

THE UNIVERSITY OF HULL

ELECTROLESS DEPOSITION OF  
GROUP EIGHT METALS

being a Thesis submitted for the Degree of

Doctor of Philosophy

in the University of Hull

by

Lee Hyland G.R.S.C., M.Sc.

October 1995

## **ABSTRACT**

Electroless plating is the controlled chemical reduction of metals without the use of an applied external potential. The use of electroless plating has a number of advantages over electroplating including the ability to deposit coatings onto complex-shaped objects which can be metallic or non-metallic, such as plastics. The most widely used electroless coating is electroless nickel prepared using sodium hypophosphite as reductant. This results in coatings which contain phosphorus. The properties of metal coatings containing non-metals are frequently superior compared to those of the pure metal.

The first part of present work was concerned with the development of an electroless plating solution capable of depositing palladium-boron coatings. The plating solution is based on EDTA-stabilised palladium (II) ions in the presence of dimethylamine borane as the reducing agent. At a pH of 10.5 the solution deposits bright adherent coatings at 1  $\mu\text{m}$  per 10 h. The plating solution operates at room temperature within narrow limits of composition and concentration: small deviations in composition from the optimum results in solution decomposition.

Characterisation of electroless palladium-boron coatings indicates that the inclusion of boron decreases the corrosion resistance of the coating. Examination of palladium-boron coatings by X-ray diffractometry show that the lattice parameter has been increased by 2.86%.

The second part of the present work was concerned with the development of pure ruthenium coatings. The plating solution developed uses hydrazine hydrate as the reducing agent with methylamine as stabiliser. The plating solution operates at a pH of

13 and at 60°C, and deposits 65% of the available ruthenium in 5 h. This corresponds to a 3 μm coating over a substrate surface area of 25 cm<sup>2</sup>.

The coatings produced are bright and adherent. The roughness of the substrate surface was found to be important to obtaining adherent coatings over 2 μm thick. A roughness in the order of 1100 Å was found to be satisfactory. Scanning electron microscopy shows the coatings to be dense with no obvious pores. The porosity of the coatings was found to be low, decreasing with increasing coating thickness. However, the electrochemical properties of the coatings indicate that ruthenium coatings have poor corrosion resistance.

The chemistry of the plating solution, particularly for ruthenium, is considered in some detail.

# CONTENTS

Title Page

Abstract

i

Contents

iii

Acknowledgements

v

1. Introduction - *Electroless deposition of metals*

1

*1.1 An Introduction to the electroless deposition process*

*1.2 The effect of incorporating a non-metal into electroless nickel coatings*

*1.3 Electroless deposition of other metals*

2. The Development and Characterisation of Electroless Palladium-Boron

Coatings

20

2.1 Introduction

21

2.2 Experimental

24

*2.2.1 Chemicals used in the study*

*2.2.2 Potentiodynamic corrosion analysis*

*2.2.3 X-ray diffractometry*

2.3 Results

30

*2.3.1 Development of an electroless palladium-boron plating solution*

*2.3.2 Characterisation of electroless palladium-boron coatings*

2.4 Discussion

42

*2.4.1 Development of an electroless palladium-boron plating solution*

*2.4.2 Characterisation of electroless palladium-boron coatings*

2.5 Conclusions

51

2.6 List of Tables

53

2.7 List of Figures	57
3. The Development and Characterisation of Electroless Ruthenium Coatings	84
3.1 Introduction	85
3.2 Experimental	87
3.2.1 Nephelometric analysis	
3.2.2 Estimation of porosity	
3.2.3 Surface profilometry	
3.3 Results	90
3.3.1 Development of an electroless ruthenium plating solution	
3.3.2 Characterisation of electroless ruthenium coatings	
3.3.3 Investigation into other possible ruthenium compounds as starting materials	
3.4 Discussion	110
3.4.1 Development of an electroless ruthenium plating solution	
3.4.2 Characterisation of electroless ruthenium coatings	
3.4.3 Investigation into other possible ruthenium compounds as starting materials	
3.5 Conclusions	132
3.6 List of Tables	136
3.7 List of Figures	143
4. Bibliography	160

## **ACKNOWLEDGEMENTS**

My thanks go to my Supervisors Professor Peter B. Wells and Dr. Ken A. Holbrook for their advice and assistance during this work. I also wish to thank Johnson Matthey plc for sponsoring this research and for the loan of palladium and ruthenium salts and complexes. In particular I would like to thank Mr. Don Cameron, Dr. Dennis Murphy and Dr. Alan Berzins of Johnson Matthey for their help and advice.

I also thank those who assisted in respect of instrumental analysis: Tony Siclair for Scanning Electron Microscopy, Bob Knight for ICP analysis of palladium coatings to determine boron content, and Jochen Schnieder for X-ray diffractometry.

# **CHAPTER 1**

## *I*ntroduction

### *Electroless Deposition of Metals*

# 1 INTRODUCTION

## 1.1 An introduction to the electroless deposition processes

Electroless deposition is the chemical reduction of metal ions in solution at a catalytic surface as opposed to reduction achieved by an applied potential. The deposit is itself catalytic and this therefore results in a continuous process. The phenomenon of electroless deposition was first observed by Brenner and Riddell in 1946.<sup>1</sup> Whilst investigating the electrodeposition of nickel-tungsten alloys in the presence of hypophosphite they observed that nickel was deposited when the applied potential was switched off. They attributed this continued plating to the chemical reduction of nickel ions by hypophosphite ions. This reaction was first performed in 1844, when Wurtz<sup>2</sup> produced black deposits of nickel powder. The first electroless coatings were reported by workers such as Breteau<sup>3</sup> and Roux<sup>4</sup> in 1911 and 1916, although their processes did not display the selective deposition of nickel and the stability characteristics of those described by Brenner and Riddell.<sup>1</sup>

The use of sodium hypophosphite to reduce nickel ions chemically resulted in deposits of nickel which were contaminated with elemental phosphorus. This incorporation of phosphorus into metal coatings is an important quality of electroless plating, because such coatings are frequently superior to those of the pure metal. Other reducing agents which have been used to electrolessly deposit a variety of metals include hydrazine, which produces coatings of high purity, and sodium borohydride, which produces coatings with incorporated boron. Therefore, by varying the composition of the plating solution it is possible to deposit metal coatings with various concentrations of phosphorus and/or boron. Each of these variants has different properties and applications.



An electroless plating solution consists of a metal salt and a reducing agent. The metal salt is normally stabilised by the addition of a complexing agent which prevents the homogenous deposition of the metal ions when the reducing agent is added. For optimum performance deposition is carried out at constant pH and temperature. To attain constant pH an appropriate buffer may be present. It is possible, however, for homogeneous deposition of the metal to occur under some conditions, allowing unwanted codeposition to occur on the walls of the plating vessel. To prevent this a stabiliser is added which may be one of four classes:<sup>5</sup> (i) compounds of group VI elements (S, Se, Te); (ii) compounds containing oxygen ( $\text{AsO}_2^-$ ,  $\text{IO}_3^-$ ,  $\text{MoO}_4^{2-}$ ); (iii) heavy metal cations ( $\text{Sn}^{2+}$ ,  $\text{Pb}^{2+}$ ,  $\text{Hg}^+$ ,  $\text{Sb}^{3+}$ ); (iv) unsaturated organic acids (maleic, itaconic). The concentration of the stabiliser may be critical to the performance of the plating solution and the quality of the coating obtained. Concentrations can be as low as 0.1 ppm for class (i), (ii) and (iii) stabilisers or as high as  $10^{-1}$  M for unsaturated organic acids. The stabilisers generally inhibit, or act as poisons to, the homogeneous catalytic processes occurring in the plating solution.

An example of an electroless nickel-phosphorus plating solution is given below.<sup>10</sup>

NiSO <sub>4</sub> .7H <sub>2</sub> O	32.05 g
Lactic acid	28.50 cm <sup>3</sup>
Propionic acid	5.01 cm <sup>3</sup>
Sodium hypophosphite	16 g
Pb <sup>2+</sup> (as Pb(NO <sub>3</sub> ) <sub>2</sub> )	4 ppb
Solution volume	1 dm <sup>3</sup>
Temperature	85°C

In the above plating solution the nickel ions from the nickel sulphate are stabilised by complexation with lactate from lactic acid. The plating solution is buffered by propionic acid. To prevent homogeneous deposition of nickel a trace amount of lead ions is added as a stabiliser. At 85°C the plating solution deposits nickel-phosphorus coatings with 9% phosphorus by weight at a rate of approximately 5  $\mu\text{m h}^{-1}$ .

Electroless deposition is not restricted to the coating of metallic materials, but can also be used to coat glass and plastic. To obtain good quality coatings on these materials the surface preparation is very important. Poor surface preparation, on any material, can lead to the coating either not adhering or exfoliating. A recent report has indicated that the type of surface preparation can influence the morphology, and therefore affect the properties, of the coating.<sup>6</sup> The first stage of any pretreatment is normally to clean the surface to remove grease, dirt and oxide layers which may be present on metallic substrates. This stage may be complicated and involve a number of soaking and electrocleaning steps. The second stage is generally an etch to improve the mechanical adherence of the coating by roughening the substrate surface. The third stage is to generate a catalytic surface on the substrate and is usually split into two parts, sensitisation and activation. Sensitisation is achieved by immersing the substrate in a solution of stannous chloride, which adsorbs the salt onto the substrate. Activation is usually achieved by an immersion in palladium chloride, which adsorbs palladium atoms onto the tin. The palladium atoms act as a catalytic surface which initiates the electroless deposition. For some metallic materials, such as nickel, because of their own catalytic properties activation can simply be performed by immersion into dilute mineral acid.

The adsorption of palladium onto the substrate surface is a general method for generating a catalytic surface but is not the only one. Different materials require specific treatment to make them suitable for electroless deposition.<sup>5</sup> The importance of cleaning and activation has been emphasised in numerous reports. For example, Shawhan and Tracy<sup>7</sup> outline the considerations necessary for the successful deposition of nickel onto stainless steel. A more specific fourteen stage process was recommended by Jeanmenne.<sup>8</sup> The first thirteen stages were concerned with the preparation of the stainless steel, with the fourteenth stage the actual deposition of nickel!

Electroless deposition onto glass and plastics is a major advantage of electroless plating but the generation of an appropriate catalytic surface necessary to initiate deposition presents problems. Pearlstein<sup>9</sup> found that attempts to coat roughened plastic surfaces which had been soaked in a solution of palladium chloride failed to result in any plating. However, a roughened surface which was immersed in chromic acid before standard treatment in stannous chloride and palladium chloride resulted in complete surface coverage of the substrate. The materials that were successfully coated included polystyrene, bakelite and glass. Roughening and immersion into chromic acid before sensitisation and activation forms the basis of surface preparation for many plastic materials.<sup>10</sup> For glass, after roughening, an etch is performed by immersion into dilute hydrofluoric acid.

The advantages of electroless plating are;

- (i) the selective deposition onto catalytically active surfaces,
- (ii) the capability of depositing coatings of uniform thickness,
- (iii) the ability for through-hole plating and the simultaneous plating of two sides,

- (iv) the ability to uniformly coat complex shaped objects,
- (v) the possibility of depositing onto non and semi-conducting materials,
- (vi) the improved properties achieved with the incorporation of a non-metal.

Since Brenner and Riddell<sup>1</sup> discovered the controlled electroless deposition of nickel by hypophosphite the number of metals which can be deposited electrolessly has grown. These metals and the reducing agents used are given below.

<i>Metal</i>	<i>Reducing Agent</i>	<i>Reference</i>
nickel	sodium hypophosphite	1
	hydrazine hydrate	11
	sodium borohydride	12
	dimethylamine borane	12
cobalt	sodium hypophosphite	1 & 13
	dimethylamine borane	14
copper	formaldehyde	15
gold	dimethylamine borane	16
silver	dimethylamine borane	17
palladium	hydrazine hydrate	18 & 19
	sodium hypophosphite	13
	tertiaryamine boranes	20
platinum	hydrazine hydrate	21
	sodium borohydride	22
rhodium	hydrazine hydrate	23
ruthenium	hydrazine hydrate	24

ruthenium	sodium hypophosphite	25
	sodium borohydride	26

It is possible to deposit electroless nickel coatings with a wide variety of phosphorus or boron compositions, which account for its wide use in the engineering and electronic industries.<sup>27</sup> For example, the incorporation of phosphorus increases the hardness and the corrosion resistance properties of the coating compared to pure nickel. Therefore, it is suitable for use in wear and/or corrosive applications in the aerospace, automotive and chemical industries.<sup>28</sup> Other applications include decorative coatings and electromagnetic radiation shielding.<sup>10</sup>

Electroless cobalt is used in the magnetic recording media industry,<sup>5</sup> because the magnetic properties of the electroless cobalt coatings can be modified depending on the deposition conditions. Electroless copper finds application in the manufacture of printed circuit boards. Electroless gold, platinum, ruthenium, silver and palladium have novel applications in the electronics industry, generally, as contacts for semi-conductor materials. Electroless gold and silver have some applications in decorative coatings and in the manufacture of jewellery.

There are other electroless deposition processes possible which have not been discussed which are beyond the scope of this study. These other processes include the electroless deposition of metal alloys, such as nickel-molybdenum-phosphorus (Ni-Mo-P), or composite coatings with silicon carbide.

## 1.2 The effect of incorporating a non-metal into electroless nickel coatings

Electroless nickel-phosphorus (Ni-P) coatings are the most widely used of all the electrolessly deposited metals. One of the advantages that electroless Ni-P and Ni-B coatings have is the improved properties which result from the inclusion of phosphorus or boron. By varying the composition of phosphorus or boron it is possible to modify the properties of the coating to make it more suitable for a particular application. This section briefly discusses how the incorporation of phosphorus or boron can impart beneficial changes on the structure and properties of metal coatings, using electroless nickel as an example.

As mentioned above the first electroless nickel coatings were deposited by Brenner and Riddell by reduction with sodium hypophosphite.<sup>1</sup> This resulted in coatings which were contaminated with phosphorus, and are the coatings usually described by the phrase “electroless nickel.” Since then many reports on the deposition of electroless Ni-P coatings which contain a variety of phosphorus compositions have been published. Generally, these reports can be divided into two groups. Firstly, those from acid plating solutions which produce the higher phosphorus variants. Riedel<sup>10</sup> reported in 1991 that there were in excess of one hundred formulations for the electroless deposition of Ni-P from acid solutions. Acid plating solutions operate in the pH range 4.6 to 5.0 and between temperatures of 85 to 95°C, and deposit coatings of 5 to 14 wt.% phosphorus at rates between 10 to 30  $\mu\text{m h}^{-1}$ . The second group, which are fewer in number, are alkaline plating solutions. These tend to be more stable than the acid variants, operating at lower temperatures (30 to 98°C), but deposit coatings at a much slower rate. The solutions operate in the pH range 8 to 11 and deposit coatings which contain 1 to 4 wt.% phosphorus.

Hydrazine hydrate based plating solutions for the deposition of high purity electroless nickel coatings were first reported by Levy in 1963.<sup>11</sup> The first major study of pure electroless nickel coatings was carried out by Dini and Coronado in 1967.<sup>29</sup> Hydrazine hydrate plating solutions operate between pH 10 to 12, at temperatures of 60 to 99°C and are capable of depositing coatings at rates about three times faster than that for Ni-P coatings. Little work on the electroless deposition of high purity nickel has been performed because of the limited requirement for the material.

Electroless Ni-B coatings were first reported by Lang in 1965, who used a plating solution based on sodium borohydride.<sup>12</sup> Plating solutions based on sodium borohydride operate at high pH, typically 11 to 14, at temperatures of 50 to 97°C, and are capable of depositing coatings which contain upto 10 wt.% boron.<sup>30</sup> Plating solutions which are based on dimethylamineborane (DMAB) operate at a lower pH, 5 to 10, between temperatures of 25 to 70°C, and deposit coatings which contain upto 5 wt.% boron at a rate of 6 to 9  $\mu\text{m h}^{-1}$ .<sup>30</sup> Generally, increasing the pH from 5 to 11 causes a decrease in the boron content from, say 4.3 to 0.2 wt.%.<sup>30</sup>

Early investigations into the structure of electroless Ni-P coatings reported that above 7 wt.% phosphorus they were amorphous.<sup>31</sup> Graham et al.<sup>32</sup> in 1965 reported that electroless Ni-P coatings with less than 7 wt.% phosphorus had a microcrystalline structure described as “a supersaturated solid solution of phosphorus dissolved in crystalline nickel.” Therefore, the structure of electroless Ni-P coatings as examined by X-ray diffractometry is dependent on the phosphorus composition. Above 7 wt.% the structure is amorphous, below it is microcrystalline. A recent report by Kumar and Nair<sup>33</sup>

claims that electroless Ni-P coatings with 4.4 to 9.1 wt.% phosphorus consist of a mixture of microcrystalline and amorphous phases.

Heat treatment of electroless Ni-P coatings results in a modification of their structure. The coatings become metallic nickel which contain nickel phosphide crystallites of formula  $\text{Ni}_3\text{P}$ . The degree of crystallisation in the coating is dependent on the temperature, the length of exposure, and phosphorus composition of the coating.<sup>34</sup>

Recent reports have indicated that the crystallisation of  $\text{Ni}_3\text{P}$  phases is preceded by the formation of intermediate nickel phosphide phases, such as  $\text{Ni}_{12}\text{P}_5$ .<sup>35,36</sup> The actual intermediate phases formed are dependent on the phosphorus content of the coating.

Electroless Ni-B coatings which contain less than 5 wt.% boron consist of two phases. "a solid solution of boron and hydrogen in a face centered cubic  $\beta$ -nickel and an amorphous phase," with coatings above 5 wt.% boron being amorphous.<sup>38</sup> Heat treatment of electroless Ni-B results in the formation of  $\text{Ni}_3\text{B}$  phases (c.f.  $\text{Ni}_3\text{P}$ ). More recent reports indicate that heat treatment results in crystallisation of nickel to the face centered cubic structure<sup>39</sup> and diffusion of boron to the surface of the coating.<sup>40</sup> Fewer studies of the structure of electroless Ni-B coatings have been reported by comparison with electroless Ni-P. The structure, before and after heat treatment, has not been completely evaluated.

The incorporation of phosphorus into electroless nickel coatings results in improved properties. For example, the microhardness of electroless Ni-P coatings ranges from 500 to 700 Knoop ( $\text{H}_\text{K}$ ), with deposits of 3 wt.% phosphorus producing the highest microhardness. An increase in phosphorus composition results in a decrease in microhardness. Heat treatment at 400°C for 1 h results in an increase in microhardness to between 800 and 1000  $\text{H}_\text{K}$ , depending on phosphorus content. The time to reach



maximum hardness is dependent on phosphorus content and heat treatment temperature.<sup>37</sup> The increase in hardness of the coatings is due to the precipitation of Ni<sub>3</sub>P crystallites described above.<sup>32</sup> A continuation of the heat treatment of electroless Ni-P coatings beyond 1 h results in a decrease in the maximum hardness attained. This is due to the Ni<sub>3</sub>P crystallites and the nickel matrix reaching the most relaxed orientation relative to each other.

The hardness of as-deposited electroless Ni-B is 700 H<sub>K</sub>,<sup>10</sup> with a maximum of approx. 1200 H<sub>K</sub> reported after heat treatment at 300°C.<sup>38</sup> Bedingfield<sup>41</sup> however, reported a value of 1000 H<sub>V</sub> after heat treatment at 300°C for 1 h. (Vickers hardness values (H<sub>V</sub>) are slightly higher than Knoop hardness values). Heat treatment at higher temperatures resulted in lower optimum hardness values.

An important mechanical property of electroless nickel coatings is in wear resistance. A review by Gould<sup>42</sup> shows that electroless Ni-P coatings have good wear resistance properties, particularly when in contact with a similar coating. Electroless Ni-P coatings which performed best were those which had been heat treated to achieve a hardness of 1000 H<sub>V</sub>.

Effective corrosion resistance can be obtained by use of electroless Ni-P coatings. The factors which may influence corrosion resistance are:<sup>5</sup>

- (i) substrate composition;
- (ii) substrate structure and finish;
- (iii) pretreatment process;
- (iv) deposit thickness;

- (v) deposit properties (composition, porosity) as determined by pH, plating solution formulation and age;
- (vi) post-plating treatments (heat treatment); and
- (vii) the corrosive environment itself.

The corrosion resistance of electroless Ni-P coatings improves with increase in phosphorus composition. This is particularly true for coatings with greater than 8 wt.% phosphorus. This is because of their amorphous structure which is relatively free from grain boundaries.<sup>10</sup> There is little evidence that the substrate composition or structure has any significant effect on the corrosion properties of electroless Ni-P coatings. Although, poor substrate surface quality may result in defects in the coating surface which may impair its corrosion performance. This was demonstrated by van Gool et al.<sup>43</sup> who studied the corrosion behaviour of electroless Ni-P in sodium chloride solution. They observed that pits were formed where coating defects were present. Similarly, with microcrystalline Ni-P coatings, pits were observed at grain boundaries.

Reports which used potentiodynamic techniques to determine corrosion properties indicate that the polarisation profile obtained varies with phosphorus content and structure of the deposit.<sup>44,45</sup> The corrosion resistance of electroless Ni-P coatings in acidic, neutral sodium chloride, and alkaline environments is claimed to be due to the formation of a passive layer which contains phosphorus.<sup>44</sup> Flis and Duquette<sup>46</sup> claimed that the phosphorus in the passive layer was in the form of phosphate. A more recent report claims that the phosphorus is in the form of phosphite.<sup>45</sup>

The corrosion resistance of electroless Ni-B in 0.5 M H<sub>2</sub>SO<sub>4</sub> and 4% NaCl shows improved resistance over nickel but impaired resistance when compared to electroless

Ni-P.<sup>47</sup> Electroless Ni-B coatings did not passivate and pits were observed when they were exposed to an acidic environment. Heat treated coatings showed no passive layer but corroded uniformly rather than by pit formation. The inferior corrosion properties of electroless Ni-B are believed to be due to the presence of grain boundaries which accompany the crystallites contained in the coating.

Hardness, wear and corrosion resistance are not the only properties improved by the incorporation of phosphorus or boron. The following list, published in 1979, shows the type of coating which is the most suitable for a particular application.<sup>27</sup>

<i>Application</i>	<i>Most Suitable Electroless Nickel Coating</i>
Wear resistance	Ni-P from acid solution
Corrosion resistance	Ni-P from acid solution or polyalloys of Ni-Sn-P, Ni-Sn-B, Ni-W-P, Ni-W-B, Ni-W-Sn-P, Ni-W-Sn-B, or Ni-Cu-P
Hardness	Ni-P from acid solution, heat treated or Ni-B with greater than 3 wt.% B
Lubricity	Ni-P from acid solution with high wt.% P
Chemical resistance	Ni-P from acid solution or polyalloy system
Solderability	Ni-B with less than 1 wt.% B or polyalloy system
Diode-bonding	Polyalloys or Ni-B with less than 1 wt.% B
Non-magnetic	Polyalloys

Magnetic (for memory)	Ni-Co-P or Ni-Co-B or Co-P or Ni-Co-Fe-P
Electrical conductivity	Ni-B with less than 0.3 wt.% B
Electrical resistance	Some polyalloys
Rhodium replacement	Ni-B with 1 to 3 wt.% B
Gold replacement	Ni-B with 0.1 to 0.3 wt.% B for soldering Ni-B with 0.5 to 1.0 wt.% B for contacts Polyalloys of P or B if below 0.5 wt.% P or B

A more comprehensive discussion on the deposition, properties and applications of electroless nickel coating can be found in “Electroless Nickel Plating” by W. Riedel.<sup>10</sup>

### 1.3 Electroless deposition of other metals

This section briefly reviews the deposition and properties of other metals which have been deposited electrolessly.

Apart from nickel, the only other metal which is deposited electrolessly on a large scale is copper, which is used in the manufacture of printed circuit boards. There are many plating solution formulations for the electroless deposition of copper, but the reductant used is almost always formaldehyde. The first comprehensive study which investigated the stability of solutions for electroless copper deposition was carried out by Goldie<sup>15</sup> in 1964. He achieved improved stability by use of a dilute solution of copper sulphate and Rochelle salt (sodium potassium tartrate) in the presence of formaldehyde. However, the deposition rate was relatively slow. Commercial plating solutions contain copper sulphate as the source of copper (II) ions which are complexed with EDTA or tartrate ions, with reduction achieved by use of formaldehyde. The stability of the solution was improved by the addition of a stabiliser. This stabiliser can effect the deposition process

and properties of the electroless copper coatings and can be selected from a long list of (generally) inorganic compounds. The list includes carbonates and phosphates, and salts of magnesium, lanthanum, gallium, thallium and ammonia; other compounds include borates, silicates and arsenates. Bielinski and Kaminski,<sup>48</sup> among others, have studied the effect of a large number of these stabilisers on the plating solution. When Bielinski and Kaminski published their results in 1987 over two hundred papers and patents had been published on the effects of such stabilisers.

The property of electroless copper which has been extensively studied is the ductility of the coating. Factors which influence this important property include, inclusion of molecular hydrogen, plating solution composition (stabilisers etc.), grain size of the coating, low temperature annealing, lattice strain, and the type of substrate.<sup>49</sup>

Other plating solution formulations which involve the use of different reducing agents have been reported, for example sodium hypophosphite<sup>50</sup> and glyoxylic acid.<sup>51</sup> The use of glyoxylic acid as reductant resulted in plating solutions which had superior stability and plating rates compared to those which used formaldehyde.<sup>51</sup>

Electroless cobalt was first deposited by Brenner and Riddell<sup>1</sup> by use of sodium hypophosphite, which resulted in electroless cobalt-phosphorus (Co-P) coatings. The main uses of electroless cobalt are in the magnetic recording and storage industry. This application was first identified by Fisher and Clinton,<sup>13</sup> who observed that electroless Co-P deposits had a high coercivity. The magnetic properties of electroless Co-P coatings can be varied by changes in the plating solution composition and operation.<sup>49</sup>

The source compound for electroless cobalt plating solutions is either cobalt chloride or cobalt sulphate. Plating solutions which involve the use of sodium hypophosphite operate between a pH of 7.0 to 9.5 and at temperatures of 17 to 77°C.<sup>5</sup> Other reductants which can be used to deposit electroless cobalt include DMAB and sodium borohydride. Deposition by use of DMAB from an acidic solution was developed by Pearlstein and Weightman in 1974.<sup>14</sup> This plating solution deposited cobalt with a rate of 13  $\mu\text{m h}^{-1}$  at 70°C. However, the more usual method for the deposition of electroless cobalt-boron (Co-B) is from an alkaline plating solution.<sup>52</sup> The use of sodium borohydride resulted in the successful deposition of Co-B at room temperature.<sup>53</sup> This plating solution operates at a high pH, typically pH 11. At still higher pH it is claimed to be possible to deposit electroless cobalt by use of formaldehyde at 30°C. For many of these electroless cobalt plating solutions, complexation of the metal ions in solution is achieved by sodium citrate, tartrate or EDTA.

The first plating solutions for the production of electroless gold coatings were developed in the early 1970's by Okinaka and co-workers.<sup>16,56</sup> These plating solutions used potassium borohydride or DMAB as reductants. An unusual feature of the use of DMAB or potassium borohydride is that pure gold coatings, and not Au-B coatings, are obtained.<sup>16</sup> The plating solutions use a gold cyanide complex in the presence of potassium cyanide to produce the stabilised gold in solution. The solution operates in alkaline conditions between 75 to 85°C with a slow deposition rate, 0.5 to 3.0  $\mu\text{m h}^{-1}$ . As well as a slow plating rate these solutions are sensitive to contamination, have poor stability, and are only capable of coating a limited number of substrates.

More recently attempts have been made to improve the stability of these plating solutions. One approach has been the addition of trace amounts of lead or thallium ions.<sup>58</sup> These additions resulted in an increased plating rate by a factor of eight. A second approach was the use of dual reducing agents. Iacovangelo<sup>58</sup> used a plating solution which contained both DMAB and hydrazine hydrate as reducing agents. The result was a bath which deposited pure gold at rates in excess of  $7 \mu\text{m h}^{-1}$ .

Plating solutions for gold which used reducing agents other than potassium borohydride or DMAB have been reported. The earliest of these used sodium hypophosphite,<sup>59</sup> though the process was not believed to be autocatalytic and the coatings produced tended to be porous with diffusion of the substrate metal to the surface of the gold. The solution operated at a neutral pH and  $93^\circ\text{C}$ , and deposited gold coatings at rates between  $2.5$  to  $5.0 \mu\text{m h}^{-1}$ . A further plating solution which used hydrazine hydrate was reported in 1962.<sup>60</sup> This solution also operated at a neutral pH and  $95^\circ\text{C}$ , depositing gold at  $1$  to  $7 \mu\text{m h}^{-1}$ . These solutions have not been investigated, or used to any extent, as those containing DMAB and potassium borohydride have been preferred.

Most recently thiourea<sup>61</sup> and ascorbic acid<sup>62</sup> have been used as reducing agents in the electroless deposition of gold. The other significant feature of these plating solutions is that they do not use the gold cyanide complexes as starting materials, but use a gold thiosulphate complex instead. The thiourea based plating solution operates at pH 9 and  $80^\circ\text{C}$  and deposits gold at a rate of  $2 \mu\text{m h}^{-1}$ . The ascorbic acid plating solution operates at pH 6 and  $60^\circ\text{C}$  with a plating rate of  $1.5$  to  $2.0 \mu\text{m h}^{-1}$ . Though the deposition rate of these solutions is slow compared to those which use DMAB or potassium borohydride, the use of a cyanide free gold complex is an advantage.

Of the other metals which can be deposited electrolessly (palladium, silver, ruthenium, platinum, rhodium and tin) only silver and palladium have been studied to any extent. The electroless deposition of palladium is discussed in detail in Section 2.1 and electroless ruthenium deposition is discussed in Section 3.1. The electroless deposition of tin by sodium hypophosphite has been reported.<sup>55</sup> This is unusual because tin does not have any catalytic properties. Molenaar,<sup>56</sup> the author of the first report, has subsequently been able to deposit coatings in excess of 20  $\mu\text{m}$ . As the process makes use of controlled disproportionation of tin (II) ions in the presence of metallic tin no reducing agent is required. Consequently, the process can not be described as truly electroless. The disproportionation of tin (II) is unaffected by the presence of tin (IV) ions in solution. Prevention of the formation of tin in the bulk of the solution was achieved by the addition of tartrate ions.

For platinum, rhodium and ruthenium few applications have been identified. As a result the electroless deposition of these materials has not been examined extensively. A number of workers have successfully deposited pure electroless platinum,<sup>5</sup> but, the properties of the coatings are not well documented. The plating solutions are based on the compounds  $\text{Na}_2\text{Pt}(\text{OH})_6$  and  $\text{K}_2\text{Pt}(\text{NO}_2)_4$  in alkaline solution. The solutions operate between 35 to 50°C and deposit pure platinum at approx. 3  $\mu\text{m h}^{-1}$ , although Rhoda and Vines<sup>21</sup> claim to have deposited platinum at a rate of 12  $\mu\text{m h}^{-1}$ . Another plating solution for the electroless deposition of platinum was described by Valsiunienne et al.<sup>22</sup> which used sodium borohydride as reductant. The plating solution contained  $\text{Na}_2\text{PtCl}_6$  as a source of platinum ions which were complexed by ethylenediamine. The stabiliser was rhodanine (2-mercapto-4-hydroxythiazole) and the solution operated at a pH of 11 and 70°C, and deposited platinum at a rate of 1.5  $\mu\text{m h}^{-1}$ .



The only recorded electroless rhodium plating solution is based on a solution of rhodium trichloride which contained excess sodium nitrite and  $\text{NH}_4\text{OH}$ .<sup>23</sup> At 60°C the addition of hydrazine hydrate resulted in a coating of rhodium. Few other details, such as the properties of the coatings, are available.

## **CHAPTER 2**

**The Development and Characterisation**

**of**

**Electroless Palladium-Boron Coatings**

## 2.1 INTRODUCTION

Little work on the development of electroless palladium systems has been carried out. The first electroless palladium plating solutions for the deposition of pure palladium were recorded by Rhoda in 1959<sup>18</sup> and 1961,<sup>19</sup> with a subsequent electroless process for depositing palladium-phosphorus coatings being reported in 1969 by Pearlstein and Weightman.<sup>63</sup>

It was not until the end of the 1980's that more work on the electroless deposition of palladium was performed. The main application for electroless palladium is in the electronics industry, there also being some interest in the nuclear industry. Ocken<sup>64</sup> has reported that an electroless coating of palladium on austenitic stainless steel prevents the incorporation of certain radionuclides found in some nuclear reactors into the stainless steel. Reports by Athanvale and Totlani<sup>65</sup> and Ocken, Pound and Lister<sup>66</sup> have been concerned with the characterisation of existing electroless palladium solutions, particularly that developed by Pearlstein and Weightman.<sup>63</sup> Others have been concerned with the development of new electroless palladium plating solutions. Steinmetz et al.<sup>67</sup> have developed an electroless palladium solution which deposits pure palladium utilising hydrazine as reductant. Chou and Chen<sup>68</sup> and Chou, Manning and Chen<sup>69</sup> have developed and characterised electroless palladium-phosphorus coatings from solutions containing sodium hypophosphite.

Examination of the patent literature on the electroless deposition of palladium reveals only two American patents;<sup>20,70</sup> these concern the deposition of palladium-boron coatings from solutions containing tertiaryamine borane reducing agents. This represents a departure from the more usual boron-containing reducing agents, sodium

borohydride and dimethylamineborane (DMAB) which are commonly used to deposit coatings of nickel,<sup>10</sup> cobalt,<sup>17</sup> gold<sup>71</sup> and silver.<sup>16</sup> Though previously having only limited use, tertiary-amine borane reducing agents are the ultimate compounds in a sequence of boron-containing reducing agents comprising, borohydride, secondary amine boranes and tertiary amine boranes.

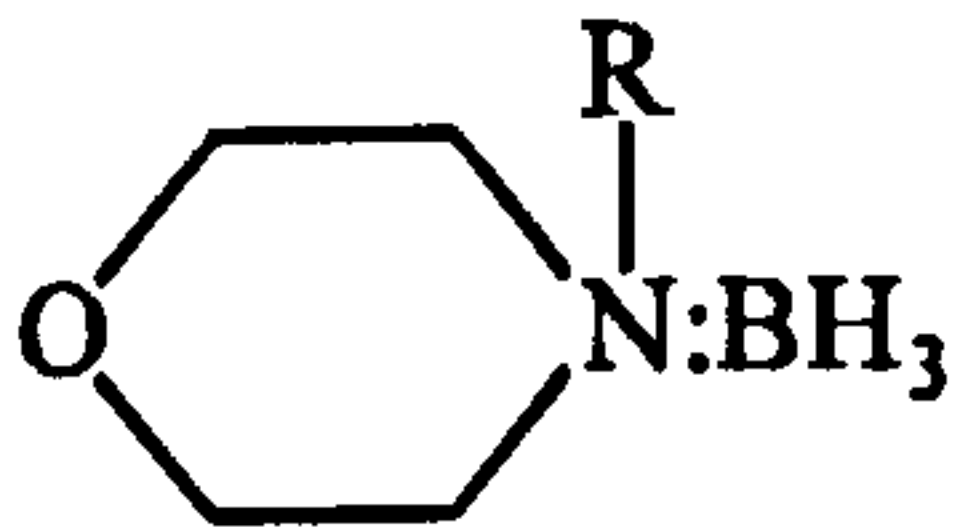
As observed from other electroless processes, the inclusion of a non-metallic element into the coating can have significant effects on the structure and properties of the coating. In many cases the effects are beneficial. One of the interesting properties of palladium is in its relationship with hydrogen, and its use in hydrogen diffusion and storage.<sup>72</sup> Expansion of the lattice by incorporation of a small atom (boron) can modify this important property of palladium.<sup>73</sup>

As the literature pertinent to the production of electroless palladium-boron coatings was limited it was decided to develop new plating solutions based on the more common reducing agents, sodium borohydride and DMAB.

The pure palladium coatings deposited by Rhoda<sup>18</sup> were found to have a lattice parameter of 3.8865 Å (c.f. JCPDS value of 3.8898 Å). The average microhardness of these coatings, as well as those deposited by Stienmetz et al.<sup>67</sup> was ca. 257 Knoop. This is above the value for bulk palladium of 70 to 250 Knoop.<sup>18</sup> The palladium-phosphorus coatings were found to have a lower microhardness. Athanvale et al.<sup>65</sup> reported a value of 173 Vickers for a coating containing 1.5 to 1.7% phosphorus. The plating solution described by Pearlstein and Weightman also deposited palladium-phosphorus coatings containing 1.5% phosphorus. Chou et al.<sup>69</sup> were able to deposit palladium-phosphorus coatings which contained 1.0 to 1.6% phosphorus from a plating solution using citrate

as complexant. Using Na<sub>2</sub>EDTA as complexant they deposited coatings containing 8% phosphorus.

Hough et al.<sup>20,70</sup> used a number of tertiary amine boranes (R<sub>3</sub>N:BH<sub>3</sub>) where R are straight chain alkyls, and N-alkyl substituted morpholine boranes having the formula



to produce electroless palladium-boron coatings. By using various combinations of reducing agents and stabilisers they were able to produce coatings which varied in appearance from black to grey to bright. The types of stabilisers used included thio-organic compounds, mercaptans, organic cyanides and thioureas. The coatings were found to contain between 1 and 3% amorphous boron and 1 to 3% crystalline PdH<sub>0.706</sub> with the remainder being amorphous palladium. Unlike palladium-phosphorus coatings the microhardness was much higher, ca. 700 Knoop.

The main uses of electroless palladium coatings is in the electronics industry, although, Ocken et al.<sup>64,66</sup> have reported that a coating of palladium-phosphorus (using the formulation of Pearlstein and Weightman<sup>63</sup>) could prevent the incorporation of <sup>60</sup>Co into stainless steel following exposure under conditions which simulated those found in primary coolant circuits of both the boiling water reactor (BWR) and the pressurised water reactor (PWR).

## **2.2 EXPERIMENTAL**

### **2.2.1 Chemicals used**

Palladium chloride, and the ruthenium compounds referred to in Chapter 3, were provided by Johnson Matthey plc.

The stainless steel sheet used as substrate was AISI 304. The maximum composition of alloying elements are (in wt.%); chromium 18.00 to 20.00, nickel 8.00 to 10.50, manganese 2.00, silicon 1.00, carbon 0.08, phosphorus, 0.045, and sulphur 0.03.

All the water used in the study was distilled water which was achieved by reverse osmosis.

### **2.2.2 Potentiodynamic corrosion analysis**

Potentiodynamic corrosion analysis allows an assessment of the corrosion characteristics of a metal sample in a few hours rather than in the weeks or months required when using other techniques. The technique is based on the potential generated when a metal electrode comes into contact with an electrolyte. This potential can be modified by the application of an external E.M.F. The applied potential, or overpotential ( $\eta$ ), results in the metal electrode being either anodically or cathodically polarised. The corrosion characteristics of an electrode are expressed as a corrosion profile. This is a graph of overpotential against the resultant current or current density.

A more detailed explanation of how the corrosion profile was obtained is as follows.

#### ***2.2.2i Theory***

A metal electrode immersed in an electrolyte has an electric double layer at its surface, the structure of which was proposed by Otto Stern.<sup>74</sup> The model, shown in Figure 1, (p.

58) combines the structures of Helmholtz<sup>75</sup> (HH) and of Gouy<sup>76</sup> and Chapman<sup>77</sup> (GC). A flow of ionic species occurs across the double layer in both the anodic (dissolution) and cathodic (deposition) directions. This flow of ions constitutes a current and can be represented by  $i_a$  (the anodic current) and  $i_c$  (the cathodic current). If the electrode is in equilibrium with the electrolyte then  $i_a = i_c$ .

The energy considerations for the flow of ions in a single direction through the electric double layer can be described by Transition State Theory. This is illustrated by Figure 2, with the energy maximum occurring at a distance  $\alpha$  (the symmetry factor) from the metal surface.

Electrochemical polarisation studies involve varying the overpotential of the material under test such that the polarisation of the electrode changes from being cathodic to anodic. As the overpotential is varied the cell potential and current density of the electrode is measured. This current density is plotted versus the cell potential to obtain the corrosion profile of the electrode. An example of such a polarisation profile is shown in Figure 3.

In electrochemical corrosion studies the currents measured are expressed as current densities, denoted by a lower case  $i$  as used in the above derivation, which has the units of  $A\ cm^{-2}$ . Capital  $I$  is used to denote a current which has the unit of Amps (A). The potential drop across the double layer at  $\eta = 0$  is known as the corrosion potential,  $E_{corr}$ , and is the potential at which corrosion begins. The current density at this potential is referred to as the corrosion current,  $i_{corr}$ , and is a measure of the rate of corrosion, given by<sup>78</sup>

$$\text{corrosion rate / mm yr}^{-1} = (M/\rho F \cdot i_{\text{corr}}) \cdot 3.2 \times 10^{10}$$

where;

$M$  = atomic mass of metal in  $\text{kg mol}^{-1}$ ,

$\rho$  = density of metal in  $\text{kg m}^{-3}$ ,

$F$  = Faraday constant ( $96,484.56 \text{ C mol}^{-1}$ ),

$i_{\text{corr}}$  = corrosion current density in  $\text{A m}^{-2}$ .

Figure 3 shows, in the ideal case, the possible processes the material under test could undergo when exposed to a corrosive environment. In the active regions either side of  $E_{\text{corr}}$  changes in current density due to overpotential can be described by the Tafel equation.

$$\eta = a \pm b \log i \quad (1)$$

For anodic polarisation;

$$\eta = \{(2.303RT/\alpha F) \log i\} - (2.303RT/\alpha F) \log i_0 \quad (2)$$

and cathodic polarisation;

$$\eta = \{(-2.303RT/(1-\alpha)F) \log i\} + (2.303RT/(1-\alpha)F) \log i_0 \quad (3)$$

where;

$R$  = the gas constant,

$T$  = temperature,

$F$  = the Faraday constant,

$\alpha$  = the symmetry factor (see Figure 2),

$i$  = the current density measured,

$i_0$  = the exchange current density (for the reaction process at equilibrium).



As the overpotential is increased above  $E_{\text{corr}}$  the potential for the formation of a metal oxide is reached with the oxide being deposited on the material surface. The oxide film results in the material becoming passive. As the metal oxide film is formed the material undergoes an active/passive transition which is seen as a decrease in the current density with increase in overpotential. Once the oxide film has formed the electrode passivates and the current density remains constant. The effectiveness of the oxide film in passivating the metal depends on the quality of the deposited film. Oxide films tend to be of poor quality. A poor oxide film will not passivate effectively, rather the material continues to corrode through the film. This can lead to the formation of pits in the substrate. Increasing the overpotential further results in a breakdown of the oxide film which is known as transpassivity.

Decreasing the potential below  $E_{\text{corr}}$  results in the metal becoming cathodically protected. This potential region is that which is studied in electroplating processes. Below this region hydrogen evolution from the electrolyte occurs. This can lead to hydrogen embrittlement of electrodeposited deposits.

Comparison of polarisation profiles of materials exposed to the same corrosive environment can be used to assess the relative corrosion resistance of each. The technique can also be used to determine whether changes in the electrode have a beneficial or detrimental effect on the corrosion resistance (e.g. the incorporation of a non-metal into an electroless coating).

The Tafel equation derived above describes the anodic and cathodic active regions of Figure 3, these being the regions either side of  $E_{\text{corr}}$ . In practice only a small part of

these regions exhibits a linear response according to the Tafel equation. At the beginning and end of these regions deviation from Tafel behaviour occurs. The effects giving rise to these deviations were first identified by Stern and Geary in 1957.<sup>79</sup> The first of these effects is a concentration effect, or concentration overpotential. This is caused by depletion of active species in the vicinity of the working electrode. This depletion results in a concentration gradient being set up and the rate of reaction becomes dependent on mass transfer mechanisms (diffusion) rather than the electron transfer process described by the Tafel equation.

The second cause of these deviations from Tafel behaviour is a result of polarisation resistance. This occurs at the opposite end of the active region from concentration polarisation effects. Polarisation resistance arises as the electrode resists being disturbed from its natural corrosion potential and occurs at small overpotentials, typically less than 0.03 V.

### *2.2.2ii Experimental*

Electrochemical polarisation measurements were carried out using a Schlumberger 1286 Electrochemical Interface with a corrosion cell designed in house in 1990 by Dr. Kalantary. The experimental arrangement is shown in Figure 4. The cell contained a working electrode of the material under test having an exposed surface area of 0.28 cm<sup>2</sup>, a platinum counter electrode, and a mercury/mercuric sulphate reference electrode. When under test the cell contained 200 cm<sup>3</sup> of 0.5 M H<sub>2</sub>SO<sub>4</sub>, which was sparged with air at 3 dm<sup>3</sup> min<sup>-1</sup>. The sparging unit was a 15 mm diameter glass tube with a glass frit at one end. The polarisation profile was obtained after 10 min; a steady

potential had usually been achieved by that time. The polarisation profile was obtained by sweeping the cell potential from -1.0 to 2.5 V at a rate of 100 mV min<sup>-1</sup>.

### 2.2.3 X-ray diffractometry of electroless palladium-boron coatings

X-ray diffraction patterns were obtained by use of a Siemens D5000 powder diffractometer. The incident radiation used was copper K<sub>α</sub>. A Soller slit was placed in the incident beam as well as a graphite secondary monochromator in the diffracted beam. The irradiated sample area of 20 x 10 mm was kept constant by means of an automatic slit arrangement.<sup>80</sup> The generator settings were 40 kV and 40 mA. The X-ray profiles were acquired in the continuous scan mode. The scan speed was varied from 0.002 to 0.020° s<sup>-1</sup>, at count times in the range of 2 to 50 s. To correct for sample displacement errors, silicon powder was placed on the sample surface as an internal standard. The arrangement is illustrated in Figure 5.

## **2.3 RESULTS**

In this section the development of the electroless palladium-boron plating solution is considered first. This is followed by a consideration of optimisation and scaling procedures and concluding with the characterisation of the palladium-boron coatings produced.

### **2.3.1 Development of an electroless palladium-boron plating solution**

#### ***2.3.1.1 Reduction of palladium solutions by DMAB [(CH<sub>3</sub>)<sub>2</sub>NH:BH<sub>3</sub>] and NaBH<sub>4</sub>***

Small scale reactions were performed to find a palladium species in solution which was stable to the presence of either dimethylamineborane (DMAB) or sodium borohydride (NaBH<sub>4</sub>).

A stock solution containing palladium was made by dissolving 0.2g PdCl<sub>2</sub> in 0.4 cm<sup>3</sup> concentrated HCl, to which was then added 16 cm<sup>3</sup> of concentrated NH<sub>4</sub>OH followed by 2.7 g NH<sub>4</sub>Cl. The solution was diluted to 90 cm<sup>3</sup> with water. The solutions under examination consisted of 3.0 or 4.5 cm<sup>3</sup> PdCl<sub>2</sub> solution with 0.2 to 0.9 cm<sup>3</sup> of complexing agent which consisted of either 0.03 M sodium citrate or 0.05 M Na<sub>2</sub>EDTA solution. The solutions were diluted such that addition of DMAB gave a total volume of 5.0 cm<sup>3</sup>. To these solutions was added 0.10, 0.15, 0.20 or 0.25 cm<sup>3</sup> DMAB solution (1g DMAB in 100 cm<sup>3</sup> water to give 0.0174 mol dm<sup>-3</sup>). Blank experiments were carried out by adding the above quantities of DMAB to 4 cm<sup>3</sup> stock palladium solution in the absence of a complexing agent. Experiments were conducted at temperatures of 22 or 55°C and at pH's of 9 or 10. In each case the pH was adjusted to the required value by the use of concentrated ammonia solution.

The addition of either DMAB or NaBH<sub>4</sub> to acidic, neutral or alkaline solutions of palladium (II) ions resulted in the immediate formation of a black precipitate. This also occurred at 22 or 55°C in the presence of the complexing agents trisodium citrate, and disodium ethylenediaminetetraacetic acid (Na<sub>2</sub>EDTA).

Adjustment of the pH of the palladium(II) solution to an alkaline value with ammonia solution resulted in the immediate formation of a black precipitate on the addition of DMAB or NaBH<sub>4</sub>. This occurred both in the presence and in the absence of complexing agents, at 22 or 55°C. However, at 22°C the addition of DMAB to an alkaline solution (pH 10) of palladium(II) ions complexed with EDTA resulted in a 0.5 h delay before a precipitate was observed. Increasing the amount of DMAB decreased this delay until addition of DMAB resulted in the immediate formation of a precipitate. Alternatively, decreasing the amount of DMAB increased the delay period to precipitation.

The use of NaBH<sub>4</sub> resulted in immediate precipitation from acidic, neutral or alkaline solution irrespective of the amount or type of complexant present.

Of the complexants examined Na<sub>2</sub>EDTA appeared to be most suitable for the formulation of a plating solution.

### *2.3.1.2 Optimisation of a palladium solution for electroless plating*

To determine the most suitable conditions for the electroless deposition of palladium from a palladium-EDTA, the composition of solutions (volume 25 or 30 cm<sup>3</sup>) was varied in the ranges given below:

Pd <sup>2+</sup>	0.006 - 0.018 g
------------------	-----------------

Na <sub>2</sub> EDTA	0.12 - 0.29 g
NH <sub>4</sub> Cl	1.00 - 2.14 g
DMAB	0.001 - 0.030 g
pH(NH <sub>4</sub> OH)	10 - 11

Plating was attempted from solutions of volume 25 or 30 cm<sup>3</sup> held at 22 or the reduced temperature of 35°C onto stainless steel (AISI 304) pretreated as described below. Variation in pH was monitored during plating. Plating solutions were made up from stock solutions in the following manner:

- (i) NH<sub>4</sub>OH was added to the palladium stock solution (Section 2.3.1) and warmed whereupon a pink precipitate formed and then dissolved;
- (ii) the solution was then cooled to room temperature and NH<sub>4</sub>Cl and Na<sub>2</sub>EDTA added;
- (iii) pH and volume were adjusted using NH<sub>4</sub>OH and water to give a stable plating solution;
- (iv) DMAB was added immediately before immersion of the substrate.

Preparation of the substrate before plating is of the first importance. Cleaning of the stainless steel was achieved by degreasing for 0.5 h in toluene followed by an anodic electroclean in 1 M KOH at 50°C with a current density of 40 mA cm<sup>-2</sup> for 300 s. Activation was achieved by immersion for 30 s in 50% H<sub>2</sub>SO<sub>4</sub> at 50°C.

An alternative procedure for activation of stainless steel was successive immersions in separate solutions of stannous chloride and palladium chloride. The preparations of the solutions were as follows: stannous chloride, 5 g SnCl<sub>2</sub> was dissolved in 30 cm<sup>3</sup> concentrated HCl and diluted to 500 cm<sup>3</sup>; palladium chloride, 0.8 g of PdCl<sub>2</sub> was

dissolved in 50 cm<sup>3</sup> concentrated HCl whereupon a 5 cm<sup>3</sup> aliquot was diluted to 500 cm<sup>3</sup> and pH 3 with 2 M NaOH and water.

The target performance was defined as a plating solution which would deposit palladium-boron coatings without decomposition. Variation of the plating solution constituents over the ranges given above was performed to attain the condition of maximum plating rate. Each component was not varied independently but moved intuitively to the optimum condition over the course of twenty experiments.

The optimum performance achieved involved the use, at 22°C, of the plating solution described below;

Pd <sup>2+</sup>	0.012 g
Na <sub>2</sub> EDTA	0.175 g
NH <sub>4</sub> Cl	1.6 g
DMAB	0.02 g
pH (NH <sub>4</sub> OH)	10.5
Total volume	30 cm <sup>3</sup>

This plating solution deposited 0.0051 g palladium over a surface area of 2.9 cm<sup>2</sup> corresponding to a coating thickness of 1.47 μm. This plating performance is achieved over 3 h and 42% of the available palladium is deposited. On standing the above plating solution decomposed by the formation of a black precipitate after about 12 h.

In an attempt to extend the plating solution life and to deposit more than 42% of the palladium, further additions of DMAB were made during plating. These further additions accelerated plating solution decomposition such that precipitation occurred within 3 h.

### *2.3.1.3 Effect of pH variation on the stability of electroless palladium solutions*

The plating solution described in Section 2.3.1.2 shows rapid decline in pH during plating (Curve 1, Figure 6). Plating solutions which showed a rapid decline in pH were observed to decompose, although good quality coatings were obtained. Increasing the  $\text{NH}_4\text{Cl}$  concentration in the plating solution (Curve 4) had no significant effect on slowing the rapid decline in pH.

In an attempt to slow the decline in pH during plating boric acid was added to the solution. In initial experiments the boric acid replaced  $\text{NH}_4\text{Cl}$ , in later experiments it was used together with  $\text{NH}_4\text{Cl}$ . The boric acid concentration was varied in the range 0.25 to 1.16 g per 30  $\text{cm}^3$  solution. The optimum concentration was determined by monitoring the rate of pH decline, solution stability, and plating rate. Plating was performed onto an electrodeposited nickel strike<sup>†</sup> onto stainless steel. [A nickel strike was used for the following reasons: (i) the surface was that of a single element rather than that of an alloy; (ii) the surface could be produced in the clean state before each experiment; (iii) nickel can be easily activated towards electroless deposition.] Activation of the nickel was achieved by a 30 s immersion in 50%  $\text{HCl}/\text{H}_2\text{O}$  at 22°C.

The addition of boric acid to the plating solution was found to slow the rate of pH decline appreciably (Curve 5, Figure 6). The addition of boric acid results in a more stable solution capable of plating for longer periods of up to, typically, 10 h.

---

<sup>†</sup> The electro-nickel strike was deposited from Wood's<sup>81</sup> solution under the following conditions. 125  $\text{cm}^3$  concentrated  $\text{HCl}$  was added to 240.27 g  $\text{NiCl}_2 \cdot 6\text{H}_2\text{O}$  dissolved in water and diluted to 1  $\text{dm}^3$ . The steel substrate was suspended in the solution between two nickel anodes and deposition was performed by applying a current density of 3  $\text{A dm}^{-2}$  for 180 s at room temperature, 22°C.



Variation of the concentration of boric acid over the range 0.25 to 1.16 g per 30 cm<sup>3</sup> plating solution resulted in an optimum value of 0.4 g. The optimum value was obtained by monitoring the pH variation, and defined as the quantity which gave a very slowly falling pH (Curve 6) but which did not impair the plating rate. Using values of less than 0.4 g resulted in a steady pH but a slower plating rate. Increasing above 0.4 g had no further beneficial effect on the plating solution.

#### *2.3.1.4 Scale up of the electroless palladium deposition process*

The plating solution volume was scaled up from 30 to 100 cm<sup>3</sup>. The palladium present was scaled up by a factor of 3 (from 0.012 to 0.036 g) resulting in a slight decrease in palladium concentration. In scaling up the solution volume in this way it was necessary to re-optimize the system, the optimum being defined by the solution stability, plating rate, and rate of pH decline. To optimize the solution the concentrations of Na<sub>2</sub>EDTA, boric acid, and NH<sub>4</sub>Cl were each increased individually by factors in the range 1.5 to 3 as follows.

Na <sub>2</sub> EDTA	0.26 - 0.525 g
NH <sub>4</sub> Cl	2.4 - 4.8 g
B(OH) <sub>3</sub>	0.6 - 1.2 g
DMAB	0.03 - 0.06 g

Though the quantity of palladium present was increased by a factor of 3 the surface area of the nickel on stainless steel substrate (Section 2.3.1.3) remained the same. During plating the variation in pH was monitored.

The result of increasing the plating solution volume from 30 to 100 cm<sup>3</sup> was that the solution tended to decompose within 1 h of DMAB addition. As a result re-

optimisation of the plating solution was necessary. For a solution of 100 cm<sup>3</sup> containing 0.036 g of palladium(II) ions this resulted in the following optimum conditions at 22°C;

Na <sub>2</sub> EDTA	0.60 g
NH <sub>4</sub> Cl	2.5 g
B(OH) <sub>3</sub>	1.0 g
DMAB	0.055 g
pH (NH <sub>4</sub> OH)	10.5

#### *2.3.1.5 Effects of the addition of lead and agitation on the stability of plating solutions*

##### **(i) Addition of lead**

The use of lead (II) ions as a stabiliser is common in electroless nickel deposition.<sup>82</sup> It was therefore decided to determine whether the presence of lead had any beneficial effect on the stability of the electroless palladium plating solution. A 50 cm<sup>3</sup> plating solution was used containing: Pd<sup>2+</sup>, 0.012 g; NH<sub>4</sub>Cl, 3.2 g; Na<sub>2</sub>EDTA, 0.4 g; pH(NH<sub>4</sub>OH) 10.5. Lead was added to 10 cm<sup>3</sup> aliquots to produce plating solutions with Pb<sup>2+</sup> concentrations of 1.3 ppb, 0.5, 1, 2, and 4 ppm. The solution was then made up to 11 cm<sup>3</sup> with 0.4 cm<sup>3</sup> DMAB and water. The solutions were left to stand to determine whether palladium would be precipitated from the solution in the absence of a substrate.

The addition of lead resulted in a *less* stable plating solution. The presence of lead hastened plating solution decomposition.

**(ii) Agitation**

- a) A 50 cm<sup>3</sup> plating solution of composition: Pd<sup>2+</sup>, 0.018 g; Na<sub>2</sub>EDTA, 0.29 g; NH<sub>4</sub>Cl, 2.4 g; B(OH)<sub>3</sub>, 0.6 g; DMAB, 0.03 g, at a pH of 10.5 was sparged with nitrogen gas at a pressure of 2 psi in the absence of a substrate.
- b) A 30 cm<sup>3</sup> plating solution of composition: Pd<sup>2+</sup>, 0.012 g; Na<sub>2</sub>EDTA, 0.20 g; NH<sub>4</sub>Cl, 1.60 g; B(OH)<sub>3</sub>, 0.30 g; DMAB, 0.03 g; at a pH of 10.5 was sparged with air at 3 dm<sup>3</sup> min<sup>-1</sup> for 2 h and then left to stand for 24 h without a substrate.
- c) A solution having the composition as in (b) was stirred whilst plating was attempted on to an electrodeposited nickel strike on to stainless steel.

The results were as follows.

Sparging nitrogen through 50 cm<sup>3</sup> of optimised plating solution before and during plating led to rapid solution decomposition. Sparging the solution with nitrogen gas in the absence of a substrate but in the presence of DMAB also resulted in rapid solution decomposition.

Sparging with air for 2 h did not result in decomposition of the solution in the absence of a substrate, although when this sparged solution was left to stand it eventually decomposed.

Alternatively, magnetic stirring of the solution in the presence of a substrate results in solution decomposition after approximately 1 h.

The action of agitation on the plating solution resulted in a decrease in the stability and performance.

## 2.3.2 Characterisation of electroless palladium coatings

### *2.3.2.1 Potentiodynamic analysis of electroless palladium coatings*

Three electroless palladium coatings were examined. The coatings were deposited onto substrates of (i) electrodeposited nickel on stainless steel and (ii) gold (gold coated copper plaques provided by Johnson Matthey). Coatings were of three types: electroless palladium-boron coatings deposited from the plating solution described in Section 2.3.1.4, pure palladium coatings<sup>†</sup> deposited as described by Rhoda,<sup>18</sup> and palladium-phosphorus coatings<sup>‡</sup> deposited as described by Pearlstein and Weightman.<sup>93</sup>

Gold substrates were activated by a 20 s immersion in 50% H<sub>2</sub>SO<sub>4</sub> at 22°C.

The results of the potentiodynamic analysis of the various electroless palladium coatings can be seen in Table 1 and Figures 7, 8, and 9. They are discussed later.

### *2.3.2.2 ICP-AES of electroless palladium coatings for determination of boron content*

Two electroless palladium-boron coatings were dissolved separately in 5 cm<sup>3</sup> 25% HNO<sub>3</sub> and diluted to 30 cm<sup>3</sup> with water. The first coating was produced from two sequential immersions in electroless palladium-boron solutions each of which decomposed producing a very dark coating. The second coating was produced from a

---

<sup>†</sup> The pure electroless palladium coatings were deposited from a 100 cm<sup>3</sup> plating solution of composition: PdCl<sub>2</sub>, 1.25 g; concentrated HCl, 1.5 cm<sup>3</sup>; NH<sub>4</sub>OH, 28 cm<sup>3</sup>; Na<sub>2</sub>EDTA, 0.8 g; at a temperature of 35°C. Hydrazine was added at a rate of 0.8 cm<sup>3</sup> (1 M solution) h<sup>-1</sup>.

<sup>‡</sup> Electroless palladium-phosphorus coatings were deposited onto gold from a 100 cm<sup>3</sup> plating solution, under the following conditions: PdCl<sub>2</sub>, 0.2 g; concentrated HCl, 0.4 cm<sup>3</sup>; NH<sub>4</sub>OH, 16 cm<sup>3</sup>; NH<sub>4</sub>Cl, 2.7 g; NaH<sub>2</sub>PO<sub>2</sub>, 1 g; at a pH of 9.8 with a temperature of 55°C.

single immersion in a solution which did not decompose, and was of a bright appearance.

Palladium analysis was performed on the above solution diluted 10 times. The emission line measured was the strongest line at  $\lambda$  340.458 nm. Calibration was made against 20.2, 10.1, and 0 ppm palladium standards in 5% nitric acid, matrix matched.

Boron analysis was performed on the neat solution using the second strongest line at  $\lambda$  249.773 nm (the strongest line at  $\lambda$  182.640 requires purging to produce a vacuum path length and was therefore not used). Calibration was performed against boron standards of 3, 2, 1, and 0 ppm in 5% nitric acid, matrix matched. In neither case was any interference from other species in solution detected.

The results of ICP-AES analysis of palladium-boron coatings for palladium and boron are, for three replicates:

for the dark grey (almost black) coating the palladium concentration was 721 ppm, and boron was 15 ppm, giving a Pd : B ratio of 47.7 : 1;

for the bright coating, palladium was 178.8 ppm and boron 2.44 ppm, giving a Pd : B ratio of 73.3 : 1.

### *2.3.2.3 X-ray diffractometry of electroless palladium-boron coatings*

The results of X-ray diffraction analysis of electroless palladium-boron coatings compared to pure electroless palladium can be seen in Table 2 and Figures 10 and 11.

The lattice expansion due to incorporation of boron was calculated using a Nelson-Riley plot.<sup>83</sup> This is a plot of Lattice Parameter ( $a$ ) versus  $1/2$  the Nelson-Riley Function (NRF), which is given by;

$$2 \times \text{NRF} = \frac{\cos^2\theta}{\sin\theta} + \frac{\cos^2\theta}{\theta}$$

Theta is obtained from;

$$\theta = (360/\pi)^{-1} \cdot (2\theta)$$

The lattice parameter (a) is given by;

$$a = d \cdot \sqrt{k}$$

where d is obtained from the equation  $n\lambda = 2d \sin \theta$ , and  $k = h^2 + k^2 + l^2$

The intercept on the y-axis of the Nelson-Riley plot is the lattice parameter.

Using the data given in Table 2 Nelson-Riley plots for the silicon powder added as an internal standard to both coatings were obtained. Plots for the two electroless palladium coatings were also obtained. The parameters measured for the pure palladium coating and silicon were compared to the Joint Council for Powder Diffraction Standards (JCPDS) values. All the Nelson-Riley plots are given in Figure 12.

The values for silicon, the internal standard, were:

JCPDS 27-1402 for silicon	5.430(88) Å;
silicon on pure electroless palladium	5.430(73) Å;
silicon on electroless palladium-boron	5.431(07) Å.

The measured lattice parameters were, for:

pure electroless palladium	3.882(8) Å;
JCPDS 5-681 for palladium	3.889(8) Å;
electroless palladium-boron	4.000(9) Å;
increase in lattice parameter	0.111(1) Å (2.86%).

The difference in measured lattice parameter of the silicon powder, in both cases, when compared to the JCPDS value can be considered to be insignificant. Therefore, indicating that the lattice parameter obtained for the palladium-boron coating shows a real increase due to the incorporation of boron.

#### *2.3.2.4 Scanning electron microscopy of electroless palladium coatings*

Electron micrographs of the electroless palladium-boron coatings were produced on a Cambridge S 360 scanning electron microscope with the samples angled at 45° to the electron beam. The coatings examined were electroless palladium-boron on:

- a) stainless steel, with coating thicknesses of 0.26 and 1.47  $\mu\text{m}$ ;
- b) electrodeposited nickel on stainless steel, with palladium-boron coating thicknesses of 2.0 and 2.7  $\mu\text{m}$ ;
- c) gold, with palladium-boron coating thickness of 0.77  $\mu\text{m}$ .

Electron micrographs (and related enlargements, as appropriate) of such electroless palladium-boron coatings are shown in Figure 13.

Figure 13(a) shows an electroless palladium-boron coating on stainless steel with a thickness of 0.26  $\mu\text{m}$ .

Figure 13(b) shows a coating on stainless steel with a thickness of 1.47  $\mu\text{m}$ .

Figure 13(c) shows a coating on nickel on stainless steel with a thickness of 2.0  $\mu\text{m}$ .

Figure 13(d) shows a coating on nickel on stainless steel with a thickness of 2.7  $\mu\text{m}$ .

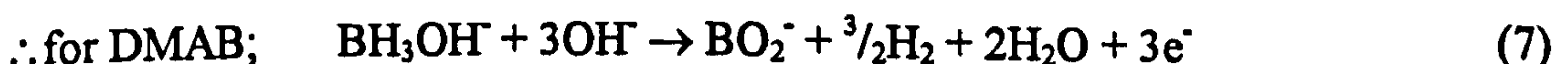
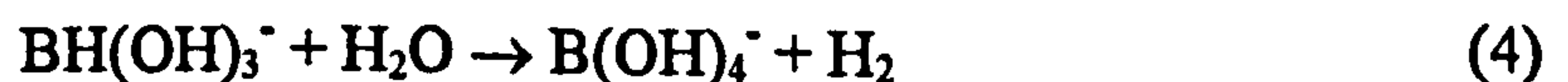
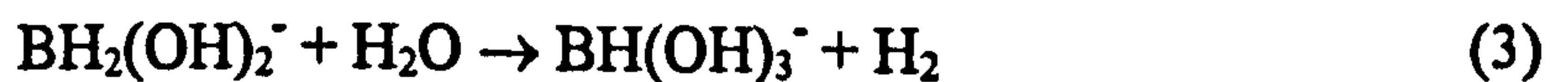
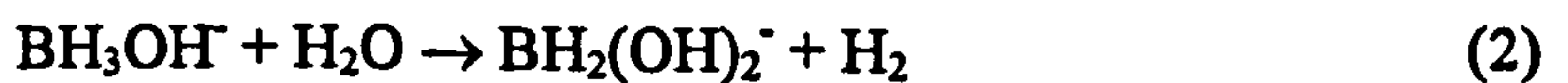
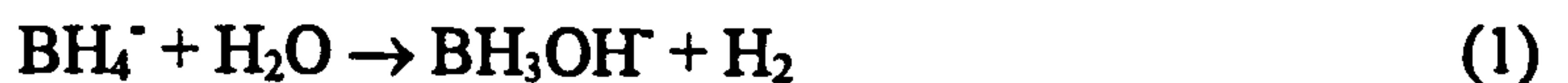
Figure 13(e) shows a coating deposited onto gold with a thickness of 0.77  $\mu\text{m}$ .

## 2.4 DISCUSSION

### 2.4.1 The Development of an electroless palladium-boron plating solution

#### *2.4.1.1 Effect of DMAB and NaBH<sub>4</sub> on palladium solutions*

Electroless plating solutions are metastable systems capable of exhibiting reduction of metal ions in controlled rates. Tetraammine palladium (II) complexes in alkaline solution are sufficiently stabilised by Na<sub>2</sub>EDTA to undergo controlled reduction by DMAB. However, the same complexes are reduced spontaneously by NaBH<sub>4</sub>. The metastability of the system towards DMAB reduction is further shown by the fact that increasing the concentration of DMAB can result in sudden precipitation of palladium. The immediate precipitation of palladium by sodium borohydride is a function of the reducing species present in the solution. Fresh aqueous solutions of sodium borohydride (or solid) contain BH<sub>4</sub><sup>-</sup> ions in solution. Fresh solutions of DMAB contain BH<sub>3</sub>OH<sup>-</sup> ions. The oxidation processes involving BH<sub>4</sub><sup>-</sup> and BH<sub>3</sub>OH<sup>-</sup> occur by replacement of H atoms by OH<sup>-</sup> according to the mechanism:

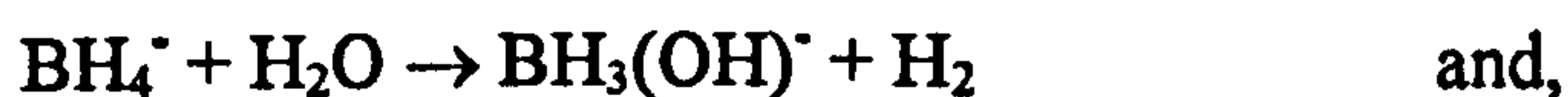


The reduction of palladium (II) ion is given simply by:

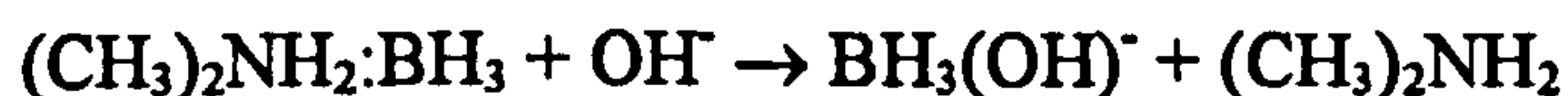




Studies by Okinaka<sup>71,84</sup> on the electroless deposition of gold using NaBH<sub>4</sub> and DMAB suggest that in both cases the reducing species is BH<sub>3</sub>OH<sup>-</sup>. According to Gardiner and Collat<sup>85</sup> the oxidation of BH<sub>3</sub>OH<sup>-</sup> occurs at a potential 0.5 V more negative than that for BH<sub>4</sub><sup>-</sup>; therefore BH<sub>3</sub>OH<sup>-</sup> will be more easily oxidised. Okinaka<sup>71</sup> observed that, when using DMAB, the rate of deposition of gold was approximately half of that observed when using NaBH<sub>4</sub>. He suggested that this was due to the kinetics of the process whereby BH<sub>3</sub>OH<sup>-</sup> is generated in solution. He proposed that the decomposition of BH<sub>4</sub><sup>-</sup> occurs in 2 steps;



the first of which is rate determining, with the second being very rapid (the second step above summarises equations 3 to 5 on the previous page). By contrast the first step in the decomposition of DMAB involves hydroxide ion in a slow step;



Remarkably the rate of decomposition of BH<sub>4</sub><sup>-</sup> and BH<sub>3</sub>(OH)<sup>-</sup> is affected in opposite senses by the concentration of OH<sup>-</sup> ions. Increasing OH<sup>-</sup> ion concentration stabilises BH<sub>4</sub><sup>-</sup> ions in solution resulting in a slower rate of decomposition, and hence a slower plating rate. For example, a report by Lo and Hwang<sup>86</sup> claims that increasing the pH from 9 to 13 decreases the rate of decomposition of BH<sub>4</sub><sup>-</sup> by over 95%. On the other hand for DMAB, an increase in OH<sup>-</sup> ion concentration destabilises the solution resulting in an increase in rate of decomposition and the plating solution crashes (a rapid bulk deposition of palladium). Thus, at a pH of 10.5 the addition of NaBH<sub>4</sub> results in rapid decomposition of BH<sub>4</sub><sup>-</sup> to BH<sub>3</sub>(OH)<sup>-</sup> giving rise to a rapid reduction of Pd(II) to Pd(0) which precipitates from solution. A plating solution containing DMAB produces

$\text{BH}_3(\text{OH})^-$  comparatively slowly resulting in a more satisfactory metastable solution. For these reasons an increase in either pH or DMAB concentration may result in gross deposition of palladium from solution, as was observed in practice.

A second factor which influences the stability of a plating solution is the degree of complexation and strength of the complex involved. Lo and Hwang<sup>86</sup> reported that the rate of decomposition of  $\text{BH}_4^-$  in an electroless nickel solution was catalysed by the concentration of free metal ion in solution. The complexed metal in solution must be sufficiently resistant to reduction by  $\text{BH}_4^-$  that it does not undergo homogeneous decomposition in the bulk of the solution. Before the addition of  $\text{Na}_2\text{EDTA}$  to the solution the palladium exists as a tetraaminepalladium (II) complex. After the addition of  $\text{Na}_2\text{EDTA}$  the palladium is thought to exist as either a Pd(II)-EDTA complex or a diamminepalladium(II)-EDTA complex. Greater stability might therefore be achieved by the introduction in the plating solution of a diammine, such as 1,2-diaminoethane. Ligands which coordinate through N rather than O are possibly a better choice because palladium generally forms stronger complexes with N-coordinating ligands. An examination of the behaviour of N-coordinating ligands in this plating solution should be the next stage in plating solution development.

#### *2.4.1.2 Optimisation of palladium-EDTA plating solution*

Though the addition of  $\text{Na}_2\text{EDTA}$  to the solution produced an increase in stability towards DMAB, too high a concentration of DMAB still resulted in decomposition of the solution. Optimum conditions were determined by gradual adjustment of the concentrations of  $\text{Na}_2\text{EDTA}$ ,  $\text{NH}_4\text{OH}$ ,  $\text{NH}_4\text{Cl}$ , and DMAB, with respect to a palladium concentration of 0.012 g in 30 cm<sup>3</sup>. The optimised condition for the solution was that at

which addition of DMAB did not result in solution decomposition, either immediately or after some time. The rate at which plating occurred was defined by the optimum stable conditions. Attempts to increase the plating rate by alteration of the conditions resulted in the decomposition of the solution and the production of a poor quality film, both in terms of thickness and appearance.

From an optimised solution it was possible to deposit over 40% of the available palladium. Prolonging the plating lifetime of the solution sometimes resulted in plating a greater percentage of palladium. Attempts to prolong the plating life of the palladium solution by the successive addition of DMAB at intervals resulted in the decomposition of the solution. This may have been due to a critical concentration of DMAB having been exceeded.

Though the solution plates for a reasonable length of time and produces a palladium coating with a high quality appearance the solution tends to eventually decompose. Therefore, even under optimum conditions, the palladium solution is not entirely stable. Decomposition under these conditions is thought to be associated with the rapid decline in pH during plating. In the absence of DMAB the palladium solution is stable at values of pH below 10. Addition of a small quantity of DMAB at values of pH below 10 results in the immediate precipitation of palladium from solution. Generally, under more stable conditions, the initial decomposition of a solution which has been plating for a few hours is quite slow. The decomposition is observed as a very gradual darkening of the solution due to the formation of particulate palladium. After a few minutes the solution darkens rapidly due to the particles catalysing the precipitation of more palladium in the bulk of the solution.

### *2.4.1.3 The effect of pH decline on solution stability*

Examination of curves 1 to 4 of Figure 6, which refer to solutions that do not contain boric acid, shows that, during the first 0.5 h of plating, there is a rapid decline in solution pH which can either continue at that rate of decline or slow and become fairly steady. Where there is a rapid decline in pH which continues beyond the first 0.5 h thick coatings are produced, but the solution decomposes earlier (generally after 4 to 5 h). Where the pH decline steadies after the first 0.5 h the solution remains stable for a longer period before decomposing (solutions generally decompose overnight) but does not produce a coating thickness of the same order as in the case of continual rapid pH decline.

Further, the initial pH of the solution appears to dictate the rate at which pH decline occurs and therefore the amount of palladium that is deposited. For example, comparison of curves 1 and 3 in Figure 6 show that low initial pH is accompanied by continued rapid decline; this plating solution gave the heavier palladium coating.

Curves 5 and 6 show the beneficial effect of the presence of boric acid. Both curves show a very slow pH decline yet these experiments produced palladium deposits of greater thickness than experiments represented by curves 2 and 3. Also, unlike solutions which do not contain boric acid, they do not decompose under the same conditions. Curve 6 appears to have no initial rapid drop in pH over the first 0.5 h, whereas curve 5 has. The experiment represented by curve 6 produced a palladium coating of greater thickness than that represented by curve 5. This observation is believed to be due to the increased boric acid concentration in curve 6.

#### *2.4.1.4 Scaling up the plating solution*

Re-optimisation of the solution was thought to be necessary due to the way in which the scaling up was performed. The amount of palladium in solution was increased from 0.012 g in 30 cm<sup>3</sup> to 0.036 g in 100 cm<sup>3</sup>, in effect the palladium concentration was decreased. As a result of this dilution the ratio of palladium to ammonia had been decreased. As seen from the previous optimisation there has to be a balance between the relative amounts of NH<sub>4</sub>OH and NH<sub>4</sub>Cl. Too high a concentration of either will result in a slow plating rate. Too low a concentration of either and the solution is liable to decompose. Therefore, as the palladium concentration has effectively decreased, less NH<sub>3</sub> from NH<sub>4</sub>OH is used to complex the palladium (II), thus increasing the NH<sub>4</sub>OH concentration. As a result less NH<sub>4</sub>Cl is required to maintain the NH<sub>4</sub>OH/NH<sub>4</sub>Cl equilibrium. As less DMAB is also used less boric acid is necessary to maintain the pH of solution. This re-optimisation resulted in a slight decline in plating rate.

#### *2.4.1.5 Other factors affecting solution stability*

Decomposition under nitrogen sparging occurred rapidly whereas under air sparging no decomposition was observed. Decomposition of an air-sparged solution sometime after sparging had ceased is probably due to the inherent instability of the solution. Nitrogen sparging displaces oxygen from solution, this is known to affect the stability and plating behaviour of electroless solutions.<sup>68,87</sup>

These sparging experiments show that oxygen dissolved in the solution has an important role in determining the reproducibility in the electroless deposition of palladium.

Stirring the palladium electroless solution shows that the solution is sensitive to excessive agitation. This may be due to stirring displacing the concentration gradient at

the coating surface. Alternatively, stirring may affect the way in which the dissolved oxygen is distributed within the solution.

The presence of lead ions in solution causes decomposition, probably by providing a mechanism whereby the reduction of palladium (II) can occur in the bulk solution.

#### *2.4.1.6 Activation procedures*

The activation procedures used for the various substrates are those which are commonly used for the activation of these materials. For stainless steel, activation using successive immersions into solutions of stannous chloride and palladium chloride resulted in a reduction of the induction period before plating, whereas activation by etching resulted in longer induction periods. Activation procedures for the other materials were found to be satisfactory.

### 2.4.2 Characterisation of electroless palladium coatings

#### *2.4.2.1 Potentiodynamic analysis of Pd-B coatings*

From Table 1 it can be seen that the addition of either phosphorus or boron resulted in a decrease in the corrosion resistance of the electroless palladium coating.

For electroless palladium and palladium-boron coatings onto electrodeposited nickel on stainless steel there is a reversed trend in values of  $E_{\text{corr}}$  (Table 1). For palladium-boron coatings  $E_{\text{corr}}$  falls with increasing thickness, and for pure palladium deposits  $E_{\text{corr}}$  increases with increasing thickness. This is due to (a) the relative positions of the  $E_{\text{corr}}$ s of palladium, nickel, and palladium-boron and (b) the roughness of the stainless steel substrate on which the nickel was electrodeposited which affected the way in which the

electroless deposits grew. It is generally known that, for smooth surfaces, a coating with a small grain size is obtained, and that for rough surfaces a larger grain size is obtained.

The  $E_{\text{corr}}$  of electroless palladium-boron coatings is about 0.1 V lower than that for pure electroless palladium. The  $E_{\text{corr}}$  of nickel lies between these two values. Therefore, on a rough surface where complete coverage of the surface is not reached until a thickness of 2  $\mu\text{m}$  is exceeded, the exposed nickel has an important effect on the  $E_{\text{corr}}$  of electroless palladium-boron and pure palladium coatings.

As the  $E_{\text{corr}}$  for electroless palladium-boron is below that for nickel, any exposed nickel being more noble, will cause an increase in the value of  $E_{\text{corr}}$ . For pure electroless palladium, the  $E_{\text{corr}}$  is above that of nickel, therefore any exposed nickel will decrease the measured  $E_{\text{corr}}$  value.

#### *2.4.2.2 Scanning electron microscopy of electroless Pd-B deposits*

Figure 13(a) to 13(d) are electron micrographs of electroless palladium-boron coatings, (a) and (b) on stainless steel and (c) and (d) on electrodeposited nickel on stainless steel. Each of the micrographs show an increase in deposit thickness, (a) 0.26, (b) 1.47, (c) 2.0, (d) 2.7  $\mu\text{m}$ . Figure 13(a) illustrates the roughness of the substrate, and shows how the coating has grown only on particular areas of the substrate. These areas correspond to the peaks of the surface roughness, with little deposition in the valleys. This results in island formation, Figure 13(b), and the islands grow until they become coherent at a nominal thickness of 2  $\mu\text{m}$ , Figure 13(c). Once the coating is thicker than a nominal 2  $\mu\text{m}$ , and becomes coherent it apparently cracks, Figure 13(d). This cracking is due either to internal stresses developed in the deposit or to mishandling of the coating. From Figure 13(d) there is no evidence that plating has continued once the coating has

cracked because there is no visible plating over the cracks. A further observation is that the cracks do not follow the grain boundaries. Mishandling is therefore the most likely source of the cracks.

Figure 13(e) shows a similar electroless palladium-boron coating deposited onto a smooth gold surface where the thickness is only 0.7  $\mu\text{m}$ . The coating is featureless and cracked, whether this is due to internal stresses or maltreatment is not clear.

#### *2.4.2.3 X-ray diffractometry*

Incorporation of boron at 1.4% by weight into an electroless palladium coating produced a change in peak position in the order of  $1^\circ$  in the X-ray diffraction pattern. The change in peak position is consistent with an increase in the lattice spacing. The measured increase was 10% in palladium volume compared to the JCPDS value; this is similar to that observed for the incorporation of hydrogen into the palladium lattice.<sup>72</sup>

A further observation is the apparent decrease in the lattice parameter of pure electroless palladium compared to the JCPDS value. The reason for this decrease is unclear.

Examination of the intensities of the peaks in the diffraction pattern for the various electroless palladium coatings, Table 3, show a change in the preferred orientation of the two electroless palladium coatings. Similarly, the preferred orientation of pure electroless palladium is different to that of the powder sample used to obtain the JCPDS pattern.



## 2.5 CONCLUSIONS

A plating solution capable of depositing electroless palladium-boron coatings has been developed. The solution containing a tetraammine palladium(II) complex stabilised by the presence of EDTA was found to be stable (or suitably metastable) to the action of DMAB but not sodium borohydride. The composition for 100 cm<sup>3</sup> of the plating solution is;

Palladium(II) ions	0.036 g
Na <sub>2</sub> EDTA	0.600 g
Boric acid	1.000 g
DMAB	0.055 g
pH (NH <sub>4</sub> OH)	10.5
Temperature	22°C

The plating solution deposits coatings under very narrow operating conditions. A small deviation from the above composition will result in premature decomposition of the plating solution. Coatings of approximately 1 µm are produced after 10 h plating, where thickness depends on the surface area of the substrate. The solution deposits approximately 40% of the available palladium. The boron content of the coatings as determined by ICP-MS was 1.4% by weight.

The presence of dissolved oxygen in the plating solution is apparently necessary for the plating solution to remain stable.

The inclusion of boron atoms into the palladium coating causes a decrease in corrosion resistance. The corrosion potential of electroless palladium-boron coatings was found to be lower than that for pure electroless palladium in aerated 0.5 M sulphuric acid.

This decrease in corrosion resistance is also seen with electroless palladium-phosphorus coatings examined.

Comparison of the X-ray diffraction patterns of pure electroless palladium and of palladium-boron coatings shows a peak shift of approximately  $1^\circ$ . This corresponds to a lattice expansion of 2.86% in length. This gives a volume expansion of approximately 10%, which is similar to the 10% volume increase observed for hydrogen inclusion into pure palladium.<sup>72</sup>

Examination of the electroless palladium-boron coatings shows them to be bright, coherent and well adhered.

## **2.6 LIST OF TABLES**

**Table 1. The potentiodynamic analysis of various electroless palladium coatings in aerated 0.5 M H<sub>2</sub>SO<sub>4</sub>**

**Table 2. Changes in X-ray peak position for electroless palladium-boron coatings**

**Table 3. X-ray peak intensities showing variation in preferred orientation of electroless palladium coatings**

**Table 1. Potentiodynamic analysis of electroless palladium coatings in aerated  
0.5 M H<sub>2</sub>SO<sub>4</sub>**

SUBSTRATE	COATING	THICKNESS /μm	E <sub>corr</sub> /mV	i <sub>corr</sub> /10 <sup>-4</sup> A cm <sup>-2</sup>
SS	-	-	-828	0.60
SS/Ni	-	-	-660	0.48
Au	-	-	-505	0.77 x 10 <sup>-2</sup>
SS/Ni	Pd-B	1.0	-714	2.4
SS/Ni	Pd-B	2.3	-745	2.9
Au	Pd-B	0.7	-750	2.1
Au	Pd-B	0.8	-738	2.8
Au	Pd-B	(thick)	-718	3.0
Au	Pd-P	4.7	-731	1.0
SS/Ni	Pd	0.9	-721	2.4
SS/Ni	Pd	2.8	-702	4.0
SS/Ni	Pd	4.3	-621	1.1
Au	Pd	4.1	-635	1.1

**Table 2. Changes in x-ray peak position for electroless palladium-boron coatings**

PEAK	<i>hkl</i>	2θ		d	
		Pd	Pd-B	Pd	Pd-B
Si	111	28.4502	28.4345	3.13464	3.13633
Au	111	38.1602	38.1234	2.35639	2.35858
Pd	111	40.1478	39.2143	2.24420	2.29545
Au	200	NV <sup>1</sup>	44.4389	-	2.04569
Pd	200	46.7261	45.5688	1.94242	1.98903
Si	220	47.3236	47.2886	1.91928	1.92062
Si	311	56.1404	56.1209	1.63697	1.63749
Au	220	64.6250	64.6530	1.44102	1.44047
Pd	220	68.2698	66.2354	1.37270	1.40984
Si	400	69.1566	69.1196	1.35724	1.35788
Si	331	76.3938	76.3846	1.24567	1.24581
Au	311	77.7708	77.5494	1.22702	1.22997
Pd	311	82.2278	79.5088	1.17143	1.20451
Au	222	NV <sup>1</sup>	81.6568	-	1.17817
Pd	222	86.7300	83.9081	1.12181	1.15219
Si	422	95.2831	94.9562	1.04500	1.04513
Au	400	NV <sup>1</sup>	98.1624	-	1.01938
Pd	400	105.1417	101.5162	0.97000	0.99457
Si	511,333	106.7263	106.7147	0.95943	0.96000
Au	331	NV <sup>1</sup>	110.8738	-	0.91796
Si	440	114.1101	114.0942	0.91788	0.91796
Au	420	NV <sup>1</sup>	115.1428	-	0.91259
Pd	331	115.1842	-	0.91238	-
Pd	420	119.6177	116.7154	0.89116	0.90479
Si	531	128.1328	-	0.85866	-
Si	533	136.8958	-	0.82818	-

<sup>1</sup> NV = not visible. Palladium coating is too thick for this gold peak to be visible

**Table 3 X-ray peak intensities showing variation in preferred orientation of electroless palladium coatings**

<i>hkl</i>	Relative Intensity			Intensity /counts s <sup>-1</sup>	
	JCPDS	pure Pd	Pd-B	pure Pd	Pd-B
111	100	100	29	2115	401
200	42	22	26	466	363
220	25	19	2	405	30
311	24	15	100	306	1378
222	8	4	1	85	12
400	3	1	33	19	457
331	13	5	-	110	-
420	11	0.5	0.5	10	6

## **2.7 LIST OF FIGURES**

Figure 1. Stern model of the electric double layer

Figure 2. Gibbs energy diagram for an ion passing through the electric double layer

Figure 3. An example of a polarisation profile

Figure 4. Schematic representation for potentiodynamic corrosion analysis

Figure 5. Diagram for x-ray diffractometry measurements

Figure 6. The variation in pH during plating for various electroless palladium-boron solutions.

Figure 7. Polarisation profiles observed for various substrates were used in the deposition of electroless palladium-boron coatings. Substrates: Curve 1, gold; Curve 2, stainless steel; Curve 3 nickel on stainless steel

Figure 8. Polarisation profiles for electroless palladium-boron coatings of various thickness. Curve 1, 0.8  $\mu\text{m}$ ; Curve 2, 2.3  $\mu\text{m}$ ; Curve 3, 1  $\mu\text{m}$

Figure 9. Polarisation profiles for pure electroless palladium coatings of various thickness. Curve 1, 1.0  $\mu\text{m}$ ; Curve 2, 4.3  $\mu\text{m}$ ; Curve 3, 4.1  $\mu\text{m}$ ; Curve 4, 2.8  $\mu\text{m}$

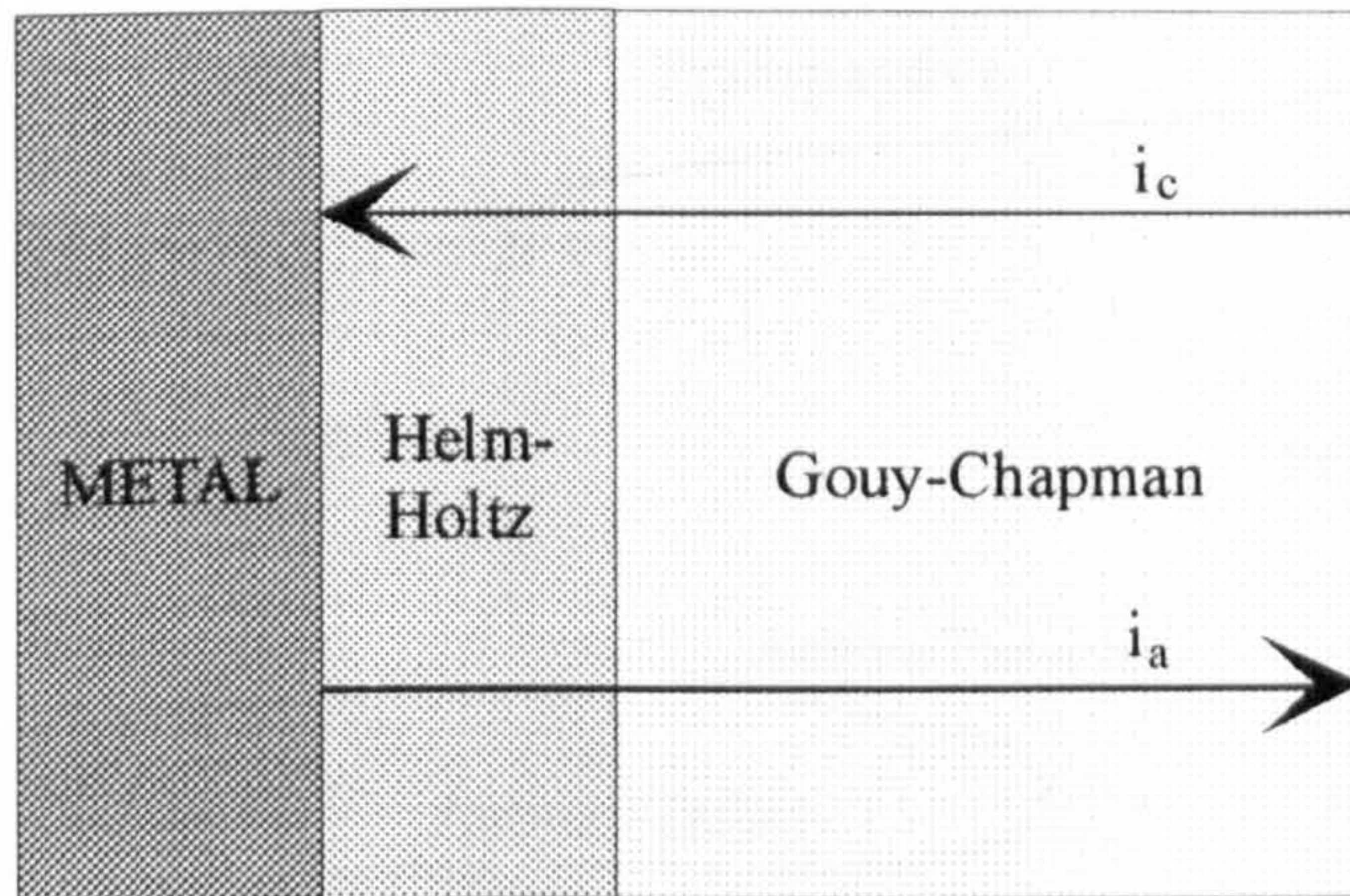
Figure 10. X-ray diffraction pattern for pure electroless palladium coatings

Figure 11. X-ray diffraction pattern for electroless palladium-boron coatings

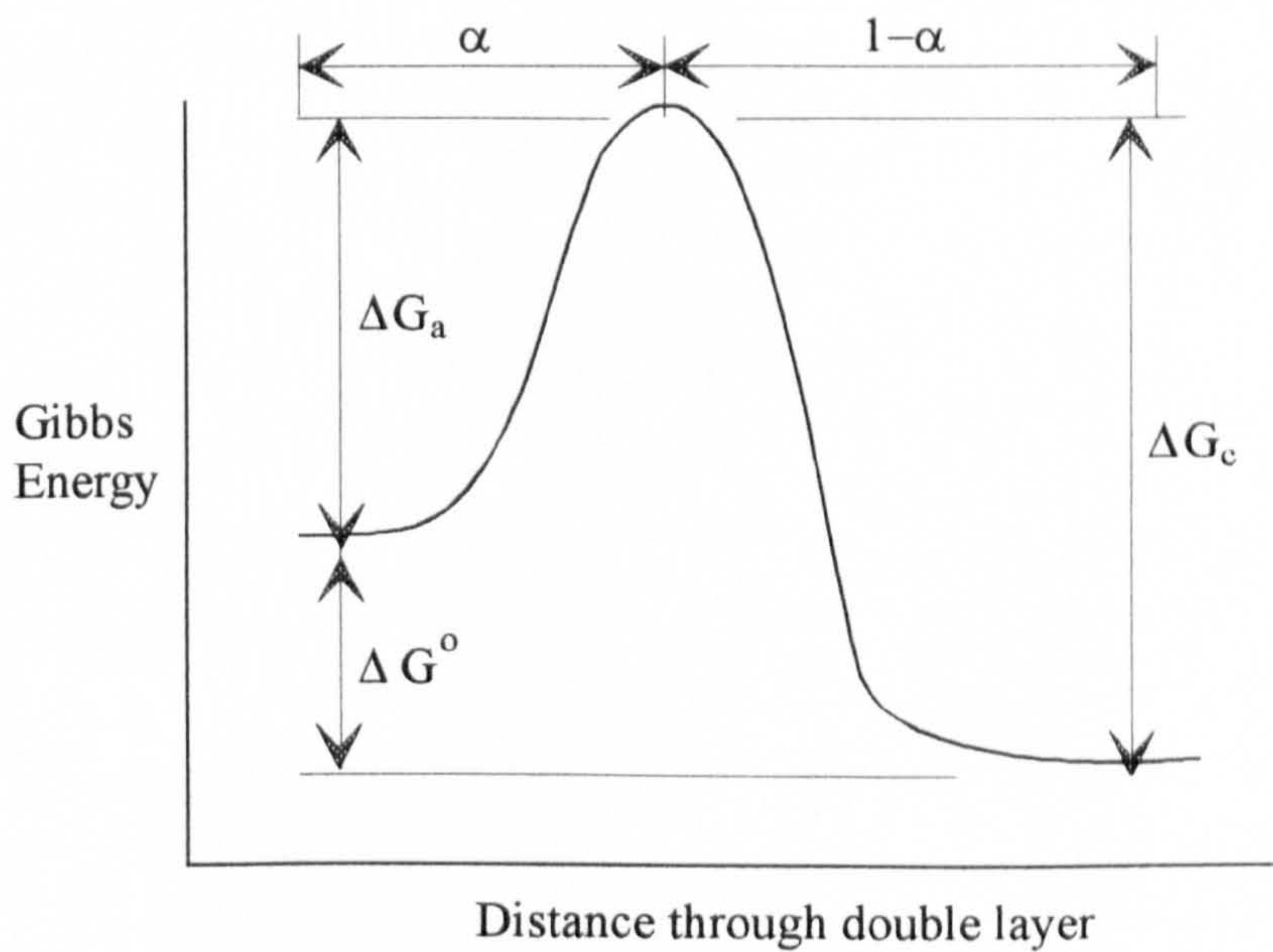
Figure 12. Nelson-Riley plots for silicon powder on (a) palladium and (b) palladium-boron coatings, and plots for (c) pure palladium and (d) palladium-boron coatings

Figure 13. Scanning electron micrographs of electroless palladium-boron coatings. (a) 0.3  $\mu\text{m}$  and (b) 1.5  $\mu\text{m}$  on stainless steel, (c) 2.0  $\mu\text{m}$  and (d) 2.7  $\mu\text{m}$  on nickel on stainless steel, and (e) 0.7  $\mu\text{m}$  on gold

**Figure 1. Stern model of electric double layer**



**Figure 2. Gibbs energy diagram for an ion passing through the electric double layer**





**Figure 3. An example of a polarisation profile**

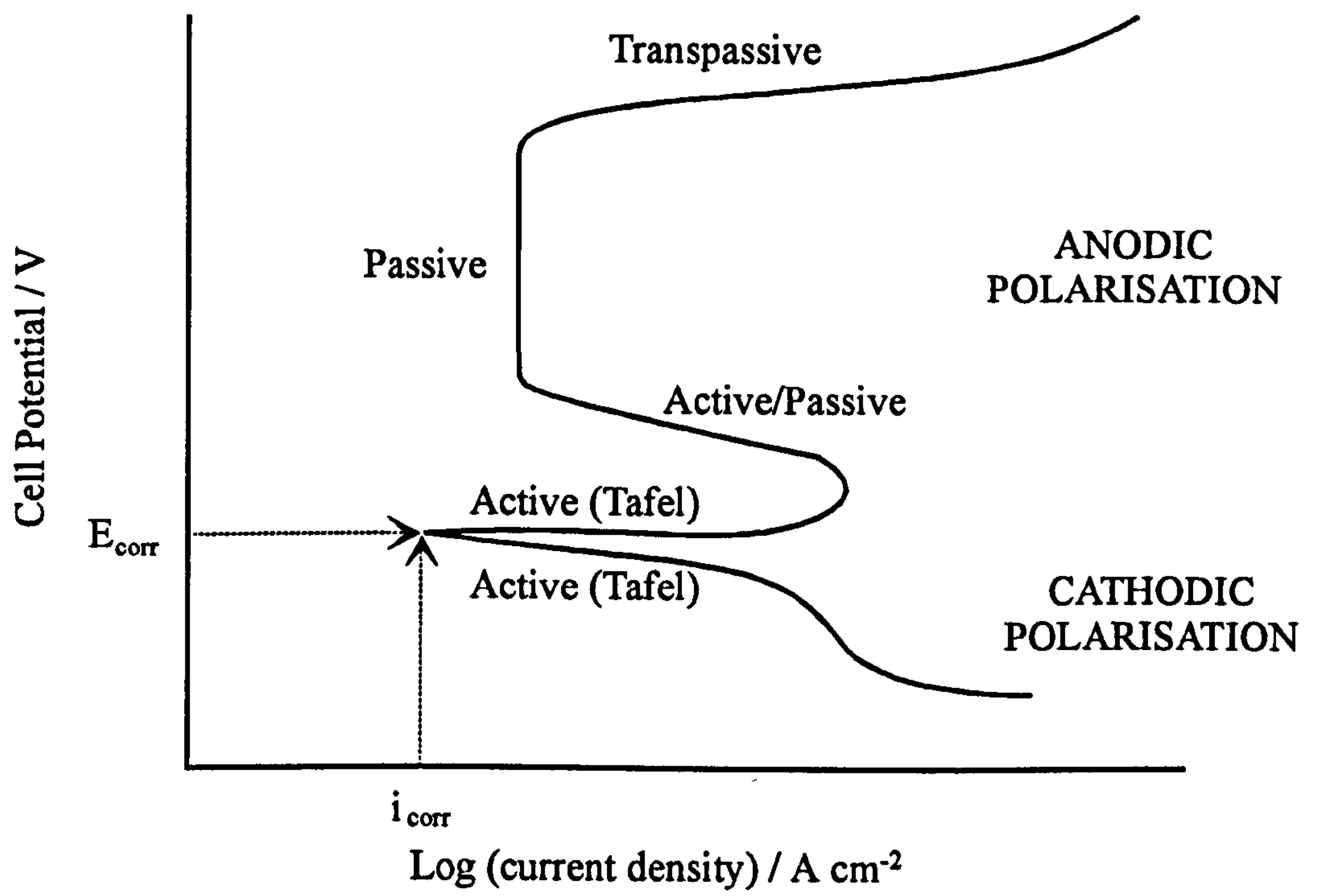
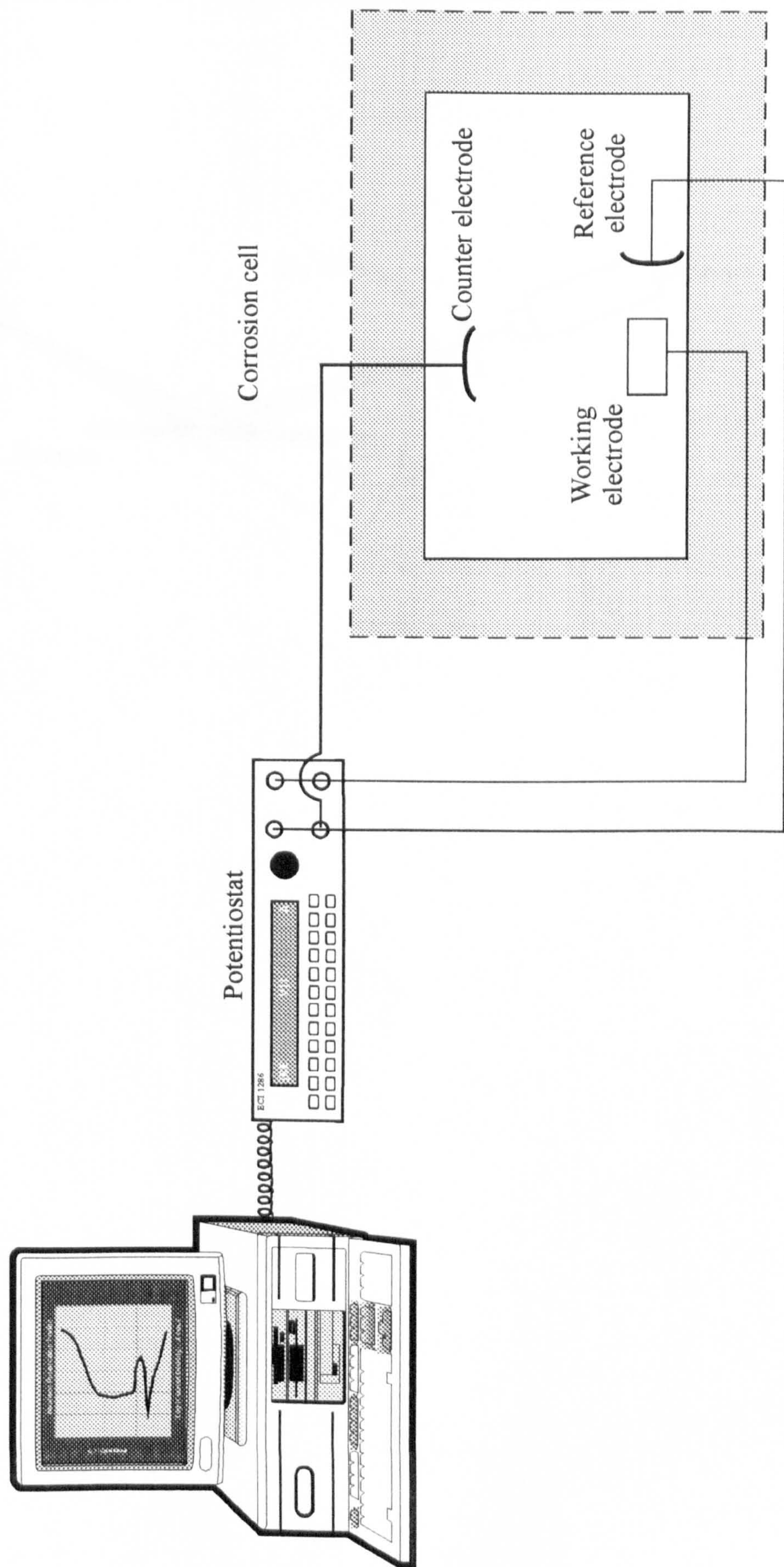
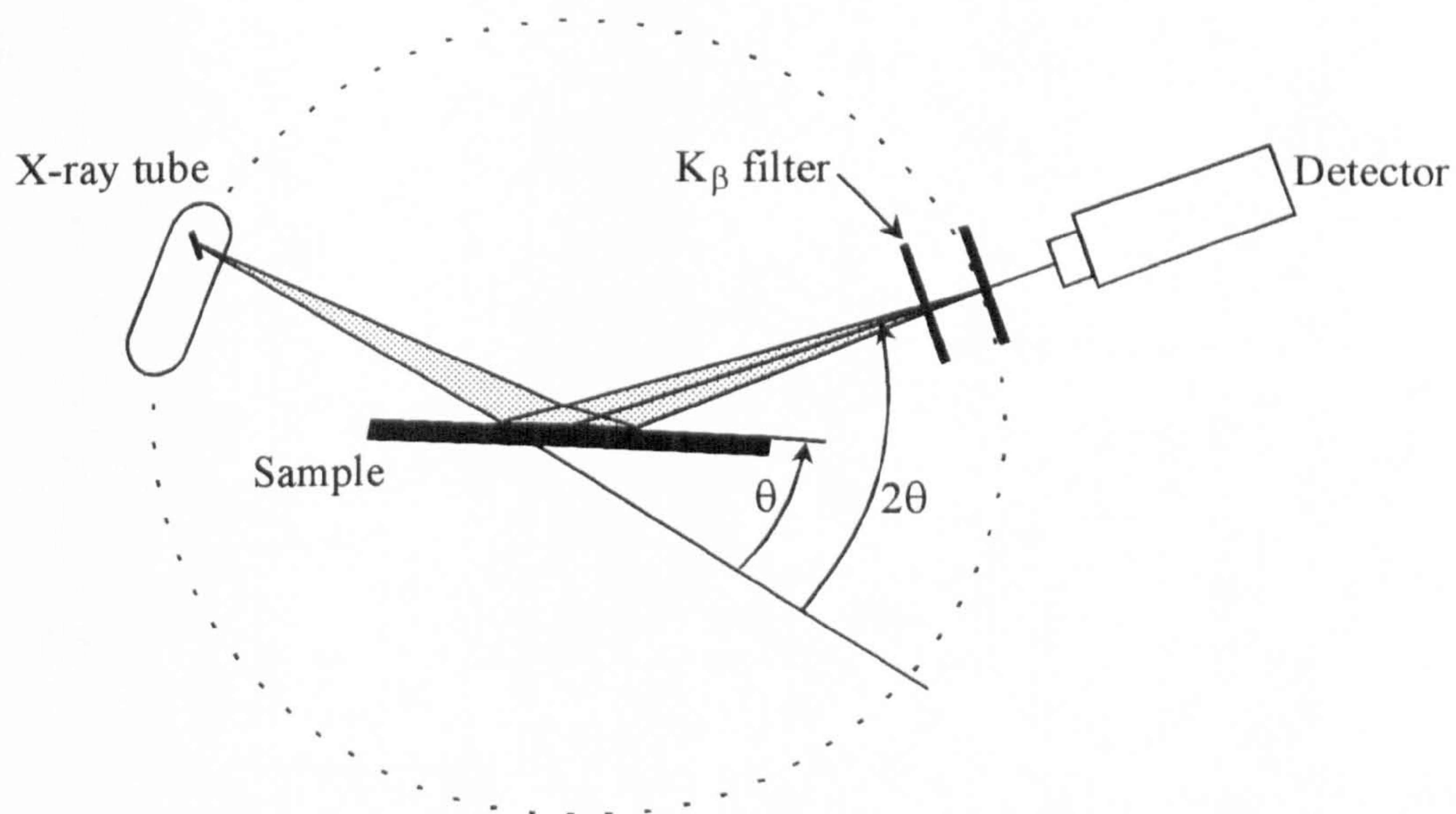


Figure 4. Schematic representation for potentiodynamic corrosion analysis



**Figure 5. Diagram for x-ray diffractometry measurements**



**Figure 6. The variation in pH during plating for various electroless palladium-boron solutions. Plating solution composition: Pd<sup>2+</sup>, 0.012 g; EDTA, 0.175 g (Curves 5 and 6, 0.199 g); NH<sub>4</sub>Cl, 1.6 g (Curve 4, 2.0 g); boric acid, 0.025 g, and Curve 6, 0.40 g, only; DMAB, 0.02 g (Curve 4, 0.03 g)**

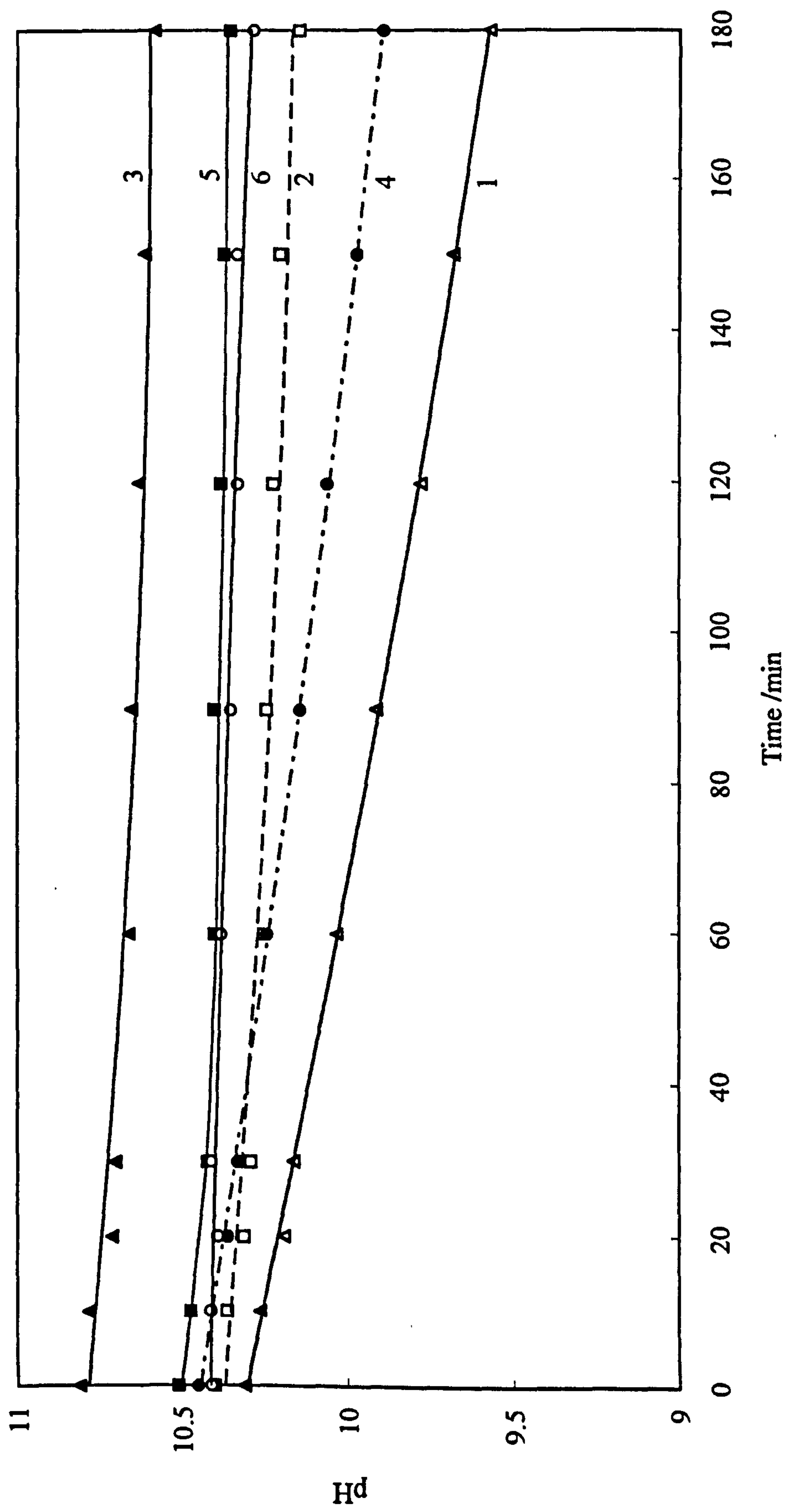


Figure 7. Polarisation profiles observed when various substrates were used in the deposition of electroless palladium-boron coatings. Substrates: Curve 1, gold; Curve 2, stainless steel; Curve 3, nickel on stainless steel

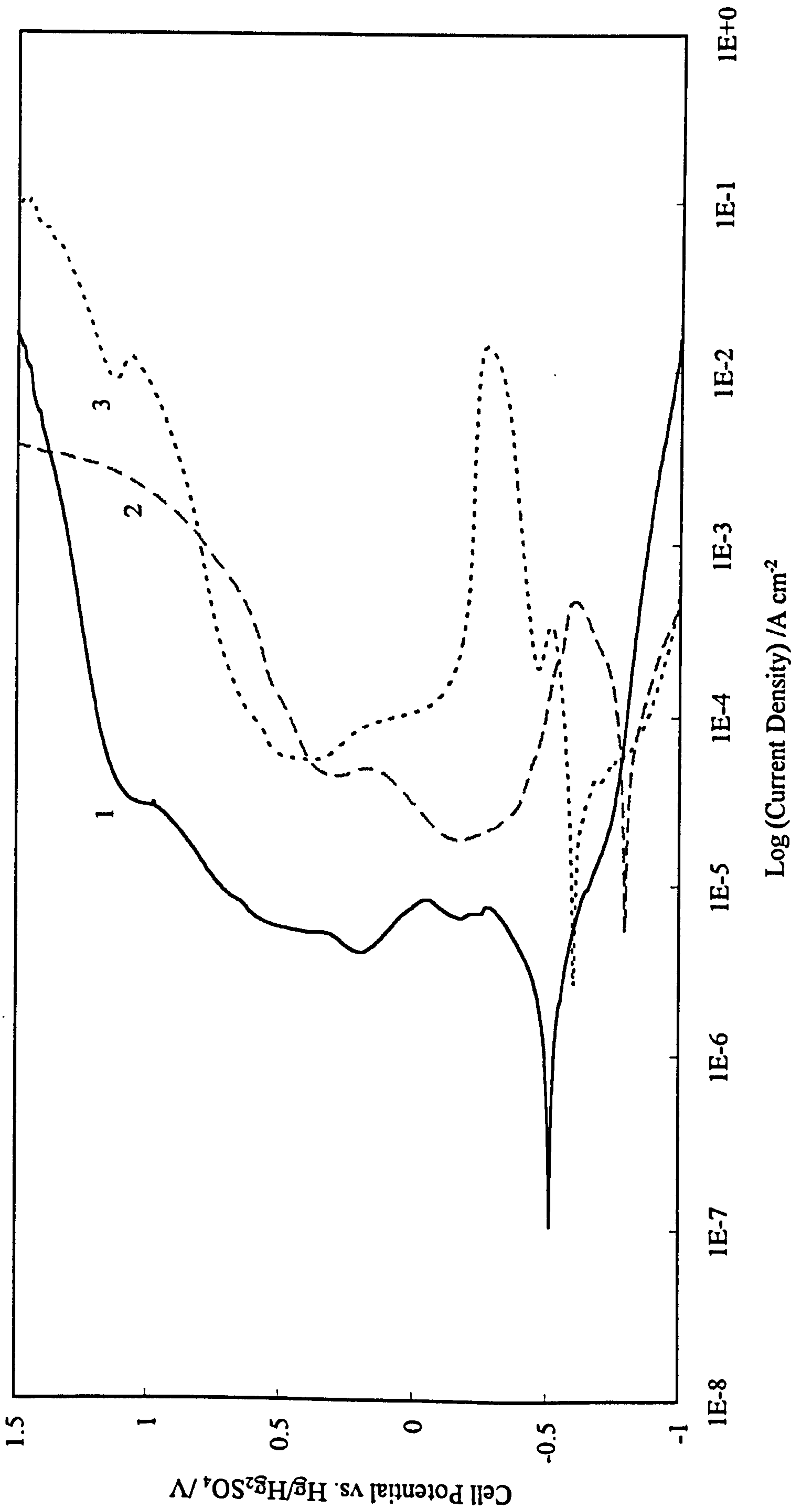


Figure 8. Polarisation profiles for electroless palladium-boron coatings of various thickness. Curve 1, 0.8  $\mu\text{m}$ ; Curve 2, 2.3  $\mu\text{m}$ ; Curve 3, 1.0  $\mu\text{m}$

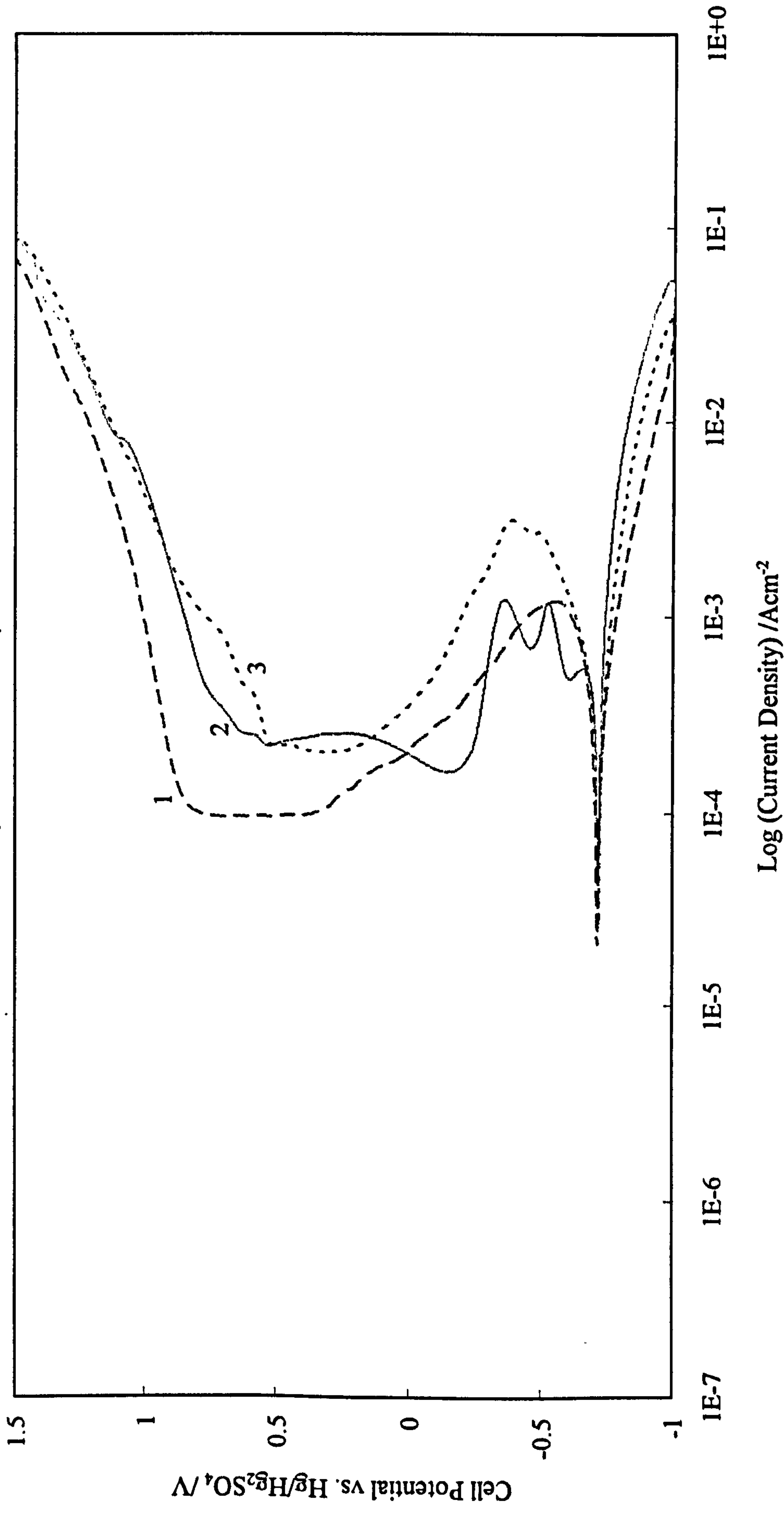
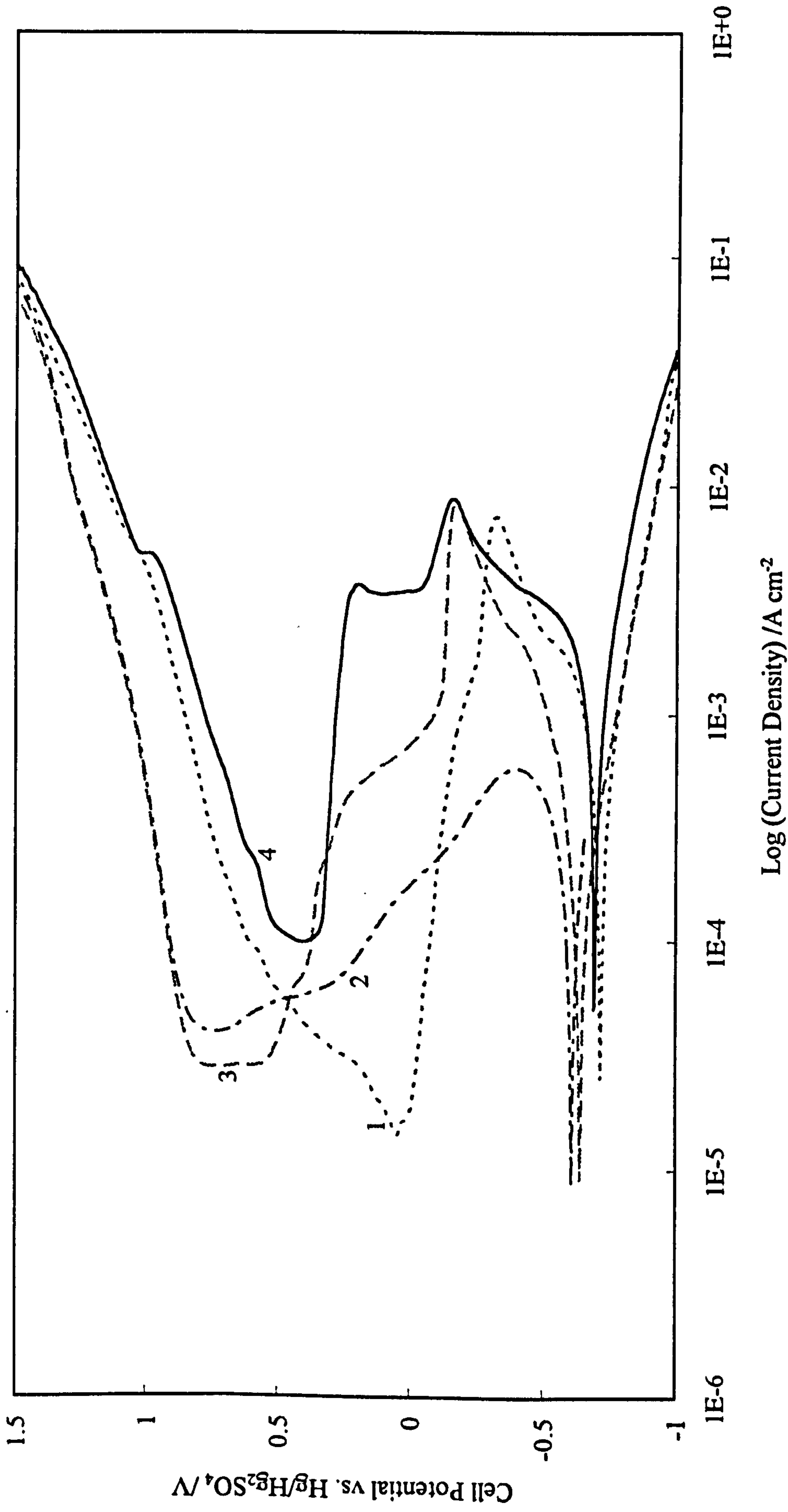


Figure 9. Polarisation profiles for pure electroless palladium coatings of various thickness. Curve 1, 1.0  $\mu\text{m}$ ; Curve 2, 4.3  $\mu\text{m}$ ; Curve 3, 4.1  $\mu\text{m}$ ; Curve 4, 2.8  $\mu\text{m}$



**Figure 10(a). X-ray diffraction pattern for electroless palladium coatings**

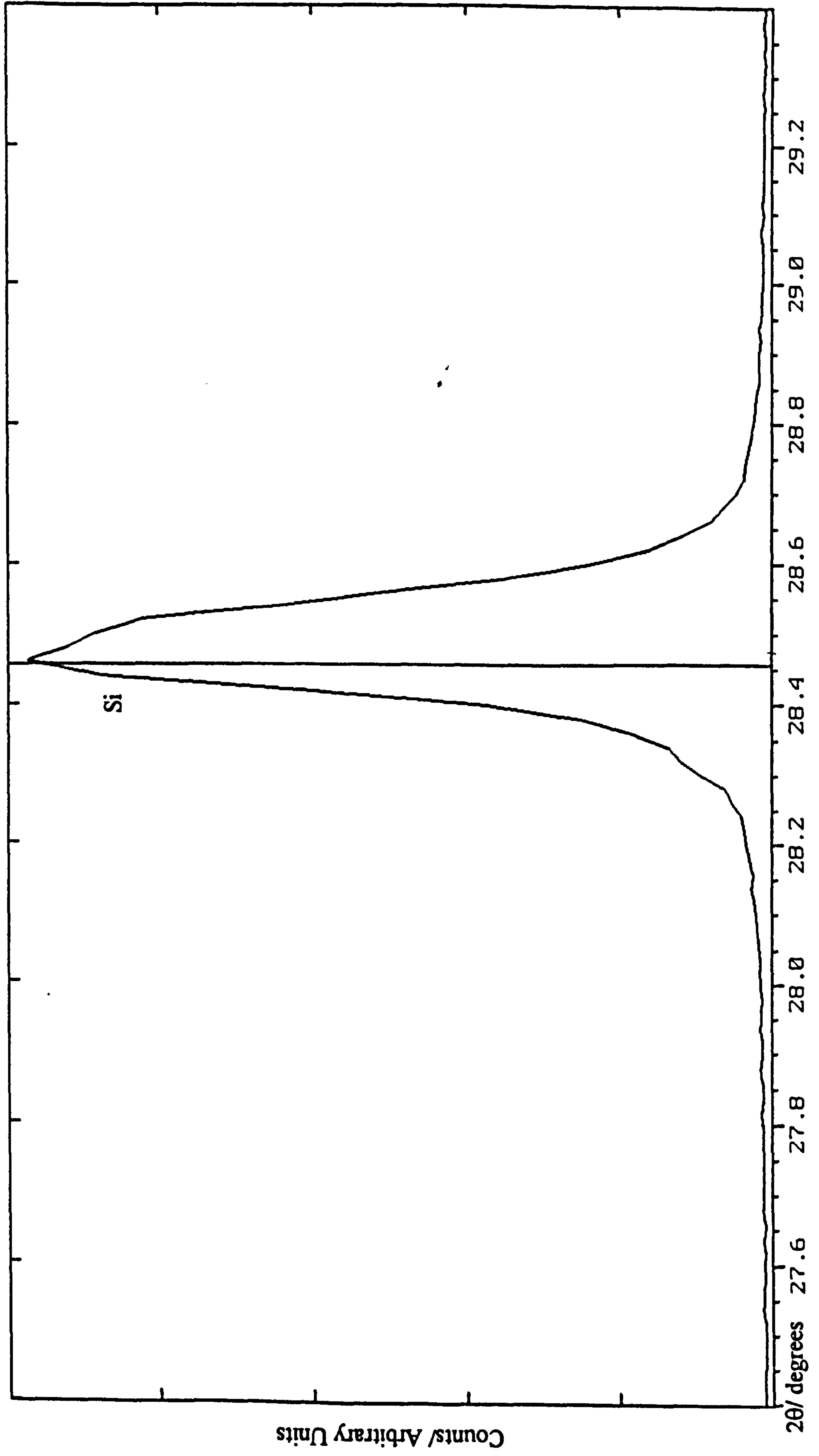
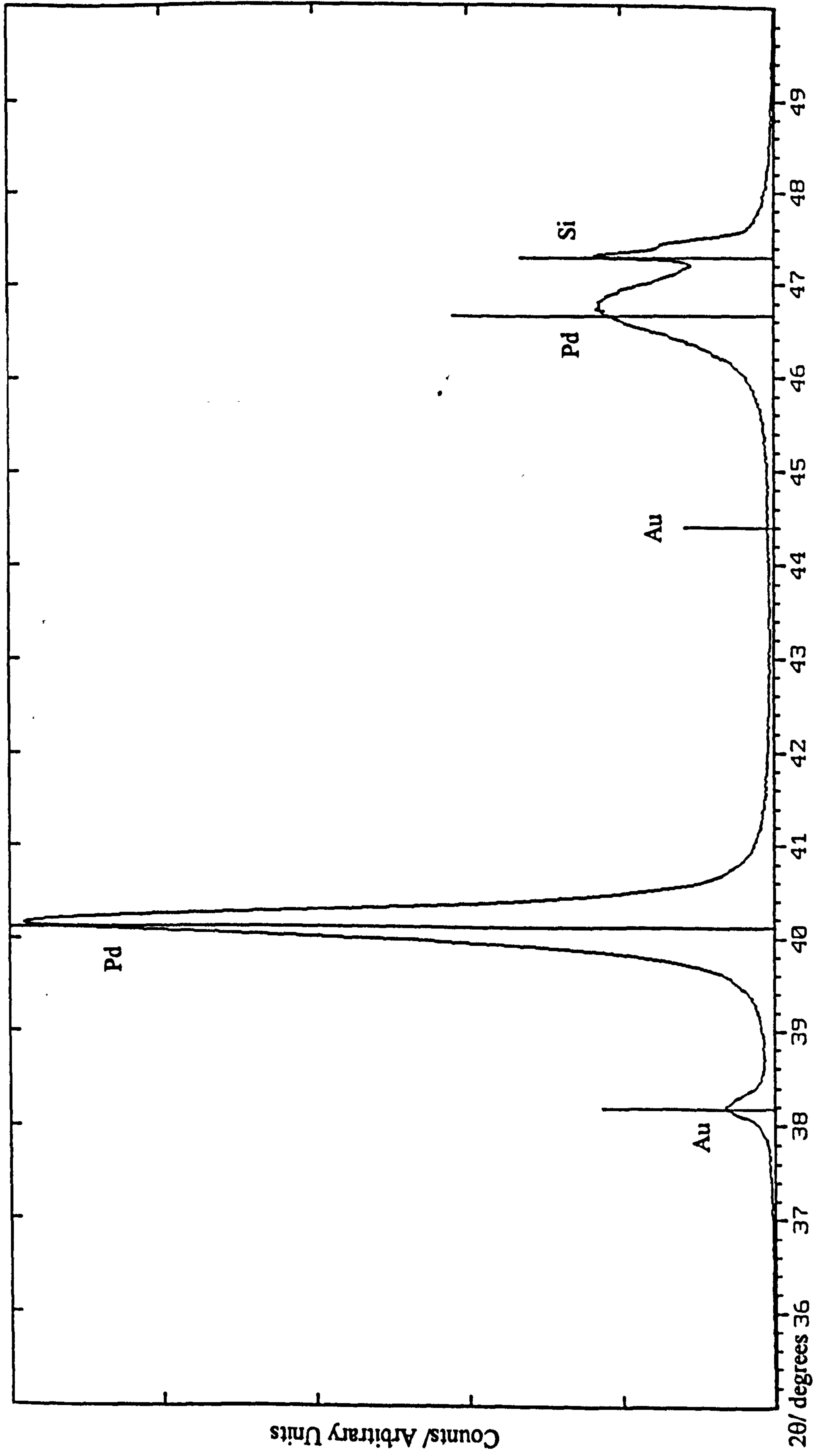




Figure 10(b). X-ray diffraction pattern for electroless palladium coatings



**Figure 10(c). X-ray diffraction pattern for electroless palladium coatings**

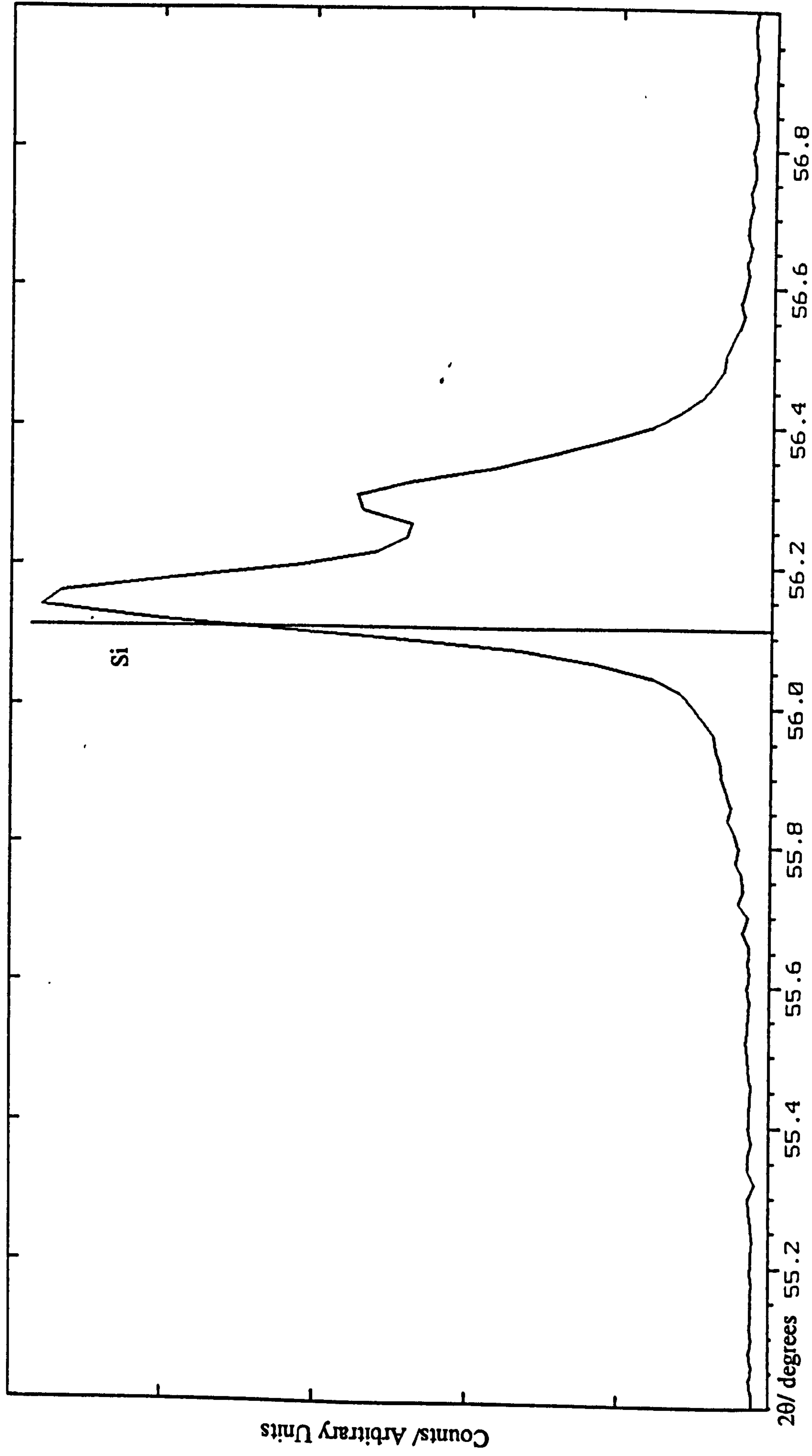


Figure 10(d). X-ray diffraction pattern for electroless palladium coatings

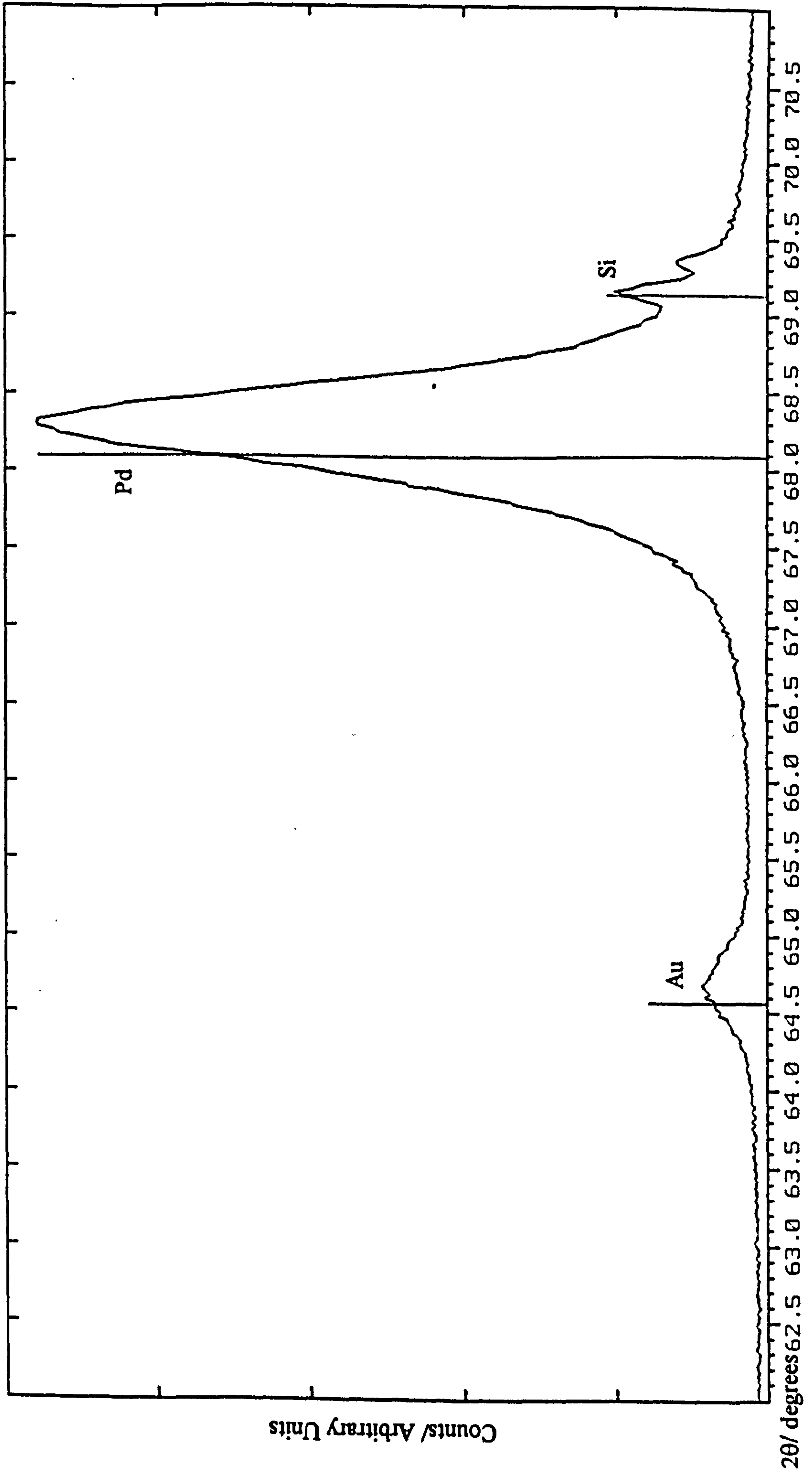


Figure 10(e). X-ray diffraction pattern for electroless palladium coatings

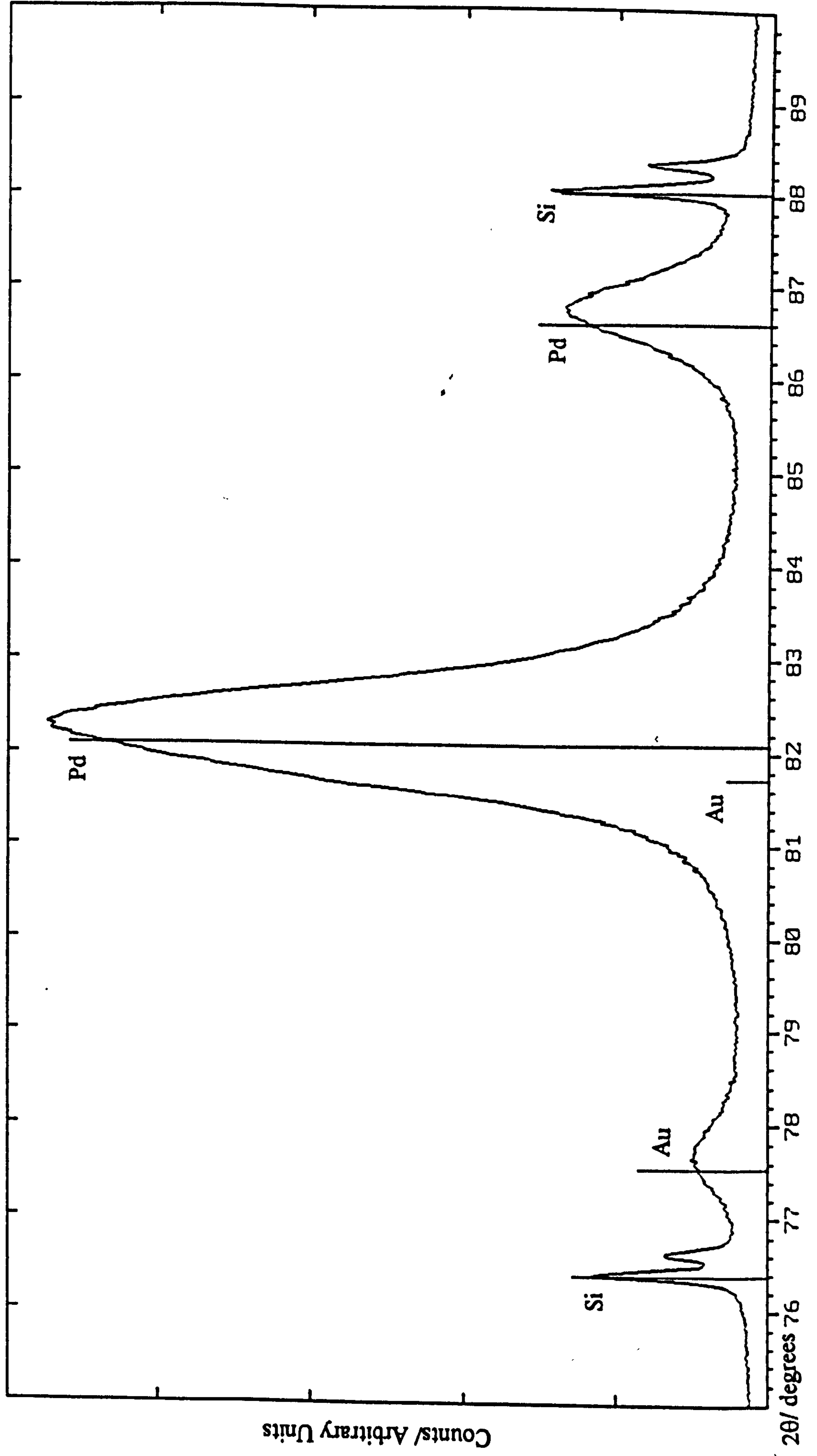


Figure 10(f). X-ray diffraction pattern for electroless palladium coatings

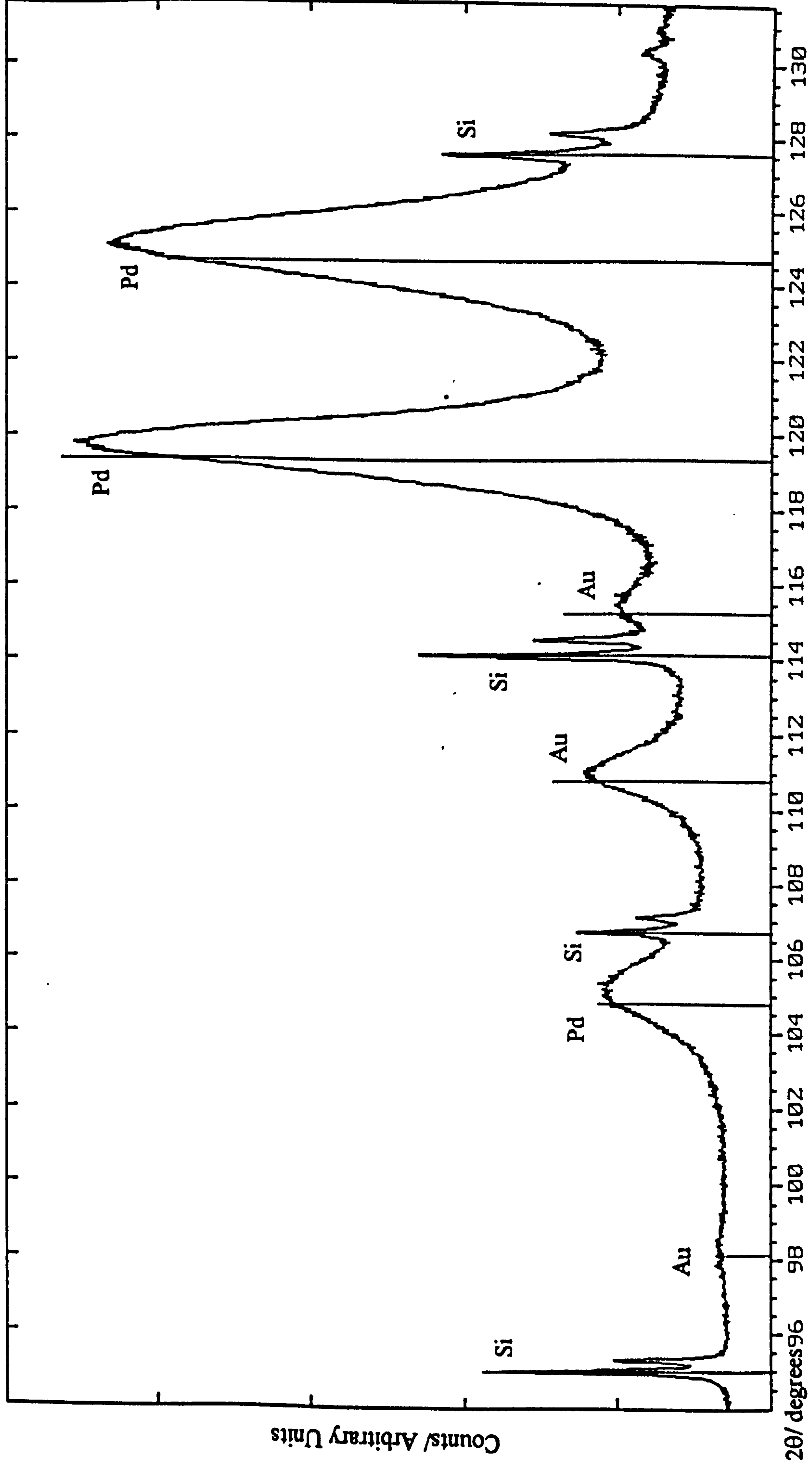


Figure 11(a). X-ray diffraction pattern for electroless palladium-boron coatings

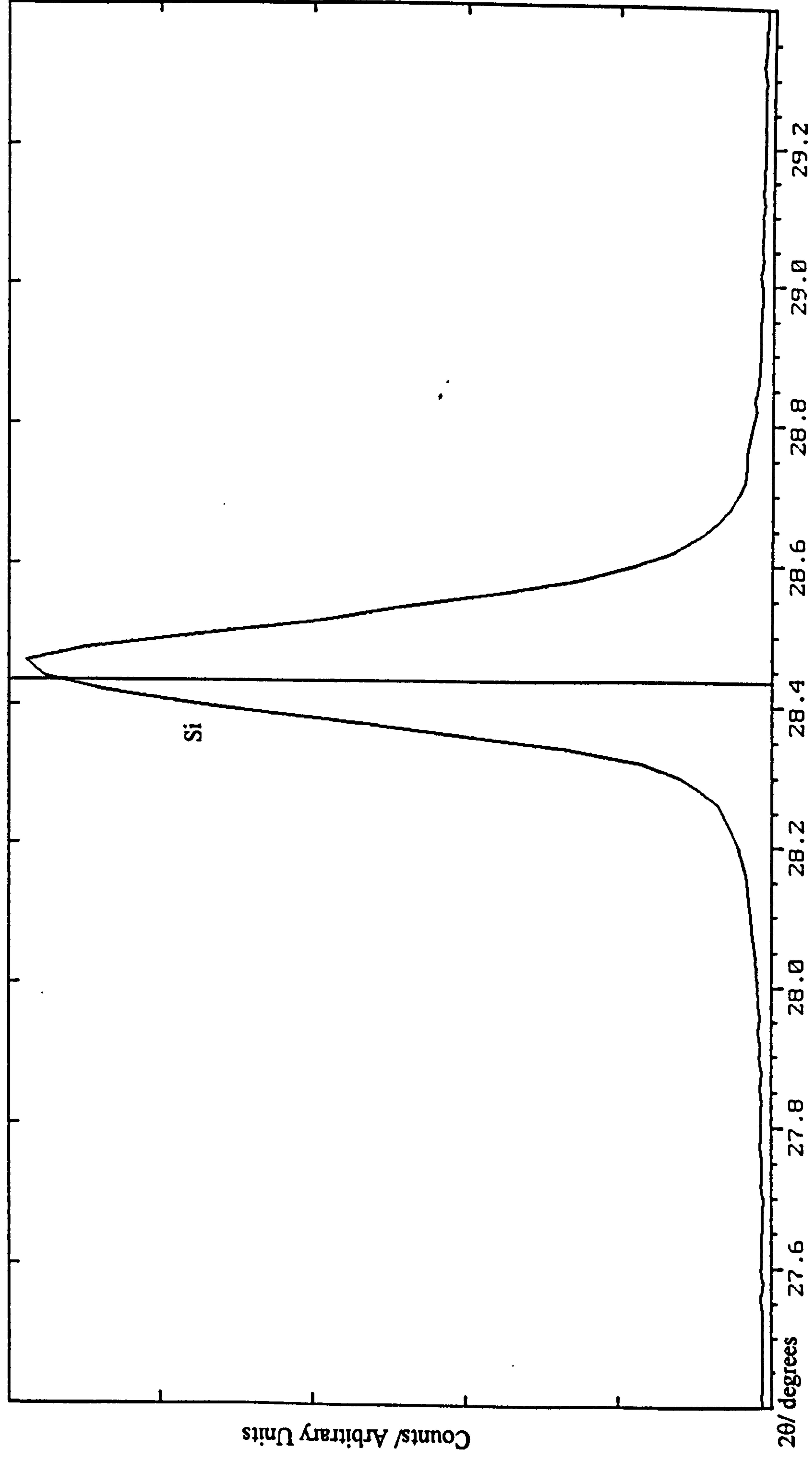


Figure 11(b). X-ray diffraction pattern for electroless palladium-boron coatings

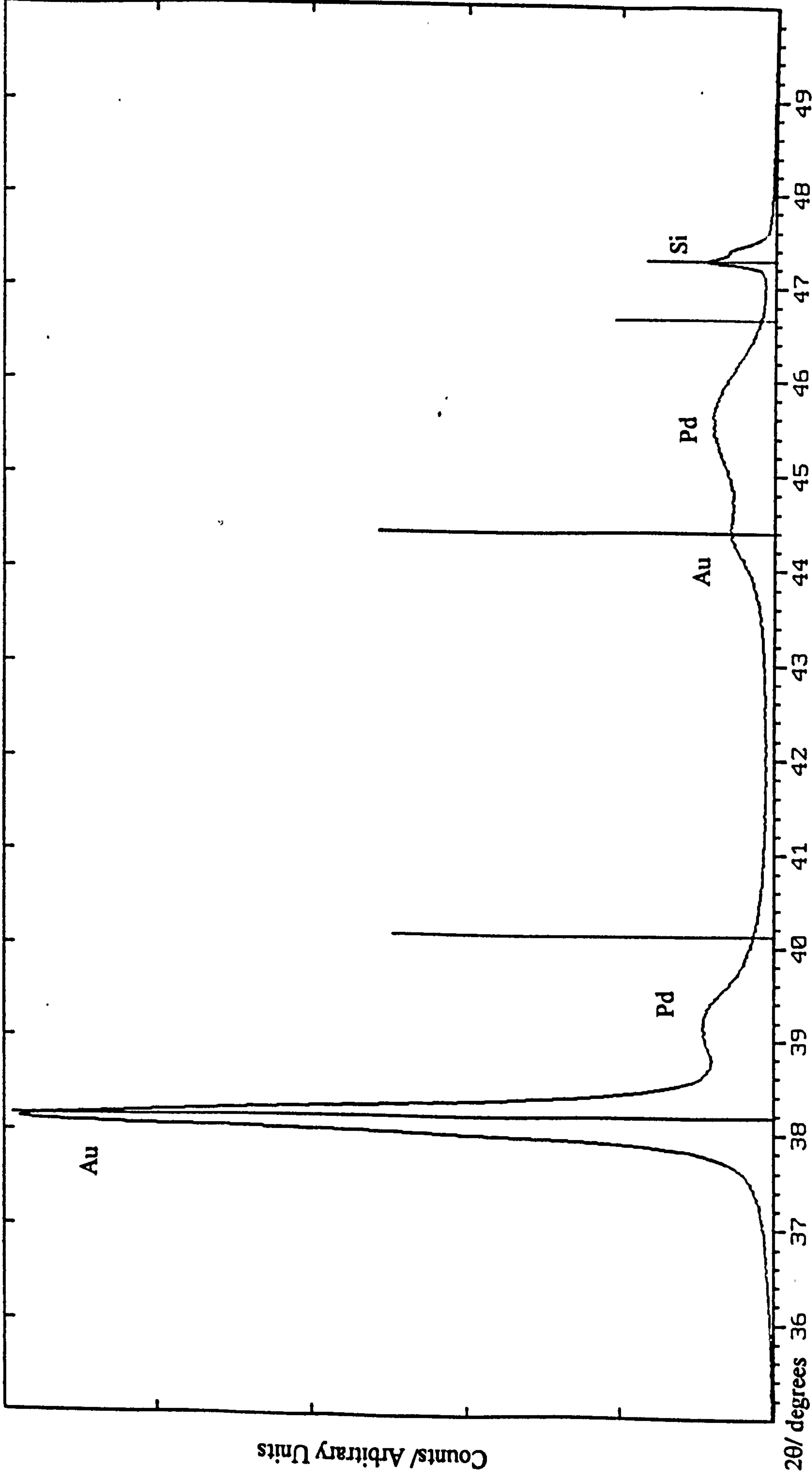


Figure 11(c). X-ray diffraction pattern for electroless palladium-boron coatings

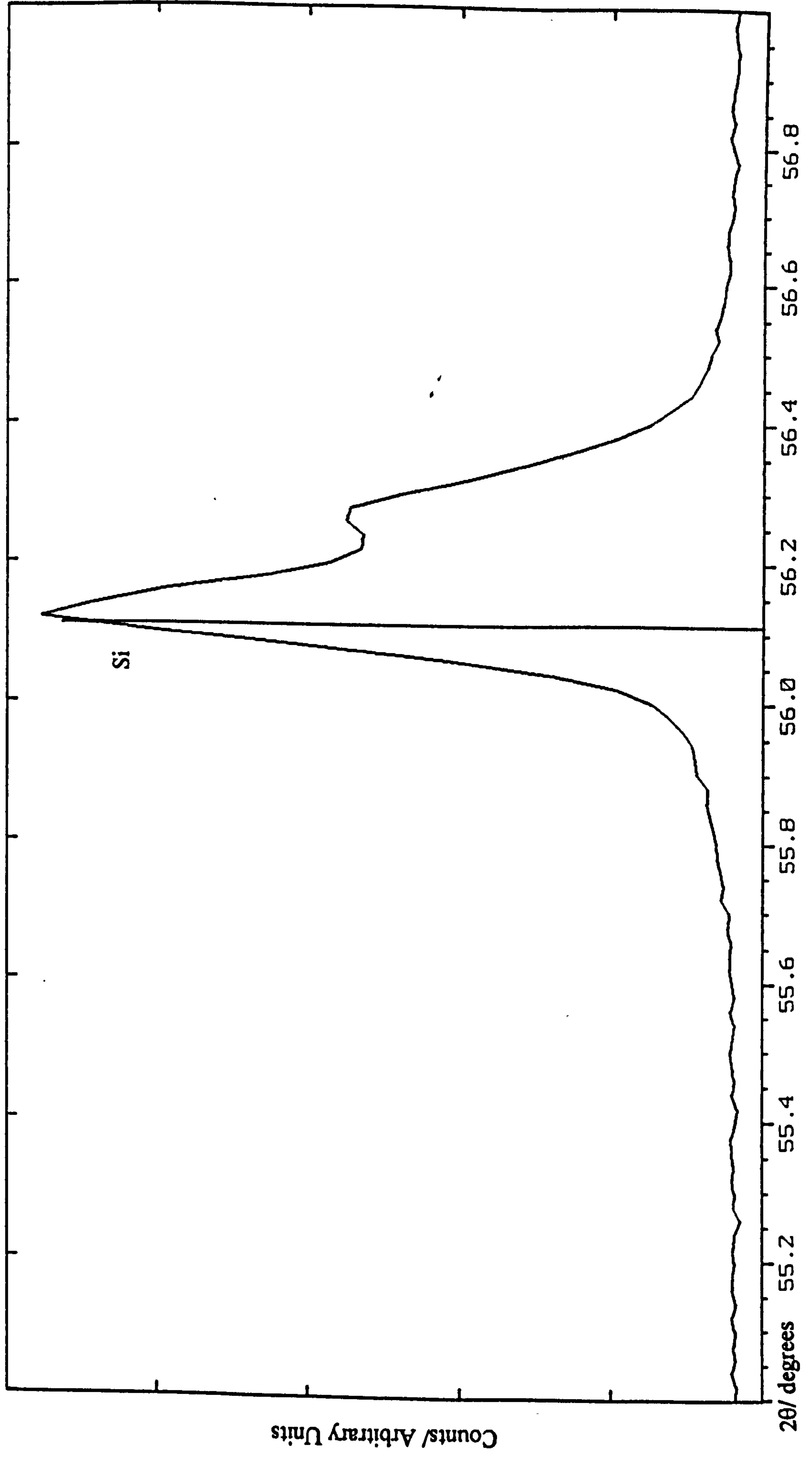




Figure 11(d). X-ray diffraction pattern for electroless palladium-boron coatings

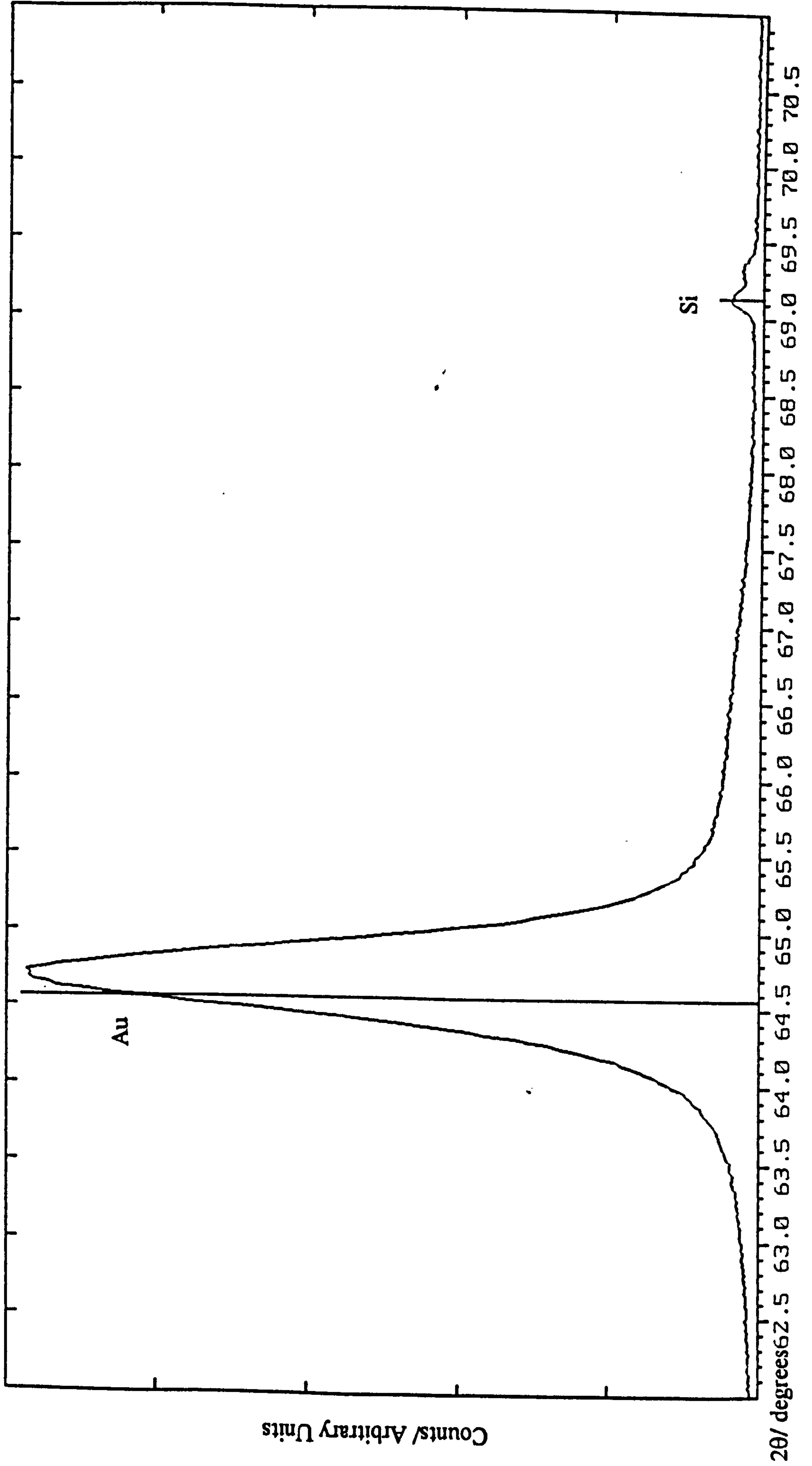


Figure 11(e). X-ray diffraction pattern for electroless palladium-boron coatings

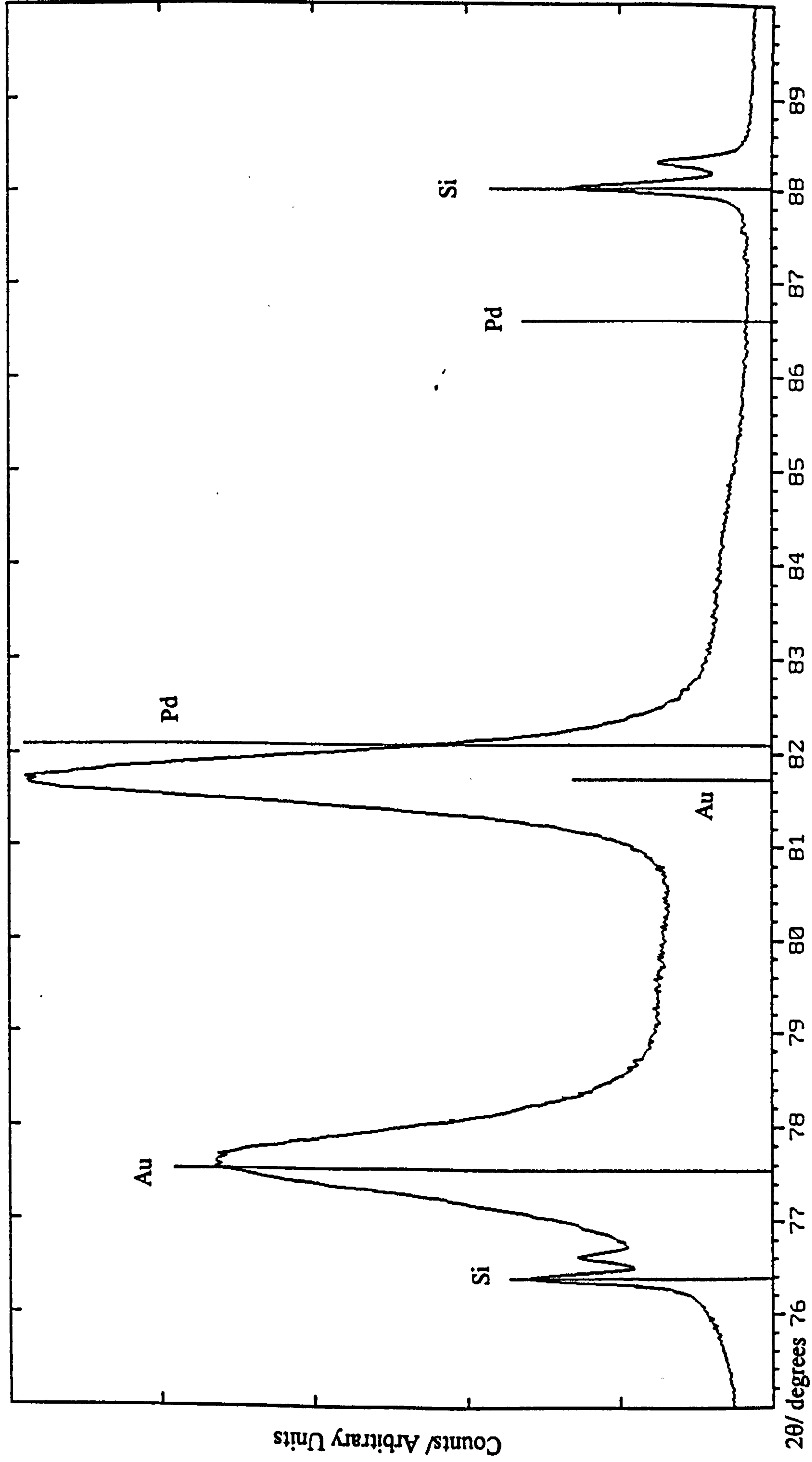


Figure 11(f). X-ray diffraction pattern for electroless palladium-boron coatings

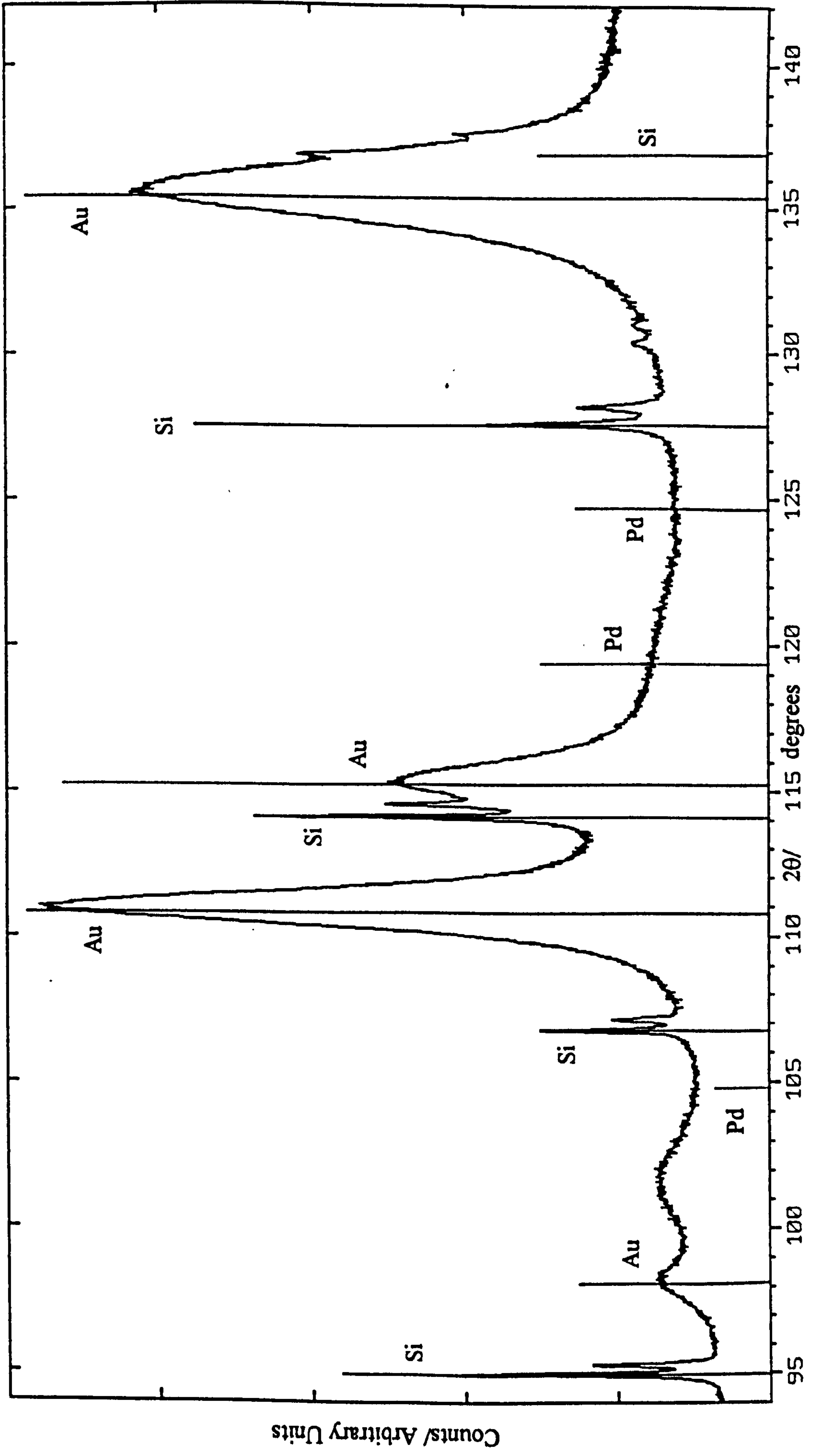
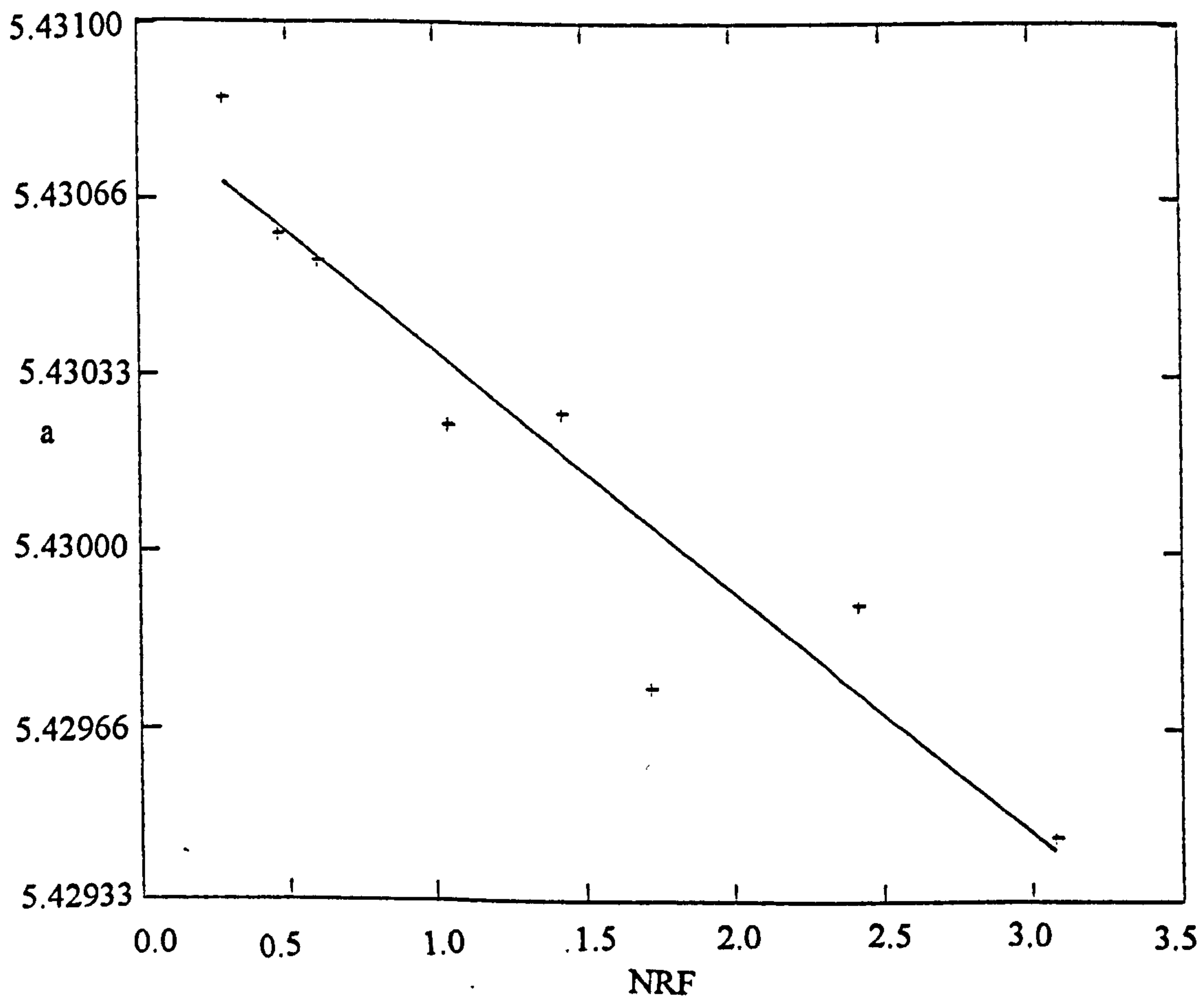
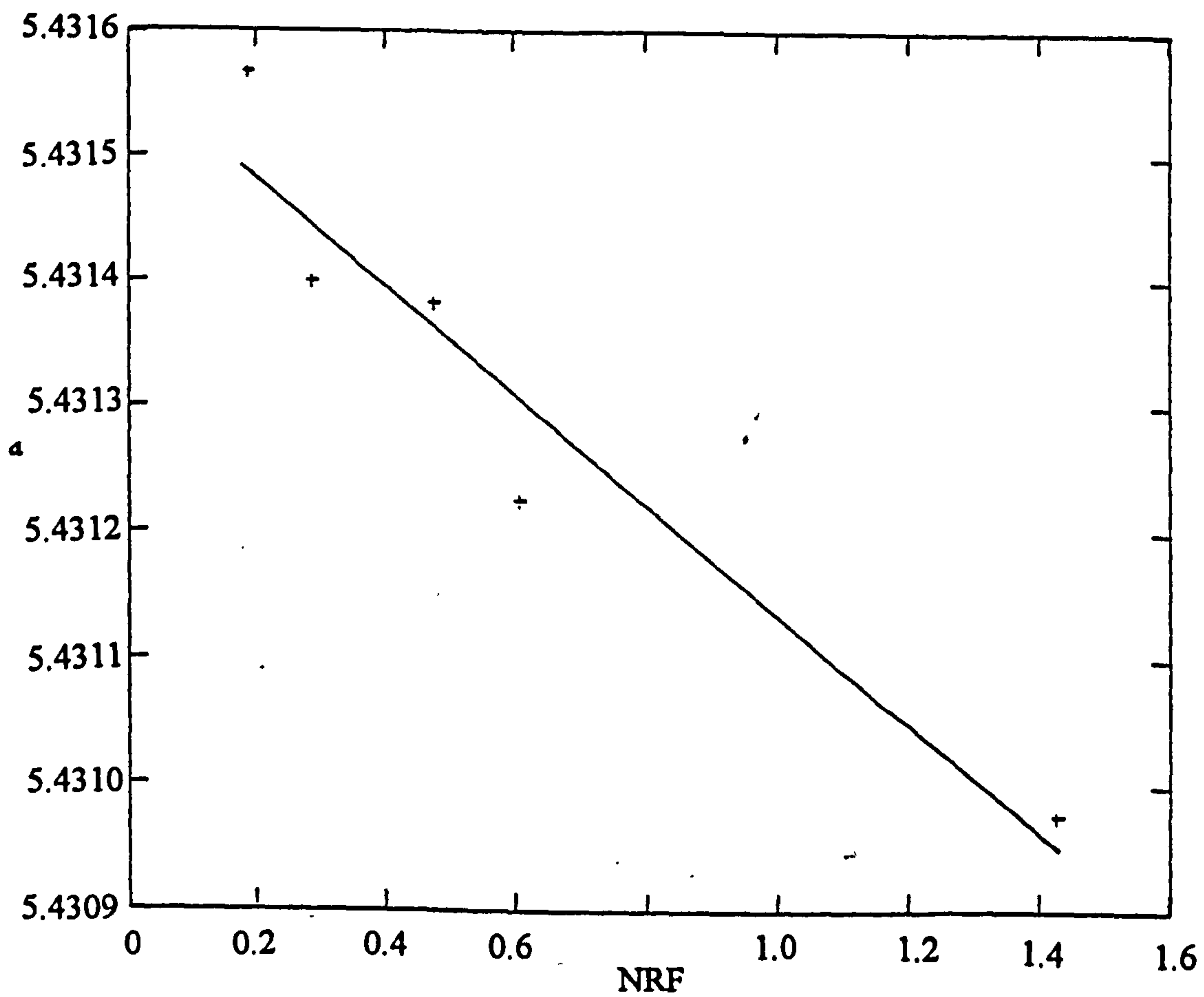


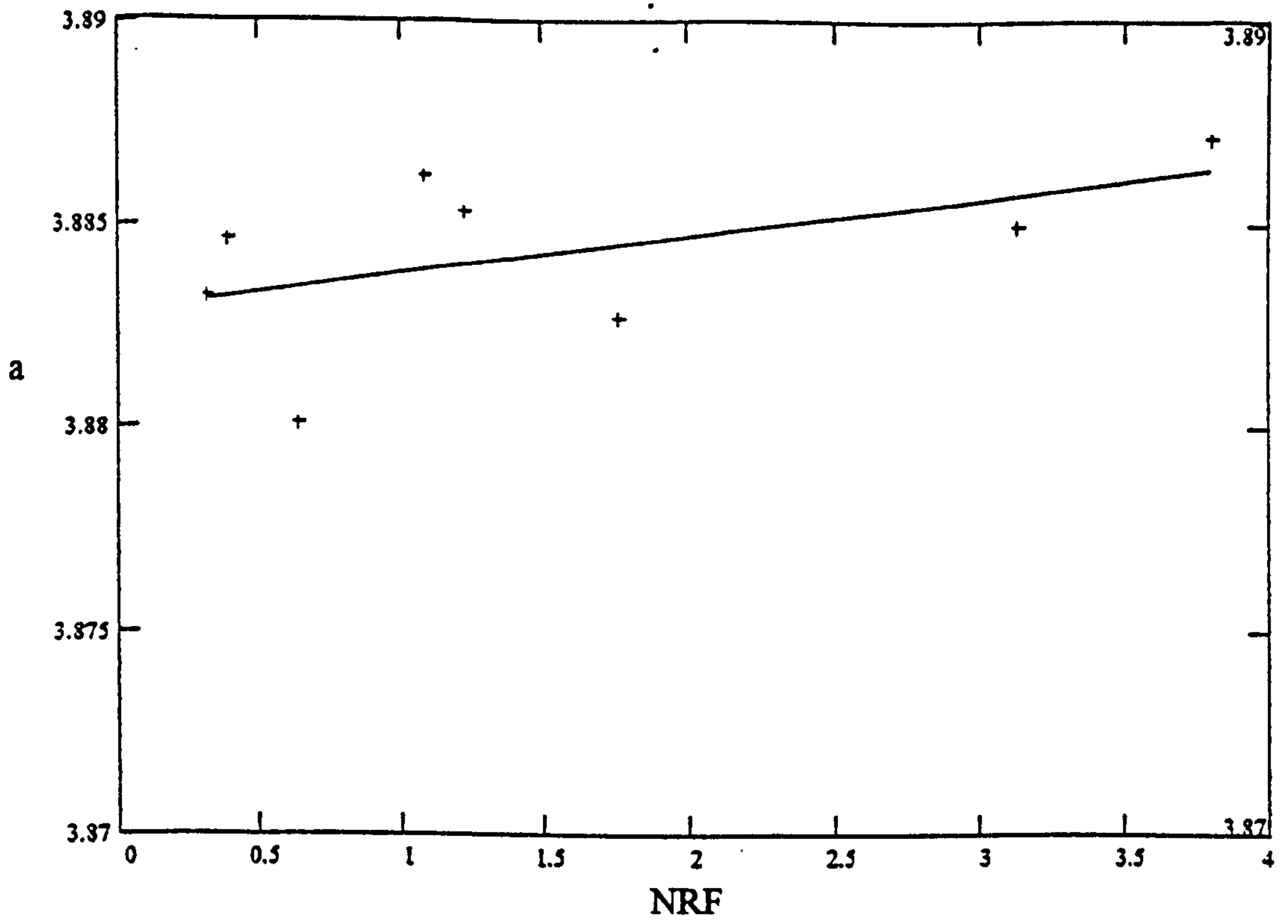
Figure 12. Nelson-Riley plots for electroless palladium coatings



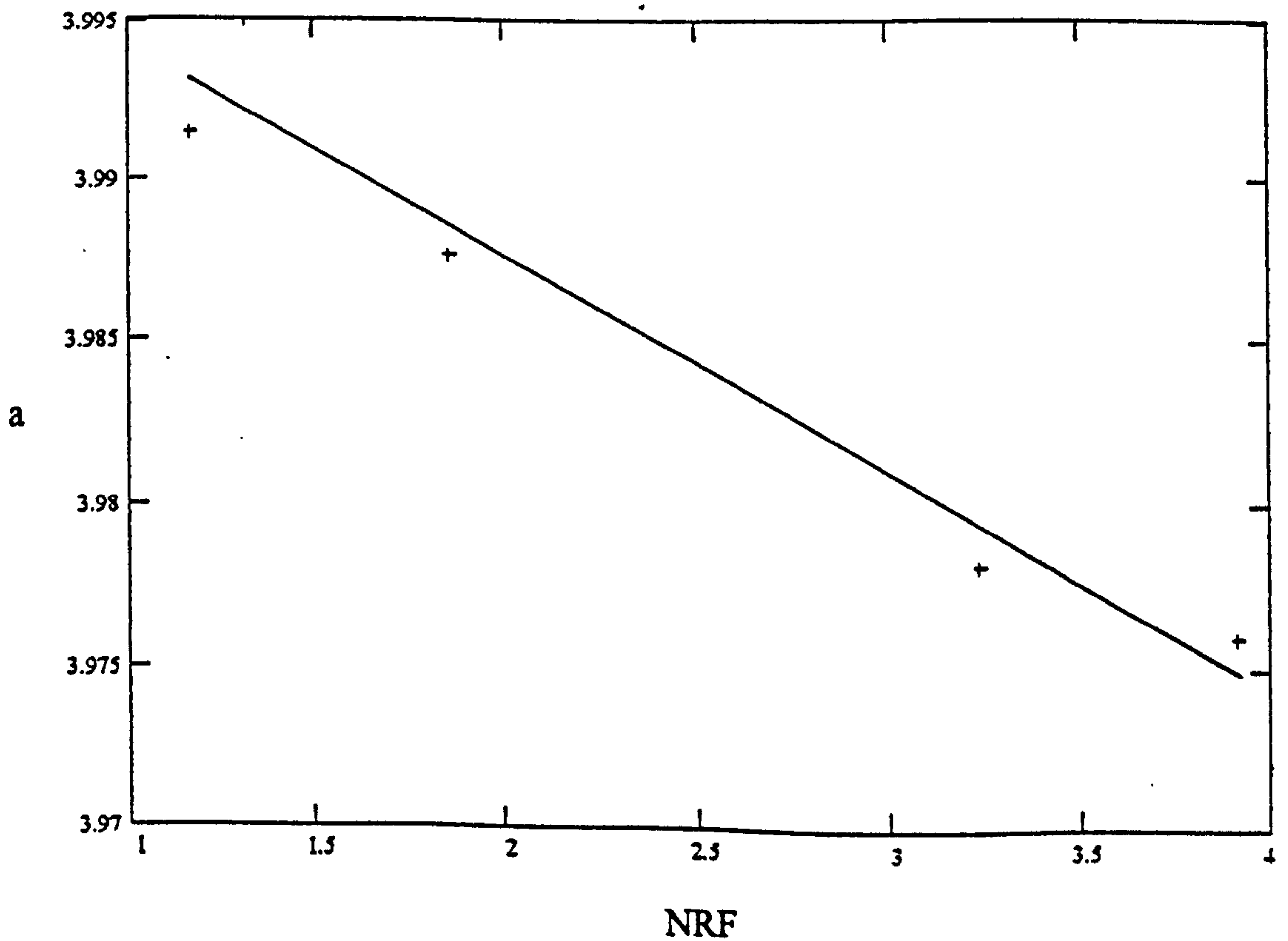
12(a) Nelson-Riley plot for silicon powder on pure electroless palladium coating



12(b) Nelson-Riley plot for silicon powder on electroless palladium-boron coating



12(c) Nelson-Riley plot for pure electroless palladium coating



12(d) Nelson-Riley plot for electroless palladium-boron coating

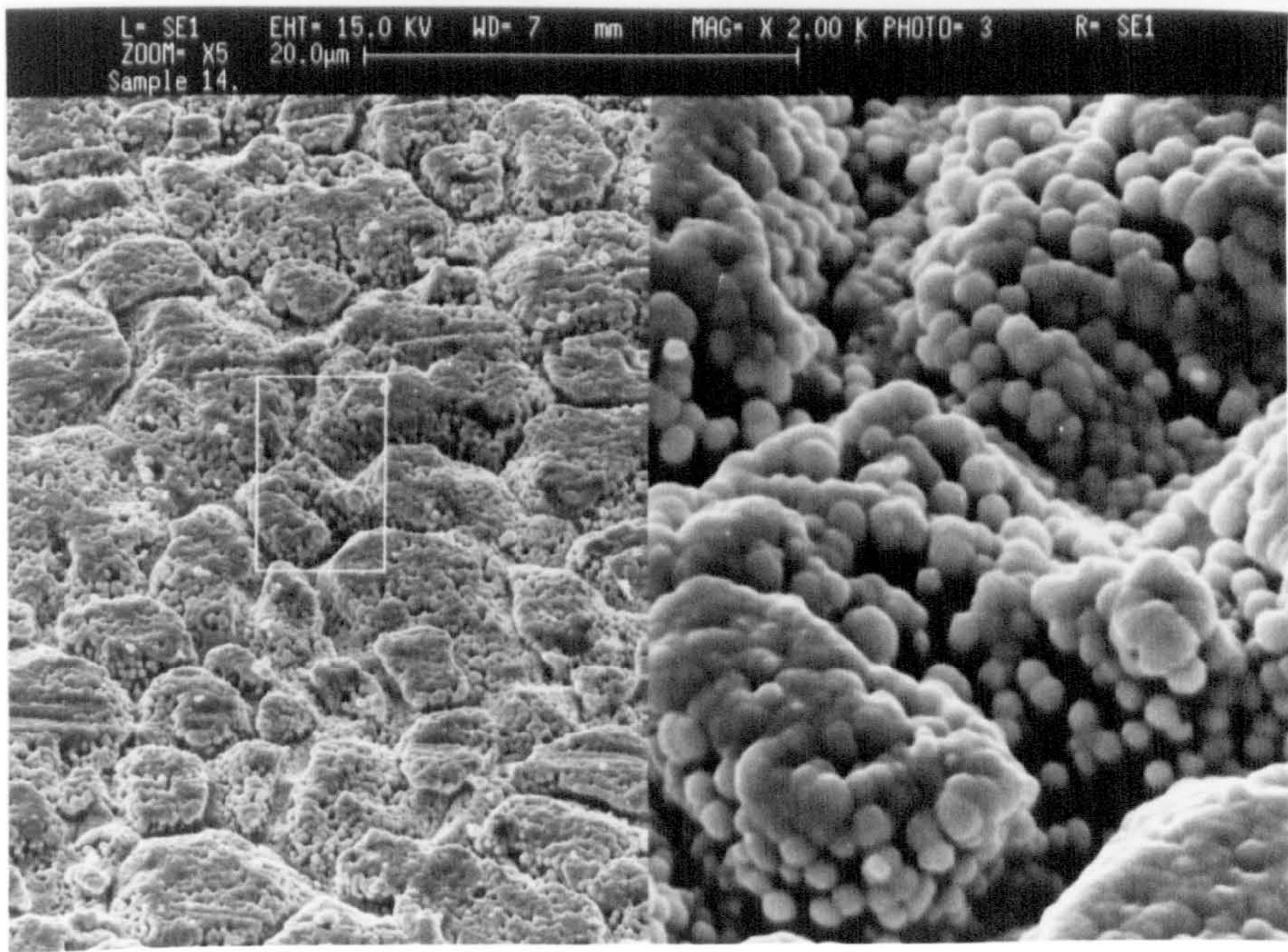


**Figure 13(a). Scanning electron micrograph of 0.3 μm electroless Pd-B on stainless steel**

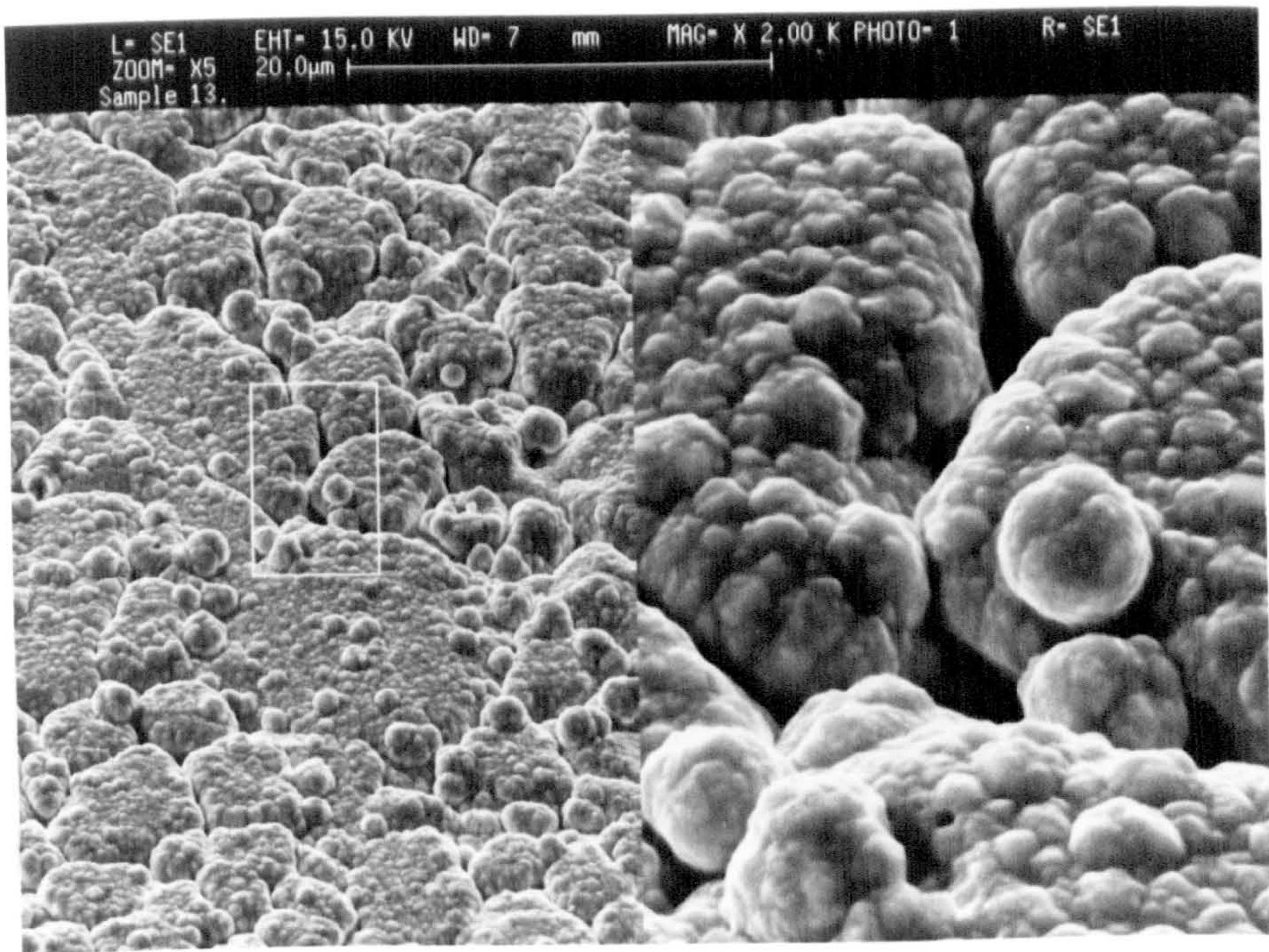


**Figure 13(b). Scanning electron micrograph of 1.5 μm electroless Pd-B on stainless steel**

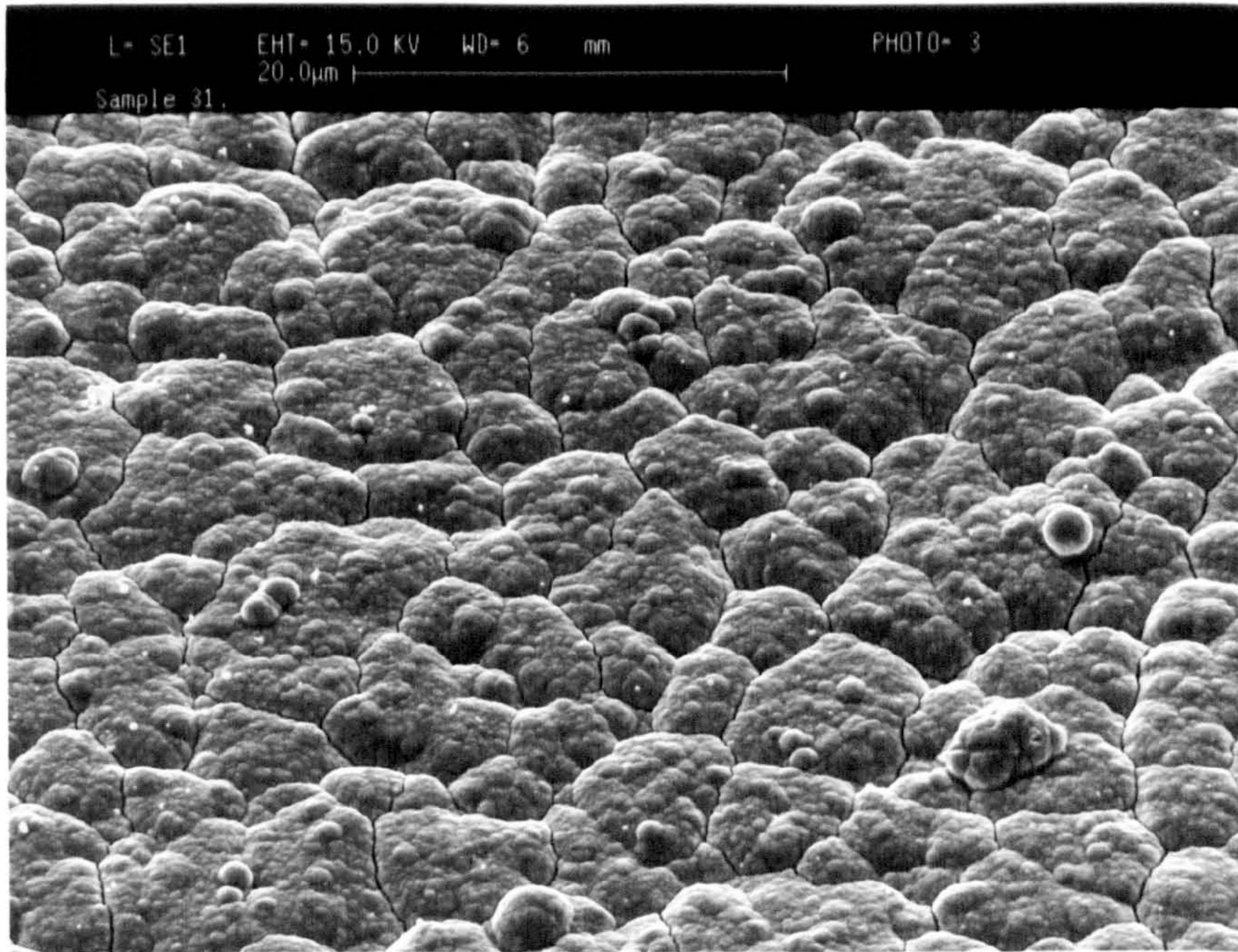


**Figure 13(c). Scanning electron micrograph of 2.0 μm electroless Pd-B on nickel on stainless steel**

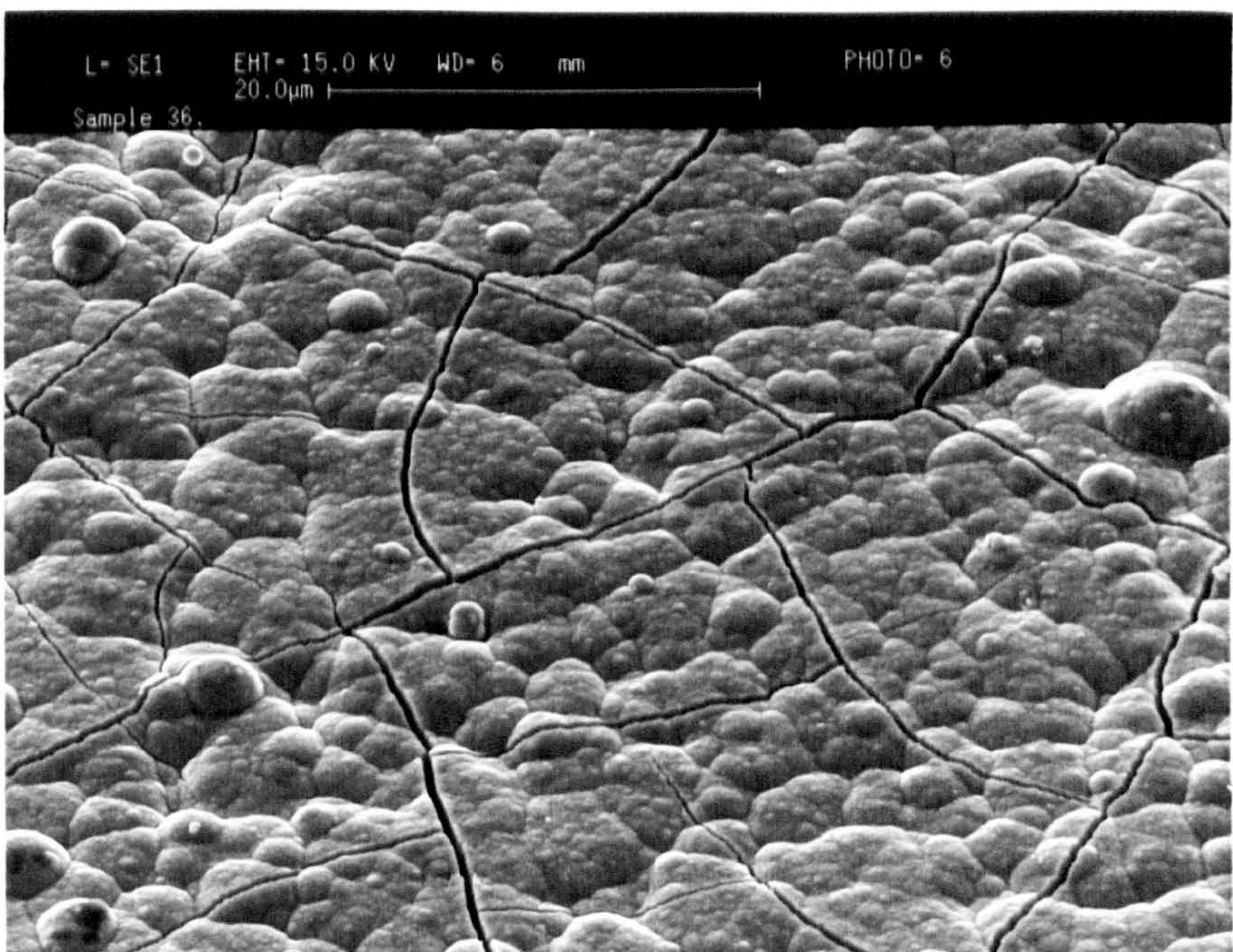


**Figure 13(d). Electron micrograph of 2.7 μm electroless Pd-B on nickel on stainless steel**



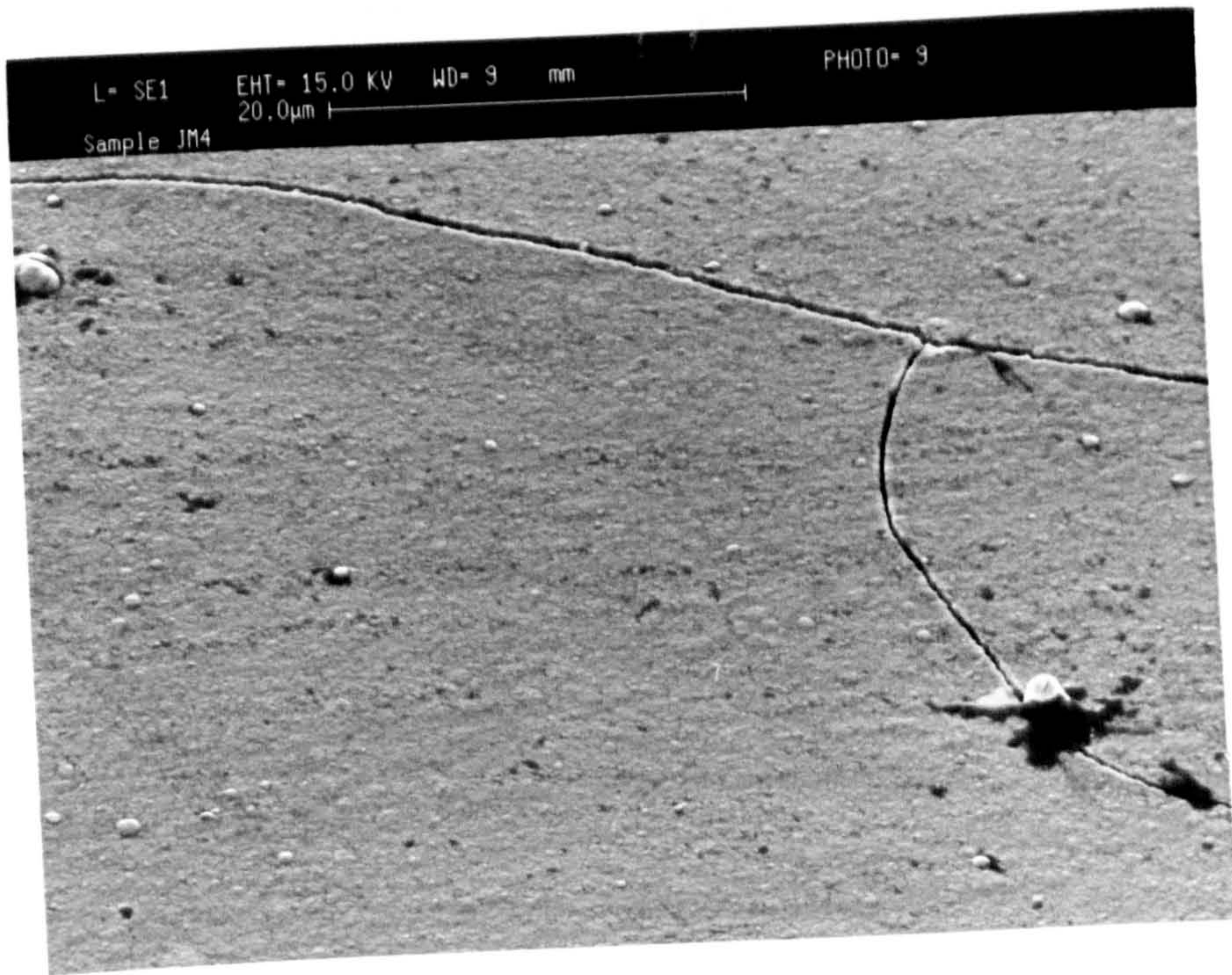


**Figure 13(e). Scanning electron micrograph of 0.7 μm electroless Pd-B on gold**

## **CHAPTER 3**

**The Development and Characterisation**

**of**

**Electroless Ruthenium Coatings**

### 3.1 INTRODUCTION

Little work has been carried out on the electroless deposition of ruthenium. The main studies are given below.

A Japanese patent<sup>24</sup> of 1984 describes a plating solution which deposited pure electroless ruthenium using hydrazine hydrate as reductant. The plating solution was stable and deposited in excess of 90% of the available ruthenium onto various materials including metals, glass and plastics. Deposition onto silicon using sodium hypophosphite was reported by Chang and Chou<sup>25</sup> in 1991. The ruthenium to phosphorus ratio was not given but the structure of the coating was described as being amorphous. Deposition of ruthenium using sodium borohydride as reductant was reported by Valsiunene and Norgailaite<sup>26</sup> in 1980; the boron content was 1%. Further deposition of pure electroless ruthenium coatings using hydrazine was recorded by Okuno<sup>96</sup> in 1990. He found that the contact resistance of electroless ruthenium coatings was unaffected by exposure to inorganic acids and alkalis. Okuno reported that the hardness of electroless ruthenium was 1030 Vickers rising to 1300 Vickers after heat treatment.

The starting materials that were used in these studies were generally nitrosyl ruthenium complexes. The complex was either generated *in situ* from "RuCl<sub>3</sub>.xH<sub>2</sub>O" and NaNO<sub>2</sub> or added as [Ru(NO)Cl<sub>5</sub>]<sup>2+</sup>. The complex was stabilised by the use of hydroxylamine,<sup>24</sup> the CdNa<sub>2</sub> salt of EDTA,<sup>25</sup> hydroxylamine sulphate,<sup>26</sup> or ammonia solution.<sup>96</sup> The plating solutions operated over a range of pH between 9.5 and 13 and temperatures of 50 to 85°C.

Useful properties of electroless ruthenium include its good resistance to chemical attack and high conductivity. Few applications for the use of electroless ruthenium coatings have been identified, hence little work on developing plating processes has been carried out. The few applications recorded are principally found in the electronics industry, where the low electrical resistivity of ruthenium has led to its possible use in contacts for semiconductor devices. Deposition of thin layers of electroless ruthenium onto silicon has been used in the production of epitaxial ruthenium silicide ( $\text{Ru}_2\text{Si}_3$ )<sup>89</sup> for use in novel devices. These novel applications include optoelectronic devices such as infra red detectors.<sup>2</sup> The property which has been identified as suitable for these novel applications is the lattice mismatch found in the ruthenium silicide. Another report has recorded that  $\text{Ru}_2\text{Si}_3$  was found to be semiconducting.<sup>90</sup> The use of electroless techniques allows for a more convenient and cheaper method for the production of epitaxial ruthenium silicides than the vapour deposition techniques currently used.<sup>25</sup>

## **3.2 EXPERIMENTAL**

### **3.2.1 Nephelometric Analysis**

Nephelometric analysis is the measurement of the intensity of scattered light, at right angles to the direction of the incident light, as a function of the concentration of the disperse phase.<sup>91</sup>

The instrument used was a Bausch and Lomb MINI 20 Nephelometer. The experimental arrangement is shown in Figure 14. The instrument was calibrated using formazin suspensions which were prepared as follows.

- i) A 400 Nephelometric Turbidity Unit (NTU) suspension was prepared by dissolving 1 g hydrazine sulphate in 100 cm<sup>3</sup> water and 10 g hexamethylenetetramine in a separate 100 cm<sup>3</sup> water. 5 cm<sup>3</sup> aliquots of each solution were mixed, and allowed to stand at room temperature for 24 h, before being diluted to 100 cm<sup>3</sup> with water.
- ii) An 80 NTU suspension was prepared by diluting a 20 cm<sup>3</sup> aliquot of 400 NTU suspension to 100 cm<sup>3</sup> with water.
- iii) An 8 NTU suspension was prepared by diluting a 10 cm<sup>3</sup> aliquot of 80 NTU suspension to 100 cm<sup>3</sup> with water.
- iv) A 0.8 NTU suspension was prepared by diluting a 1 cm<sup>3</sup> aliquot of 80 NTU suspension to 100 cm<sup>3</sup> with turbidity free water (prepared by filtering distilled water through a 0.45 µm membrane filter).

N.B. Formazin standards are unstable. The 400 NTU suspension is stable for 1 month, the 80 NTU for 12 h, 8 NTU for 8 h, and 0.8 NTU 1 h, after which the formazin decomposes.

Calibration of the instrument was achieved after a 60 s warm up. A vial two-thirds full with an 80 NTU suspension was placed in the Nephelometer, and covered with the shield, then the scale was adjusted to 0-100 NTU. After preconditioning for 60 s the reading was adjusted to 80 NTU. This was repeated using the 8 NTU suspension, changing the scale to 0-80 NTU and adjusting reading to 8 NTU after 60 s. Similarly for the 0.8 NTU suspension. The calibration was checked by obtaining a reading for the 0 to 100 and 0 to 10 NTU standards which were provided with the Nephelometer. This was performed in the same manner as described above. If the readings for these formazin standards was in the ranges indicated then the calibration was deemed to be satisfactory.

Measurement of the colloids (to be described later) and plating solution was performed by placing a vial which was two-thirds full into the instrument and adjusting the scale until a reading could be obtained.

### 3.2.2 Estimation of porosity

The porosity of electroless ruthenium coatings was estimated by immersing the coated substrate into a solution of ammonium persulphate. The persulphate had no effect on the ruthenium but dissolved any exposed copper.

The copper panels used had dimensions of 35 x 35 mm giving a nominal surface area of 24.5 cm<sup>2</sup>. The ruthenium coated panels were clamped between two aluminium discs as shown in Figure 15. The exposed surface area was 11.5 cm<sup>2</sup>. The assembly was then immersed for 2 h in a 10 g dm<sup>-3</sup> ammonium persulphate solution with no agitation. The

ammonium persulphate solutions were then analysed by ICP-OES to determine the copper concentration.

### 3.2.3 Surface profilometry

Surface profiles were obtained using a Dektak<sup>3</sup> ST Surface Profile Measuring System. Measurements were made by moving a sample under a diamond tipped stylus. The vertical movement of the stylus caused by the surface was measured electronically and related to the horizontal distance moved. A plot of vertical movement against horizontal movement is used to calculate the roughness of the surface. A diagram illustrating the experimental arrangement is shown in Figure 16.

The value of surface roughness,  $R_a$ , is the Arithmetic Average Roughness. It is calculated as the arithmetic deviation from the mean line of the trace.

In the experiment the stylus force, scan length, and speed are set before the analysis is performed. For the materials in this study a scan length of 5 mm was used with a low scan speed and high resolution. This corresponds to 8,000 data points over the scan length. The stylus force was 30 mg.

### **3.3 RESULTS**

#### **3.3.1 Development of an Electroless Ruthenium Plating Solution**

##### ***3.3.1.1 Attempts to precipitate ruthenium from solutions of $RuCl_3 \cdot xH_2O$***

Dissolution of " $RuCl_3 \cdot xH_2O$ " in water produced a very deep brown solution with a pH of 1. The addition of either 1 M NaOH or  $NH_4OH$  to " $RuCl_3 \cdot xH_2O$ " resulted in the deep brown colour changing to a deep green. The green colour is also obtained if a mixture of 1 M NaOH and  $NH_4OH$  was added.

The addition of disodium-EDTA, sodium oxalate, or sodium glycolate to a solution of " $RuCl_3 \cdot xH_2O$ " did not result in any visible change in the solution. In the presence of any of these complexants the addition of 1 M NaOH or  $NH_4OH$  resulted in the formation of a green solution. Addition of  $NH_4Cl$  to " $RuCl_3 \cdot xH_2O$ " produced a yellow colour which became green on the addition of alkali.

The action of dimethylamineborane (DMAB) on a solution of " $RuCl_3 \cdot xH_2O$ " resulted in a yellow colour and the evolution of a gas. The solution colour gradually faded until it became colourless. Leaving this solution to stand for 16 h resulted in the formation of a black precipitate. Adjustment of the pH of the " $RuCl_3 \cdot xH_2O$ " solution to pH 11 with NaOH produced a green solution, and adding DMAB resulted in the solution becoming darker with the formation of a black precipitate. When the precipitate had settled it was noted that the solution had become colourless.

The addition of  $NaBH_4$  solution to " $RuCl_3 \cdot xH_2O$ " solution resulted in the immediate formation of a black precipitate. When  $NaBH_4$  was added to a solution of " $RuCl_3 \cdot xH_2O$ " at pH 11, adjusted using NaOH, the evolution of a gas was observed.



The solution developed a pale purple colour, which darkened and gave the appearance of becoming "dirty." Leaving the solution to stand for 16 h resulted in a black precipitate and a colourless solution.

The addition of sodium hypophosphite to " $\text{RuCl}_3 \cdot x\text{H}_2\text{O}$ " solution resulted in a yellow colour. Over a 4 h period no precipitate was observed and the yellow colour did not appear to diminish. When sodium hypophosphite was added to an alkaline solution of " $\text{RuCl}_3 \cdot x\text{H}_2\text{O}$ " (pH 11 after NaOH addition) there were no observable changes in the solution, with the green colour remaining constant.

The addition of  $\text{NaBH}_4$  to " $\text{RuCl}_3 \cdot x\text{H}_2\text{O}$ " which contained disodium-EDTA (which was added to stabilise the ruthenium ions in solution) at pH 11 immediately produced a black precipitate.

Alkaline solutions of " $\text{RuCl}_3 \cdot x\text{H}_2\text{O}$ " containing either sodium oxalate or sodium glycolate evolved a gas on the addition of DMAB. After 1 h a black precipitate appeared. As in previous experiments, after allowing the precipitate to settle it was observed that the solution had become colourless.

To a stable alkaline solution of " $\text{RuCl}_3 \cdot x\text{H}_2\text{O}$ " (pH 11, adjusted with NaOH and  $\text{NH}_4\text{OH}$ ) in the presence of sodium hypophosphite a piece of palladium-activated nickel was immersed. Within a few minutes the evolution of a gas (possibly hydrogen) was observed from the nickel surface. The rate of hydrogen evolution was significantly increased by warming the solution to  $30^\circ\text{C}$ . After 1 h the solution had become colourless, the evolution of hydrogen at the nickel surface had ceased, and no black precipitate was observed. Immersion of a piece of activated nickel into an alkaline (to

pH 11 with NaOH only) solution of “ $\text{RuCl}_3 \cdot x\text{H}_2\text{O}$ ” containing sodium hypophosphite and in which  $\text{NH}_4\text{Cl}$  had been added instead of  $\text{NH}_4\text{OH}$ , resulted in the evolution of hydrogen at the activated nickel surface. The solution became colourless and no black precipitate was observed. In both of these experiments a deposit of ruthenium was obtained on the nickel surface.

Replacing sodium hypophosphite with hydrazine hydrate as the reductant in an alkaline solution of “ $\text{RuCl}_3 \cdot x\text{H}_2\text{O}$ ” (adjusted using NaOH and  $\text{NH}_4\text{OH}$ ) resulted in a yellow solution. A few seconds after immersion of a palladium-activated nickel surface, at room temperature, evolution of hydrogen was observed. A deposit of ruthenium was obtained on the nickel substrate. Leaving the solution to stand for 16 h resulted in a colourless solution and there was no observable precipitate.

The results of these experiments show that precipitation of ruthenium can be achieved from alkaline solution by DMAB and  $\text{NaBH}_4$  in the presence or absence of complexants. Attempts to precipitate ruthenium from alkaline solution using sodium hypophosphite and hydrazine hydrate were unsuccessful. However, when an activated nickel substrate was immersed electroless deposition of ruthenium was observed.

### *3.3.1.2 Attempts to deposit ruthenium from a “ $\text{RuCl}_3 \cdot x\text{H}_2\text{O}$ ” solution using hydrazine hydrate as reductant*

During the preparation of ruthenium plating solutions it was observed that the addition of 0.3 g of NaOH, dissolved in  $10 \text{ cm}^3$  of water, to a small quantity of “ $\text{RuCl}_3 \cdot x\text{H}_2\text{O}$ ” solution resulted in the formation of a black precipitate. The addition of sodium oxalate before the addition of NaOH prevented the formation of the precipitate and gave the

expected green solution. Similarly, the addition of large quantities of  $\text{NH}_4\text{OH}$  to small volumes of " $\text{RuCl}_3 \cdot x\text{H}_2\text{O}$ " solution resulted in the formation of a black precipitate. The addition of 0.3 g NaOH to 0.06 g " $\text{RuCl}_3 \cdot x\text{H}_2\text{O}$ " in the presence of sodium oxalate produced a solution showing a pH of 13. The addition of 5  $\text{cm}^3$   $\text{NH}_4\text{OH}$  had no measurable effect on the pH. Clearly, the presence of sodium oxalate is advantageous in retaining ruthenium in solution.

The addition of hydrazine hydrate to a solution containing " $\text{RuCl}_3 \cdot x\text{H}_2\text{O}$ ," sodium oxalate, NaOH, and  $\text{NH}_4\text{OH}$  to pH 13 at  $50^\circ\text{C}$  did not result in any observable change in the solution. Immersion of a palladium activated nickel substrate resulted in the evolution of hydrogen from the surface. The solution remained green in colour throughout the 2 h of immersion, and 7% of the available ruthenium was deposited.

Additions of 1 M NaOH in the range 4.5 to 9  $\text{cm}^3$  for a plating solution containing 0.06 g " $\text{RuCl}_3 \cdot x\text{H}_2\text{O}$ ," 3  $\text{cm}^3$  0.25 M sodium oxalate, 5  $\text{cm}^3$   $\text{NH}_4\text{OH}$ , and 1  $\text{cm}^3$  1 M hydrazine hydrate, resulted in an increase in the amount of ruthenium deposited. For a solution containing 4.5  $\text{cm}^3$  1 M NaOH the amount of ruthenium deposited was 8% and this value rose to 15% for a solution containing 9  $\text{cm}^3$ . A second addition of 1  $\text{cm}^3$  1 M hydrazine hydrate after 1 h to a solution containing 9  $\text{cm}^3$  1 M NaOH resulted in the amount of ruthenium deposited being increased to 16% over 2 h. In both cases, where 9  $\text{cm}^3$  NaOH was used, the nominal coating thickness was the same though the latter deposited more ruthenium over a larger surface area. An area of 4.6  $\text{cm}^2$  was used in the first instance whilst 5.1  $\text{cm}^2$  was used in the latter.

The effect of a variation in  $\text{NH}_4\text{OH}$  volume on the amount of ruthenium deposited was investigated using a solution consisting of 0.06 g " $\text{RuCl}_3 \cdot x\text{H}_2\text{O}$ ," 3  $\text{cm}^3$  0.25 M sodium oxalate, 7.5  $\text{cm}^3$  1 M NaOH, and 1  $\text{cm}^3$  1 M hydrazine hydrate. The  $\text{NH}_4\text{OH}$  volume was varied from 0 to 10  $\text{cm}^3$ . In a solution which contained no  $\text{NH}_4\text{OH}$  a black precipitate was obtained when the solution was warmed, consequently no plating was possible. For such a solution containing 2  $\text{cm}^3$   $\text{NH}_4\text{OH}$  a black precipitate was obtained on the addition of hydrazine hydrate, and thus no plating was possible. With the other volumes of  $\text{NH}_4\text{OH}$  deposition of ruthenium was obtained. The amount of ruthenium deposited from a plating solution containing 4  $\text{cm}^3$   $\text{NH}_4\text{OH}$  was 9% rising to 11% for 10  $\text{cm}^3$   $\text{NH}_4\text{OH}$ . A repeat experiment which used 5  $\text{cm}^3$   $\text{NH}_4\text{OH}$  deposited 20% of the available ruthenium in solution. In this repeat experiment the surface area of the copper substrate was larger (7.6  $\text{cm}^2$  as opposed to 4.5  $\text{cm}^2$  in the first) although the coating thickness in the two experiments was the same. Both experiments gave a coating thickness of 0.5  $\mu\text{m}$ .

The results of varying the concentrations of NaOH and  $\text{NH}_4\text{OH}$  on ruthenium deposition are summarised in Table 4 (page 137). The amount of ruthenium deposited increased with increasing concentration of NaOH. The dependence was less clear for  $\text{NH}_4\text{OH}$  because of variations in the surface area of the substrate from experiment to experiment.

A solution containing 0.06 g " $\text{RuCl}_3 \cdot x\text{H}_2\text{O}$ " and 3  $\text{cm}^3$  0.25 M sodium oxalate adjusted to pH 9.5 using dropwise additions of NaOH appeared to be stable when heated to 50°C. The addition of 0.5  $\text{cm}^3$  1 M hydrazine hydrate did not result in any deposition of ruthenium. Repetition of this experiment using additions of NaOH and  $\text{NH}_4\text{OH}$  to give

pH 9.5 resulted in a black precipitate being produced when the solution was similarly heated.

Adjustment of a solution containing 0.06 g “RuCl<sub>3</sub>.xH<sub>2</sub>O” and 3 cm<sup>3</sup> 0.25 M sodium oxalate to pH 11 using NaOH resulted in the formation of a black precipitate on the addition of hydrazine hydrate. Repetition of this experiment using NaOH and NH<sub>4</sub>OH to adjust the pH to 11 resulted in a black precipitate when the solution was heated.

During the plating experiments it was observed that the sides of the polypropylene plating vessels were coated in ruthenium. Consequently the plating vessels had a short experimental lifetime, even though most of the extraneous ruthenium could be removed from the vessel sides by wiping with acetone.

The ruthenium deposits produced on the substrate were of a metallic and bright appearance. They adhered well to the copper with no signs of exfoliation, and if flexed the coating did not readily lose its adherence.

The experiments show that, to deposit ruthenium electrolessly from an alkaline solution using hydrazine hydrate as reductant a number of factors must be met: (i) the presence of sodium oxalate and NH<sub>4</sub>OH to stabilise the ruthenium ions in solution, and (ii) the pH of the plating solution, at room temperature, is 13.

### *3.3.1.3 Attempts to deposit ruthenium from solutions of [Ru(NH<sub>3</sub>)<sub>6</sub>]Cl<sub>3</sub> using hydrazine hydrate as reductant*

Initial experiments were performed using solutions consisting of 0.08 g [Ru(NH<sub>3</sub>)<sub>6</sub>]Cl<sub>3</sub> (which gave the same amount of ruthenium ions in solution as 0.06 g “RuCl<sub>3</sub>.xH<sub>2</sub>O”)

7.5 cm<sup>3</sup> 1 M NaOH, 5 cm<sup>3</sup> NH<sub>4</sub>OH and 1 cm<sup>3</sup> 1 M hydrazine hydrate. As observed for solutions based on "RuCl<sub>3</sub>.xH<sub>2</sub>O," an extraneous deposit of ruthenium formed on the sides of the plating vessel. Consequently, further experiments contained 1 cm<sup>3</sup> 0.25 M methylamine solution. The inclusion of this small quantity of methylamine appeared to improve the plating performance. The plating solution containing methylamine deposited 20% of the available ruthenium onto 5 cm<sup>2</sup> substrate from a 50 cm<sup>3</sup> solution at 60°C over 2 h. This corresponded to a coating thickness of 0.8 μm.

A number of comments can be made about the behaviour of an electroless ruthenium plating solution based on hexaammine ruthenium trichloride, [Ru(NH<sub>3</sub>)<sub>6</sub>]Cl<sub>3</sub>, which was observed in most of the electroless plating performed. These are as follows.

[Ru(NH<sub>3</sub>)<sub>6</sub>]Cl<sub>3</sub> is a pale yellow powder which gave a colourless or pale yellow solution depending on concentration. The addition of NaOH to aqueous [Ru(NH<sub>3</sub>)<sub>6</sub>]Cl<sub>3</sub> produced a solution which was, at first, intense yellow in colour but which became brown when exposed to air at room temperature. The darkening occurred after a few minutes exposure. The addition of NH<sub>4</sub>OH to [Ru(NH<sub>3</sub>)<sub>6</sub>]Cl<sub>3</sub> solution resulted in a less intense yellow colour than that observed after the addition of NaOH. Addition of NH<sub>4</sub>OH to the yellow solution of [Ru(NH<sub>3</sub>)<sub>6</sub>]Cl<sub>3</sub> and NaOH had no noticeable effect on the colour change. The addition of methylamine before addition of NaOH appeared to slow or prevent the yellow colour darkening to brown. Similarly, the addition of methylamine after the addition of NaOH prevented the yellow colour becoming brown. The pale yellow solution, obtained by the dropwise addition of 1 M NaOH to a [Ru(NH<sub>3</sub>)<sub>6</sub>]Cl<sub>3</sub> solution, turned colourless on the addition of methylamine.

Successful plating was indicated by the evolution of hydrogen from an immersed copper substrate. Hydrogen evolution was usually observed within a few seconds of immersion, with full surface coverage of the copper occurring after 5 to 10 minutes as judged by the colour of the substrate. Generally the colour changes during plating were: (i) an intense yellow on the addition of NaOH, (ii) after heating and addition of hydrazine hydrate the solution paled until it became almost colourless, (iii) the solution then began to develop a pale green colour, (iv) the pale green colour darkened to deep green by which time plating appeared to have ceased. Normally, after 6 h plating the solution would be a light green in colour. When this solution was exposed to air at room temperature it would become dark green, appearing almost black. After a few days a black precipitate formed and the supernatant solution was colourless. As with deposition from a solution based on "RuCl<sub>3</sub>.xH<sub>2</sub>O" most experiments using [Ru(NH<sub>3</sub>)<sub>6</sub>]Cl<sub>3</sub> gave a ruthenium deposit on the sides of the plating vessel. In most experiments the deposition of this extraneous ruthenium appeared after 3 to 4 h plating.

The plating performance of a 50 cm<sup>3</sup> plating solution consisting of 0.08 g [Ru(NH<sub>3</sub>)<sub>6</sub>]Cl<sub>3</sub>, 1 cm<sup>3</sup> 0.25 M methylamine, 18 cm<sup>3</sup> 1 M NaOH, and 3 cm<sup>3</sup> NH<sub>4</sub>OH with 1 cm<sup>3</sup> 1 M hydrazine hydrate added at 0.5 h intervals deposited 20% of the ruthenium in solution over a 2 h period. This corresponded to a coating thickness of 0.83 μm over a surface area of 5.1 cm<sup>2</sup>. At the end of this 2 h period no extraneous ruthenium was observed. Repeating this experiment using only a single addition of 2 cm<sup>3</sup> 1 M hydrazine hydrate resulted in deposition of 18% of the available ruthenium over a 3 h period.

The best plating performance was achieved from a 150 cm<sup>3</sup> plating solution with a composition of 0.48 g [Ru(NH<sub>3</sub>)<sub>6</sub>]Cl<sub>3</sub>, 6 cm<sup>3</sup> 0.25 M methylamine, 45 cm<sup>3</sup> 1 M NaOH, 7.5 cm<sup>3</sup> NH<sub>4</sub>OH and 6 cm<sup>3</sup> 1 M hydrazine hydrate, at a temperature of 60 °C. The solution deposited coatings of 2.8 μm over 18.5 cm<sup>2</sup> substrate area in 6 h. This corresponded to 41% of the ruthenium present in solution. Multiple repeats of this experiment, in which a new polypropylene container was used, resulted in more than 65% of the available ruthenium being deposited. After 6 h plating in the new container there was only a very small amount of extraneous ruthenium visible.

In a blank experiment, a 50 cm<sup>3</sup> plating solution of the composition used above, containing 2 cm<sup>3</sup> 1 M hydrazine hydrate with a further addition at 2 h, was allowed to stand at 50°C for 6 h exposed to air in the absence of a copper substrate. After 0.5 h a light deposit of ruthenium was observed on the sides of the container. After 3 h this deposit had become quite heavy, covering most of the container sides, and the solution had become a pale yellow colour. A further 2 h plating resulted in no noticeable increase in the amount of extraneous ruthenium deposited, though the solution had begun to darken. After 6 h the solution had become a deep yellow/brown colour, which became dark green on standing for 16 h at room temperature exposed to the atmosphere.

Additions of hydrazine hydrate in excess of 6 cm<sup>3</sup> at the beginning of the experiment or during the first 3 h of plating resulted in a lower amount of ruthenium being deposited. Typically 6% as compared to the 65% achieved in experiments which had only a single addition of 6 cm<sup>3</sup>. Further additions of hydrazine hydrate after 3 h appeared to have no effect on plating performance.



It was possible, using a new polypropylene beaker under optimum conditions, to deposit a ruthenium coating without depositing extraneous ruthenium on the beaker sides. In these circumstances the beaker can be used for 6 or 7 plating experiments as opposed to 1 or 2 where the first plating experiment resulted in a heavy deposit of extraneous ruthenium. Use of a beaker which had had a heavy extraneous ruthenium deposit resulted in further experiments also having a heavy extraneous ruthenium deposit. Generally, use of new beakers would result in 50 to 65% of available ruthenium being deposited over 6 h without an extraneous deposit being observed.

The effect of varying the NaOH concentration in the plating solution on ruthenium deposition can be seen in Figure 17. The omission of NaOH resulted in no plating occurring. The maximum ruthenium deposition of 68% occurred at a NaOH concentration of 45 cm<sup>3</sup> for a 1 M solution. Increasing the NaOH concentration further resulted in a decline in the amount of ruthenium deposited.

The effect of varying NH<sub>4</sub>OH concentration on ruthenium deposition is shown in Figure 18. Using no or small quantities of NH<sub>4</sub>OH (circa 2 cm<sup>3</sup> 28% solution) resulted in very little deposition of ruthenium from solution. These solutions developed a green colour between 1 and 2 h plating. This is in contrast to solutions which contained over 5 cm<sup>3</sup> 28% NH<sub>4</sub>OH which deposited over 50% of the available ruthenium and developed a green colour after 4 to 5 h plating. From Figure 18 the optimum NH<sub>4</sub>OH concentration is 7.5 cm<sup>3</sup> of a concentrated solution.

Observations from experiments using "RuCl<sub>3</sub>.xH<sub>2</sub>O" indicated that the surface area of the substrate may influence the ruthenium deposition. The effect of surface area on the

amount of ruthenium deposited from a solution using  $[\text{Ru}(\text{NH}_3)_6]\text{Cl}_3$  is shown in Figure 19. It can be seen that the optimum substrate surface area for a 150 cm<sup>3</sup> plating solution is 25 cm<sup>2</sup>. Increasing or decreasing the surface area of the substrate induces a decline in the amount of ruthenium deposited. Using 25 cm<sup>2</sup> substrate surface area resulted in a coating thickness of circa 3.2 μm. A decrease to 15 cm<sup>2</sup> gave a 5 μm coating and to 10 cm<sup>2</sup> a 7 μm coating for a single immersion. The behaviour of the plating solution was the same using smaller substrates as using substrates of 25 cm<sup>2</sup> surface area. Similarly, increasing the substrate surface area to 35 cm<sup>2</sup> saw a fall in coating thickness to 2.3 μm and for 50 cm<sup>2</sup> a decline to 1.3 μm.

The variation in pH for an electroless plating solution during plating is shown in Figure 20. On mixing the components at room temperature the observed pH was 13; on heating the solution to 60°C the pH declined by approximately 1 pH unit to 12. The addition of hydrazine hydrate had no measurable effect on the pH. During the first 0.5 h of plating it was observed that the pH declines by approximately 0.5 a pH unit, thereafter remaining constant. Observations made during plating indicated that extraneous deposition of ruthenium occurred between 3 and 4 h plating. After 4 h the evolution of hydrogen at the substrate surface had almost ceased. Between 4 and 5 h the solution showed signs of beginning to darken and after 5 h there was no further evolution of hydrogen. After 6 h immersion the solution had become a dark brown-green colour.

Figure 21 compares the variation in pH for a plating solution which was exposed to air and one in which the atmosphere was contained. It can be seen from Figure 21 that for a contained system, the pH initially declined, but after 0.5 h the pH began to rise back

towards the original value and then remained constant. Use of a closed plating system, where the gases evolved from the solution are not allowed to escape to the atmosphere, had a significant effect on the performance of the plating solution. The amount of ruthenium deposited over a 6 h period was reduced from 65 to 30%. The evolution of hydrogen from the substrate surface continued beyond 4 h, and was observed after 6 h, unlike the open system in which plating appeared to have declined considerably after 4 h and ceased after 5 h. Although the enclosed vessels were made of glass no extraneous deposition of ruthenium was observed, even after five consecutive 6 h plating experiments. Leaving the solution enclosed in the vessel for 16 h resulted in a dark green solution. After several days there was no black precipitate such as would have been produced had the plating solution been exposed to air.

Plating in an inert atmosphere for 2 h, obtained by having a flow of argon gas across the surface of the plating solution, resulted in gross deposition of ruthenium onto the sides of the plating vessel. The plating solution had become pale green and ruthenium particulates were observed in the solution, with 24% of the ruthenium deposited onto the copper substrate.

Sparging the solution with air had a detrimental effect on the behaviour of the solution. After 20 minutes the solution had become very dark brown in colour. Continuing to sparge air for a further 2 h resulted in the solution becoming a very dark green colour. The green colour was similar to that which was observed in exhausted plating solutions which had been left at room temperature unagitated for 16 h and exposed to air.

It was considered that the green colour which developed during plating might be due to the formation of colloidal ruthenium, which would provide an alternative site for the electroless deposition of ruthenium. To determine if a colloid was produced during deposition the plating solution was examined by Nephelometric analysis (see Section 3.2.1). The results for the plating solution were compared to solutions which were known to contain colloidal material. The colloids prepared were manganese dioxide<sup>†</sup> and von Weimarn's gold.<sup>‡</sup> The results of the analyses are shown in Table 5.

The performance of the plating solution was found to be irreproducible. An experiment which deposited 65% of the ruthenium present in solution might be followed by one which deposited 20 or 30% under experimentally identical conditions. This was more prevalent for plating solutions where preparation involved the addition of 15 cm<sup>3</sup> 3 M NaOH to 0.48 g [Ru(NH<sub>3</sub>)<sub>6</sub>]Cl<sub>3</sub> dissolved in a small volume (circa 30 to 40 cm<sup>3</sup>) of water. The sequence of addition of methylamine, NaOH and NH<sub>4</sub>OH did not appear to have any effect on plating performance, although the addition of methylamine before NaOH or NH<sub>4</sub>OH generally prevented the brown colour from developing after a few

---

<sup>†</sup>25 cm<sup>3</sup> of 0.01 M potassium permanganate solution was diluted to 50 cm<sup>3</sup> and heated to boiling point. Then while stirring, a drop of 28% NH<sub>4</sub>OH was added every three minutes with the temperature maintained at approx. 90°C. The solution turned from red to deep brown. Testing for complete reduction of the permanganate was achieved by coagulation of the colloid by the addition of NaCl, no violet colour indicated complete reduction.

<sup>‡</sup>15 cm<sup>3</sup> of 0.1% gold chloride was added to 200 cm<sup>3</sup> boiling water. 1 cm<sup>3</sup> of 0.05 M Rochelle salts was added dropwise and boiling continued. A blue gold colloid appeared after 60 s. The large particles of the dark blue gold colloid were gradually dispersed into smaller particles of a deep red gold colloid.

minutes. To minimise this irreproducibility, plating solutions were prepared as follows. 0.48 g  $[\text{Ru}(\text{NH}_3)_6]\text{Cl}_3$  was dissolved in 50 cm<sup>3</sup> of water to which was added 6 cm<sup>3</sup> 0.25 M methylamine, then 45 cm<sup>3</sup> 1 M NaOH, and then 15 cm<sup>3</sup>  $\text{NH}_4\text{OH}$ ; the total volume was made up to 144 cm<sup>3</sup> with water. The additions were made under constant magnetic stirring. The plating solution was then heated to 60°C and maintained at that temperature for a short time (total time = 0.5 h) whereupon 6 cm<sup>3</sup> 1 M hydrazine hydrate was added, followed immediately by the immersion of the activated substrate. Solutions prepared under these conditions produced a consistent plating performance of 60% or better.

Coatings of thickness greater than 3 μm were obtained by immersion of the substrate in a sequence of plating solutions, until the desired thickness was reached. When a copper substrate coated in ruthenium was immersed into a second plating solution deposition occurred as for a freshly activated copper substrate. Coatings of ruthenium required no activation procedure when immersed into a second plating solution. Indeed, a coating that had been exposed to air for a number days did not require activation when immersed into a fresh plating solution.

Table 6 compares the immersion of a single copper substrate for 3 h in four successive plating solutions to a separate copper substrate immersed in each of the plating solutions. The immersion of a copper substrate in a sequence of plating solutions showed no decline in the amount of ruthenium deposited with thickness as the two substrates in each solution were coated in ruthenium to the same extent. The results in Table 6 are for a solution which did not contain methylamine, but similar results were obtained for plating solutions which contained methylamine, and are shown in Table 7.

Electroless ruthenium was successfully deposited onto a number of metals from the plating solution based on  $\text{Ru}(\text{NH}_3)_6\text{Cl}_3$ . The successful substrates and the activation procedures were:

Copper	60 s immersion in $\text{PdCl}_2$ solution at room temperature;
Nickel	60 s immersion in $\text{PdCl}_2$ solution at room temperature;
Gold	30 s immersion in 50% $\text{H}_2\text{SO}_4$ at $50^\circ\text{C}$ , water rinse, and a 60 s immersion in $\text{PdCl}_2$ solution at room temperature;
AISI 304 SS	30 s immersion in 50% $\text{H}_2\text{SO}_4$ at $50^\circ\text{C}$ ;
Electroless Ni-P	30 s immersion in 50% $\text{HCl}$ , water rinse and a 60 s immersion in $\text{PdCl}_2$ solution at room temperature;
Nickel superalloy (MAR M002)	30 s immersion in 50% $\text{HCl}$ , water rinse, a 60 s immersion in $\text{SnCl}_2$ and a 60 s immersion in $\text{PdCl}_2$ solution both at room temperature.

Initial experiments to deposit ruthenium onto nickel superalloy, nickel, and gold substrates resulted in exfoliation of the coating after a single immersion. Exfoliation was not observed on copper substrates, even after several sequential immersions. Table 8 gives a comparison of the average surface roughness of the various substrates obtained by surface profilometry. It can be seen that a coating of  $10\ \mu\text{m}$  was possible on copper with an average roughness in excess of  $1100\ \text{\AA}$ . The topography of nickel and copper substrates is shown in the electron micrographs in Figures 22 and 23. The micrograph of nickel (Figure 22) shows a flat and featureless surface which had an  $R_a$  of  $183\ \text{\AA}$ . The micrograph of copper (Figure 23) shows an uneven surface which had an  $R_a$  of  $1185\ \text{\AA}$ . The exfoliation of the ruthenium coating from the nickel superalloy was

overcome by roughening the surface. This was achieved by grit blasting the surface using 200  $\mu\text{m}$  alumina particles. Subsequently it was possible to deposit coatings of 10  $\mu\text{m}$  without any indication of exfoliation.

### 3.3.2 Characterisation of Electroless Ruthenium Coatings

#### *3.3.2.1 Scanning electron microscopy*

Topological detail of the growth of ruthenium coatings obtained by scanning electron microscopy is shown in the micrographs of Figure 24. Figure 24(a) shows a micrograph of a 1  $\mu\text{m}$  ruthenium coating, 24(b) a 2  $\mu\text{m}$  coating, 24(c) a 5  $\mu\text{m}$  coating, and 24(d) a 10  $\mu\text{m}$  coating. Comparison of Figures 24(a) and (b) with Figure 23 shows how the ruthenium coating has followed the contours of the copper substrate. A 5  $\mu\text{m}$  coating, however, shows no discernible trace of the underlying copper morphology. The unevenness of the copper substrate has been “filled in.” Examination of the values of  $R_a$  in Table 9 indicates a large decline in  $R_a$  with the deposition of a 2  $\mu\text{m}$  coating. The value of  $R_a$  then increases to above the value for copper as the coating thickness increases. Increasing the thickness above 5  $\mu\text{m}$  sees an increased merging of the grains of the coating to give a smoother texture.

Generally the coatings are adherent, continuous and coherent with no observable deformations. Examination of fracture cross-sections of 5 and 10  $\mu\text{m}$  coatings as shown in Figures 25(a) and (b) indicate that the coatings are dense with no discernible pores.

#### *3.3.2.2 Action of ammonium persulphate*

The dissolution of copper through electroless ruthenium coatings was used to estimate the porosity of coatings. The results of the action of ammonium persulphate on

ruthenium coatings of various thickness are given in Table 10. It can be seen that the amount of dissolved copper decreases with increasing coating thickness. The amount of copper dissolved through the 10  $\mu\text{m}$  coating was greater than that dissolved through an electrodeposited gold coating on copper which was used as a standard.

### *3.3.2.3 Potentiodynamic corrosion analysis*

Potentiodynamic corrosion analysis is described in Section 2.2.2.2ii. The analysis was performed under two conditions. The first with an air sparge, as described in 2.2.2.2ii, and secondly with an argon sparge. Argon was used to both de-aerate the 0.5 M  $\text{H}_2\text{SO}_4$  beforehand and to sparge the solution during the analysis. Corrosion analysis was performed on electroless ruthenium coatings, and on sheets of copper, palladium, and platinum. The results of the analyses are shown in Table 11 and Figures 26 (using an air sparge) and 27 (using an argon sparge).

It can be seen from Table 11 that the  $E_{\text{corr}}$  for ruthenium, palladium and platinum is lower than that of copper indicating that copper is more corrosion resistant. The corrosion profiles in Figures 18 and 19 show that the platinum group metals tested corrode at a faster rate than copper. Immersing each of the above materials in aerated or de-aerated  $\text{H}_2\text{SO}_4$  and measuring the cell potential gives the potential of that system. These values are the open circuit potentials (OCP) given in Table 11.

### 3.3.3 Investigation into Other Ruthenium Compounds as Starting Materials

#### *3.3.3.1 Ammonium pentachloroaquo ruthenium (III) $\{(\text{NH}_4)_2[\text{RuCl}_5(\text{H}_2\text{O})]\}$*

Dissolution of  $(\text{NH}_4)_2[\text{RuCl}_5(\text{H}_2\text{O})]$  in water produced a deep yellow-brown colour. When used in solution as a direct replacement for  $[\text{Ru}(\text{NH}_3)_6]\text{Cl}_3$ , without the presence



of methylamine, the solution produced a black precipitate. The addition of NaOH to a solution of  $(\text{NH}_4)_2[\text{RuCl}_5(\text{H}_2\text{O})]$  produced a deep green solution to which the addition of  $\text{NH}_4\text{OH}$  had no visible effect. On standing, the solution changed from a green colour to turquoise and then to a dirty grey. The addition of hydrazine hydrate to this solution at room temperature had no observable effect, though subsequent heating resulted in a gas being evolved from solution followed by the formation of a black precipitate.

The addition of  $\text{Na}_2\text{-EDTA}$  to a solution of  $(\text{NH}_4)_2[\text{RuCl}_5(\text{H}_2\text{O})]$  produced no colour change. The subsequent addition of NaOH altered the solution colour from deep yellow to brown. Further additions of  $\text{NH}_4\text{OH}$  and hydrazine hydrate had no visible effect on the solution. On heating to  $60^\circ\text{C}$  and the immersion of an activated copper substrate no plating was observed, even after 3 h, although after 1 h the solution had become inky blue.

The replacement of  $\text{Na}_2\text{-EDTA}$  with 1,2-diaminoethane resulted in a green precipitate on addition to a solution of  $(\text{NH}_4)_2[\text{RuCl}_5(\text{H}_2\text{O})]$ . The precipitate was dissolved by addition of NaOH to produce a deep yellow solution. The addition of  $\text{NH}_4\text{OH}$  did not dissolve the precipitate. Further addition of  $\text{NH}_4\text{OH}$  and hydrazine hydrate to the deep yellow solution followed by heating resulted in no deposition of ruthenium onto an activated copper substrate.

Changing from a chelate which bonds via its nitrogen atom to one which bonds through oxygen, such as oxalic acid, resulted in the formation of a black precipitate when hydrazine hydrate was added to an NaOH/ $\text{NH}_4\text{OH}$  alkaline solution of  $(\text{NH}_4)_2[\text{RuCl}_5(\text{H}_2\text{O})]$ . The addition of NaOH to the deep yellow solution of

$(\text{NH}_4)_2[\text{RuCl}_5(\text{H}_2\text{O})]$  and oxalic acid produced a green solution which became blue-green then a dirty green.  $\text{NH}_4\text{OH}$  addition appeared to darken the colour of the solution. Addition of hydrazine hydrate and heating resulted in the evolution of a gas from the solution followed by the formation of a black precipitate.

The use of methylamine to stabilise  $(\text{NH}_4)_2[\text{RuCl}_5(\text{H}_2\text{O})]$  solution resulted in the successful deposition of ruthenium onto copper. The addition of methylamine did not affect the colour of the  $(\text{NH}_4)_2[\text{RuCl}_5(\text{H}_2\text{O})]$  solution. However, the addition of  $\text{NaOH}$  resulted in the formation of a blue colour in solution and the production of a precipitate. After a few moments the precipitate dissolved to give a deep yellow solution. Further addition of  $\text{NH}_4\text{OH}$  had no visible effect, although heating brought a brown colour to the solution. Hydrazine hydrate caused the solution to become lighter, and within a few minutes a deposit of ruthenium was observed on the activated copper. After 2 h the solution was pale yellow in colour. Plating on to copper had appeared to have ceased, and no extraneous deposition of ruthenium was observed.

### *3.3.3.2 Potassium pentachloronitrosyl ruthenium (III) $\{K_2[\text{RuCl}_5(\text{NO})]\}$*

Dissolution of  $K_2[\text{RuCl}_5(\text{NO})]$  in water produced a deep pink solution, on which the addition of  $\text{NaOH}$  and/or  $\text{NH}_4\text{OH}$  had no effect. Similarly the addition of hydrazine hydrate had no effect. Heating a solution containing  $K_2[\text{RuCl}_5(\text{NO})]$ ,  $\text{NaOH}$ ,  $\text{NH}_4\text{OH}$ , and hydrazine hydrate resulted in a yellow solution. Immersing activated copper in this solution resulted in the deposition of ruthenium on the copper within a few minutes. Over a 1 h period the solution became a pale red colour with a quite heavy deposit of ruthenium on the sides of the container.

The use of  $[\text{RuCl}_5(\text{H}_2\text{O})]^{2-}$  without any further complexation does not result in a stable plating solution. However, complexation with chelates such as EDTA or 1,2-diaminoethane results in a ruthenium complex which is too stable to undergo electroless reduction. Weaker chelates, like oxalate ions, are insufficiently strong to prevent solution decomposition and thus no electroless deposition. The addition of methylamine to a solution of  $[\text{RuCl}_5(\text{H}_2\text{O})]^{2-}$  resulted in electroless deposition. This is a result of the ruthenium ions becoming complexed with methylamine ligands to produce a complex of the form  $[\text{Ru}(\text{NH}_2\text{CH}_3)_6]^{3+}$ . Although complexation at all six coordination points maybe unlikely. Though similar to  $[\text{Ru}(\text{NH}_3)_6]\text{Cl}_3$  it may be more stable and prevent the extraneous deposition of ruthenium occurring. The Ru-NO arrangement is very stable, but not too stable to prevent electroless deposition. However, the complex as a whole is insufficiently stable to produce a useable plating solution.

## 3.4 DISCUSSION

### 3.4.1 Development of an Electroless Ruthenium Plating Solution

#### *3.4.1.1 Attempts to precipitate ruthenium from solutions of $RuCl_3 \cdot xH_2O$*

The use of commercial " $RuCl_3 \cdot xH_2O$ " was determined by its availability though it is far from a simple compound. " $RuCl_3 \cdot xH_2O$ " as supplied has an average oxidation state nearer to IV than the III.<sup>92</sup> The material has been defined as<sup>92</sup> "...a heterogeneous, ill defined mixture of variable oxidation-state, oxochloro and hydroxychloro, monomeric and polymeric ruthenium complexes, frequently containing even nitrosyl derivatives."

Although the starting material is complex the deposition of ruthenium by electroless processes utilising " $RuCl_3 \cdot xH_2O$ " has been reported.<sup>25,93</sup>

The initial objective was to determine the action of the common reducing agents used in electroless processes on solutions of " $RuCl_3 \cdot xH_2O$ ." The performance of the reducing agent was assessed under both acidic and alkaline conditions with and without the presence of a complexant. In acid solutions, " $RuCl_3 \cdot xH_2O$ " gave a deep brown solution to which the addition of a base resulted in the formation of a green solution and no observable precipitate. From the literature,<sup>94</sup> the addition of NaOH to a solution of " $RuCl_3 \cdot xH_2O$ " should result in the precipitation of ruthenium oxide. The oxide produced has repeatedly been redefined. Cotton and Wilkinson<sup>94</sup> describe the precipitate as a hydrous oxide of the type  $Ru_2O_3 \cdot xH_2O$ , whereas Seddon and Seddon<sup>92</sup> record the precipitate as  $RuO_2 \cdot xH_2O$ , and Griffith<sup>95</sup> as  $Ru^{IV}O(OH)_2$ . Though no precipitate was observed on the addition of NaOH to " $RuCl_3 \cdot xH_2O$ " solution, the green colour may indicate the formation of mixed ruthenium oxides/hydroxides which do not precipitate. Cotton and Wilkinson<sup>94</sup> have reported that under the right alkaline

conditions, though none was specified, the hydrous oxide produced by the addition of NaOH may become colloidal.

Though no precipitate was observed in these small scale test tube reactions, later studies showed that addition of large volumes of high concentration NaOH or  $\text{NH}_4\text{OH}$  to small volumes of " $\text{RuCl}_3 \cdot x\text{H}_2\text{O}$ " solution did result in the formation of a black precipitate. Equally, it was possible to add small volumes of high concentration NaOH to similar volumes of " $\text{RuCl}_3 \cdot x\text{H}_2\text{O}$ " to produce a green solution without the formation of a black precipitate. It is therefore reasonable to assume that the precipitation of ruthenium oxide from solution is pH dependent. At modest alkalinities (possibly  $\text{pH} < 11$ ) the ruthenium hydroxide species do not precipitate but at higher alkalinities they precipitate as the hydrated oxide.

In the presence of a complexing agent, such as oxalate or EDTA ions, the addition of NaOH and/or  $\text{NH}_4\text{OH}$  to  $\text{pH} 13$  resulted in a green solution with no precipitate observed. This is due to the complexant stabilising the ruthenium ions in solution thus preventing the formation of ruthenium oxides. A summary of the reactions of " $\text{RuCl}_3 \cdot x\text{H}_2\text{O}$ " in solution can be seen in Figure 28.

The addition of DMAB and sodium borohydride as reductants to solutions of " $\text{RuCl}_3 \cdot x\text{H}_2\text{O}$ " resulted in the formation of a black precipitate of hydrous ruthenium oxide. The gas evolved after the addition of these reductants was hydrogen. The evolution of hydrogen is a result of the breakdown of the reductant due to the pH of solution and the reduction of the higher oxidation states of ruthenium to lower states (eg IV to III). After this reduction the formation of ruthenium oxide occurs. From

Chapter 2, The Development of Electroless Palladium-Boron Coatings the mechanisms of the breakdown of DMAB and sodium borohydride were given as:



Equation (1) is the first step in the breakdown of sodium borohydride and Equation (2) the first step for DMAB. As the boron species break down further more hydrogen is evolved. The addition of sodium borohydride and DMAB to solutions of “ $\text{RuCl}_3 \cdot x\text{H}_2\text{O}$ ” produced a black precipitate irrespective of pH and the presence of complexant. Sodium borohydride reduction of ruthenium ions occurs more rapidly than that of DMAB. This is because the rate of Equation (1) is retarded by increasing hydroxide ion concentration, whereas the rate of Equation (2) is increased as hydroxide ion concentration increases. As a result, the electroless deposition of ruthenium from solutions of “ $\text{RuCl}_3 \cdot x\text{H}_2\text{O}$ ” which use boron-containing reductants is not possible. However, a report by Valsiuniene and Norgaiulaite<sup>26</sup> recorded that at  $\text{pH} > 13$  the electroless deposition of ruthenium can be achieved using sodium borohydride as reducing agent if the source of ruthenium ions was ruthenium nitrosyl hydroxide. This indicates that stability towards reducing agents can be achieved by use of the appropriate complexants, in the same way that complexation prevents the formation of hydrous ruthenium oxides on the addition of alkalis.

The use of sodium hypophosphite as reductant did not result in the formation of ruthenium oxide, in either acid or alkaline conditions. This is because the hypophosphite ion is more stable in alkaline solution (pH 11) than either the borohydride ion or DMAB. Similarly, hydrazine is more stable than borohydride ion,

and DMAB under alkaline conditions. The use of sodium hypophosphite or hydrazine resulted in the electroless deposition of ruthenium from alkaline solution. The gases evolved at the surface of the substrate are hydrogen in the case of sodium hypophosphite, and hydrogen and nitrogen in the case of hydrazine.

These observations for the electroless deposition of ruthenium from alkaline solutions when sodium hypophosphite and hydrazine are used as reductants are consistent with reported electroless ruthenium plating solutions using "RuCl<sub>3</sub>.xH<sub>2</sub>O." Chang and Chou<sup>25</sup> reported a "RuCl<sub>3</sub>.xH<sub>2</sub>O" plating solution where reduction was achieved using sodium hypophosphite at pH 9.5. A system using hydrazine hydrochloride as reductant at pH 11 was reported by Nagata et al.<sup>93</sup> In their report the presence of a complexant was not disclosed.

#### *3.4.1.2 Attempts to deposit ruthenium from a "RuCl<sub>3</sub>.xH<sub>2</sub>O" solution using hydrazine hydrate as reductant*

One of the desired properties of electroless ruthenium coatings in the present work was that the metal should be deposited in the pure state without the inclusion of a non metal. Consequently, sodium hypophosphite was rejected as reducing agent, and hydrazine hydrate was a logical choice. The most informative report which described the use of hydrazine hydrate was published by Okuno.<sup>96</sup> In this work an unspecified ruthenium compound was successfully used to deposit electroless ruthenium coatings from a plating solution at pH 13. This contrasts with the use of hydrazine hydrochloride used by Nagata et al.<sup>93</sup>

By use of the same relative quantities of ruthenium ions, NaOH, NH<sub>4</sub>OH, and hydrazine hydrate as those reported by Okuno<sup>96</sup> it was possible to deposit electroless ruthenium coatings. Contrary to Okuno's experience, it was necessary in this work to include a complexing agent to prevent the addition of alkali resulting in the precipitation of ruthenium oxide. In this study the complexant chosen was sodium oxalate. The observed precipitation of ruthenium oxide may indicate that Okuno had used a different source of ruthenium ions, such as the hydroxy nitrosyl ruthenium (III) complex used by Valsiuniene and Norgaiulaite.<sup>26</sup> The performance of this solution was not of the same standard as those previously reported.<sup>25,26,93,96</sup>

Throughout 2 h of plating the solution remained green with no indication of solution becoming colourless as was observed in the small scale reactions described in the previous section. This may be due to the small amount of ruthenium deposited from solution (approximately 7%). Alternatively, the higher pH (13 as opposed to 11) may have a different influence on the chemistry of the solution.

An increase in the concentration of NaOH by a factor of 2 had no significant effect on the pH of solution. The measured pH of these solutions was 13. An estimation of the pH (using  $\text{pH} = -\log_{10} a_{\text{H}^+}$ ) sees an increase in pH from 12.9 to 13.2 by an increase in NaOH concentration from 0.1 to 0.2 M.

Similarly, at such a high concentration of OH<sup>-</sup> ions the addition of NH<sub>4</sub>OH solution will have no significant effect on the pH. In plating solutions which did not contain NH<sub>4</sub>OH the deposition of ruthenium was not possible. Similarly, with small quantities of NH<sub>4</sub>OH deposition did not occur. The addition of NH<sub>4</sub>OH may result in the formation



of "hydroxy amine ruthenium" or "amine ruthenium" based complexes in solution which are more amenable to reduction than "hydroxy ruthenium" based complexes. With all of these complexes it is necessary to have a small amount of oxalate ion present ( $[\text{oxalate}] = [\text{Ru ions}]$ ) to prevent precipitation of ruthenium oxide at high pH. Table 4 shows that there may be little effect in variation of  $\text{NH}_4\text{OH}$  concentration on the deposition of ruthenium from solution. Although, this small effect may be obscured by the possible effect of substrate surface area.

Attempts to deposit ruthenium from sodium oxalate stabilised solutions of " $\text{RuCl}_3 \cdot x\text{H}_2\text{O}$ " below pH 13 resulted in the precipitation of ruthenium oxide when the solution was heated. This is in contrast to the results of the small scale reactions (previous section (3.4.1.1)) where warming a pH 11 solution of " $\text{RuCl}_3 \cdot x\text{H}_2\text{O}$ " without sodium oxalate did not produce a precipitate.

The appearance of extraneous deposition of ruthenium on the sides of the polypropylene containers is possibly due to the ease with which reduction of the ruthenium complexes in solution occurs. Consequently, the use of surfaces contaminated with ruthenium resulted in the deposition of ruthenium on these surfaces, even if the extraneous deposit from the previous experiment had apparently been removed.

To overcome the problems of extraneous deposition of ruthenium and to improve the performance of the plating solution the stability of the ruthenium complexes in solution had to be improved. This was achieved by use of different complexants or by changing the initial ruthenium reagent. The best electroless deposition of ruthenium from a

solution of “RuCl<sub>3</sub>.xH<sub>2</sub>O” was achieved from a 50 cm<sup>3</sup> plating solution at 50°C with the composition:

“RuCl <sub>3</sub> .xH <sub>2</sub> O”	0.06 g
1 M NaOH	7.5 cm <sup>3</sup>
28% NH <sub>4</sub> OH	5.0 cm <sup>3</sup>
0.25 M Na <sub>2</sub> (COO) <sub>2</sub>	1 cm <sup>3</sup>
1 M N <sub>2</sub> H <sub>4</sub> .H <sub>2</sub> O	1 cm <sup>3</sup>
pH	13

The effect of changing the ruthenium reagent is described in the next section.

#### *3.4.1.3 Attempts to deposit electroless ruthenium from a [Ru(NH<sub>3</sub>)<sub>6</sub>]Cl<sub>3</sub> solution using hydrazine hydrate as reductant*

The change to [Ru(NH<sub>3</sub>)<sub>6</sub>]Cl<sub>3</sub> as the source of ruthenium was made because the compound provided only one ruthenium species in solution. The use of [Ru(NH<sub>3</sub>)<sub>6</sub>]Cl<sub>3</sub> with NaOH and NH<sub>4</sub>OH concentrations as listed above resulted in a similar performance. The solution deposited ruthenium onto a copper substrate and as an extraneous deposit on the sides of the plating vessel. The addition of methylamine was made in an attempt to stabilise the ruthenium complex and prevent the extraneous deposit. This addition appeared to have some beneficial effect on the behaviour of the plating solution, though some extraneous ruthenium deposition was still observed.

The use of solutions of [Ru(NH<sub>3</sub>)<sub>6</sub>]Cl<sub>3</sub> which contained methylamine did result in an improvement in plating performance. But, like plating solutions based on “RuCl<sub>3</sub>.xH<sub>2</sub>O,” decomposition of the solution was observed. Examination of the

literature on ruthenium chemistry yielded few clues as to the possible causes of the decomposition of  $[\text{Ru}(\text{NH}_3)_6]\text{Cl}_3$  solutions. A summary of the chemistry of hexaammine ruthenium (II) and (III) complexes is given in Figure 29.

Dissolution of  $[\text{Ru}(\text{NH}_3)_6]\text{Cl}_3$  in water produced a colourless solution of  $[\text{Ru}(\text{NH}_3)_6]^{3+}$  ions. These ions are reportedly stable in acidic, neutral and alkaline solution, and are inert to substitution. It has been calculated that the half life time for the dissociation of an ammine group is of the order of 3 years.<sup>94</sup> In alkaline solution the formation of an intense yellow colour has been attributed to the formation of the deprotonated species  $[\text{Ru}(\text{NH}_3)_5\text{NH}_2]^{2+}$ ,<sup>91</sup> the  $\text{pK}_a$  of which has been calculated to be 12.4.<sup>97</sup> When the solution was left exposed to air, the intense yellow colour became a deeper yellow and eventually brown. At  $\text{pH} \geq 11$ , in the presence of oxygen, oxidation of a single ammine group to nitrosyl can be achieved.<sup>98,99</sup> The reaction produces a 30% yield of  $[\text{Ru}(\text{NH}_3)_5\text{NO}]^{2+}$ . This reaction is typical of hexaammine ruthenium (III) solution chemistry. These reactions tend to involve oxidation/reduction of an ammine ligand such that the new ligand coordinates to ruthenium through the same nitrogen atom.

The development of the deep yellow/brown colour is prevented, or slowed, by the addition of methylamine before the addition of alkali. Ultra-violet spectrophotometry of  $[\text{Ru}(\text{NH}_3)_6]\text{Cl}_3$  in neutral solution gave a single absorbance at 275 nm, which corresponds to the reported value.<sup>100</sup> In alkaline solution two absorbances were obtained at 275 and 400 nm (which corresponds to  $[\text{Ru}(\text{NH}_3)_5\text{NH}_2]^{2+}$ ).<sup>92</sup> When the solution was allowed develop a deep yellow/brown colour, bands at 275 and 380 nm were observed. The results indicate that only a fraction of the hexaammine is converted

into the new species. It may be that an equilibrium is set up between the hexaammine and the unidentified species, which maybe  $[\text{Ru}(\text{NH}_3)_5\text{NO}]^{2+}$ .

The action of  $\text{OH}^-$  on  $[\text{Ru}(\text{NH}_3)_6]\text{Cl}_3$  to produce the deprotonated species complicated the behaviour of the plating solution. Before the addition of hydrazine hydrate the plating solution did not contain unique ruthenium species. After the addition of hydrazine hydrate, reduction of all these species present occurred. This resulted in the solution initially becoming pale yellow. During plating, the solution slowly became green and eventually, when plating stopped and there had been sufficient exposure to air, a black precipitate was obtained. It must be remembered that when plating was attempted in a closed system with a limited supply of air the green solution did not subsequently produce a precipitate. It is proposed that the reduction of the various ruthenium (III) species to ruthenium metal proceeds via a two-step process. The first, which occurs in the bulk of the solution is the reduction of the ruthenium (III) species to their ruthenium (II) analogues, this is associated with the solution becoming pale in colour. The second step is the reduction of the ruthenium (II) species to ruthenium metal. This two-step process is unlike other electroless plating processes where the metal complex to be reduced is not affected by the presence of the reducing agent in the bulk of solution. Reduction of these metal complexes to the metal occurs only at the catalytic surface of the substrate. The chemical reduction of ruthenium (III) to ruthenium (II) may be achieved using hydrazine hydrate via an outer sphere mechanism.<sup>94</sup> The standard electrode potentials of some ruthenium (III)/(II) couples are given in Table 12. These potentials indicate the ease with which oxidation/reduction between ruthenium (II) and ruthenium (III) complexes can be achieved.

The solution phase reduction of ruthenium (III) to ruthenium (II) results in a further complication to the plating process because the ruthenium (II) ammines are far less stable in alkaline solution than their ruthenium (III) analogues. The chemistry of ruthenium (II) ammines was first investigated by Lever and Powell in 1959<sup>101</sup> and was the subject of a review by Ford.<sup>100</sup>

Lever and Powell<sup>101</sup> reported that the exposure to air of the yellow crystals of hexaammine ruthenium (II) dichloride resulted in the crystals becoming green then blue. In aqueous solution hexaammine ruthenium (II) is moderately stable, especially in the absence of oxygen. In neutral solution hexaammine ruthenium (II) undergoes stepwise acid catalysed aquation which results in a number of unidentified products.<sup>100</sup> In the presence of  $\text{NH}_4\text{OH}$  hexaammine ruthenium (II) decomposes rapidly, especially if oxygen is present, to give as yet unidentified products.<sup>92</sup> In acid solution the decomposition of hexaammine ruthenium (II) results in three products, a blue compound which has an absorbance at 590 nm, a compound with an absorbance in the u.v. spectrum at 262 nm, and a pentaammine ruthenium (III) species.<sup>102</sup> At low pH (circa pH 6) the decomposition products that predominate are the pentaammine ruthenium (III) species and the unidentified species with an absorbance at 262 nm. The appearance of the green colour in the plating solution is consistent with the decomposition of hexaammine ruthenium (II). Its gradual appearance in the plating solution may be due to the competing reactions of decomposition and reduction. As more ruthenium (II) ammines decomposes the potential for the plating solution to deposit ruthenium becomes impaired.

*Extraneous deposition of ruthenium.* As with plating solutions based on "RuCl<sub>3</sub>.xH<sub>2</sub>O" which use hydrazine hydrate, the deposition of extraneous ruthenium is observed. Such deposition on the sides of the plating vessel is possibly an indication of the instability of the plating solution and the ease by which ruthenium (II), and possibly ruthenium (III), can be reduced to ruthenium metal. This instability is particularly noticeable if the plating vessel surfaces are contaminated. The contamination is not necessarily restricted to ruthenium particulates from previous plating experiments. However, it was possible to deposit 68% of the available ruthenium without a simultaneous extraneous deposit when a new plating vessel was used. The extraneous deposition of ruthenium resulted in other technical difficulties. Due to the chemical inertness of the ruthenium it was not possible to remove it all from the sides of the polypropylene plating vessels. As a consequence the plating vessels had only a limited practical plating lifetime.

*Scale up of the plating solution.* The first stage in the development of the electroless ruthenium plating solution involved the deposition of ruthenium from 50 cm<sup>3</sup> plating solutions. These solutions successfully deposited 20% of the available ruthenium onto a copper substrate in 2 h. Scaling up the plating solution to 150 cm<sup>3</sup> involved an increase in the concentration of the main plating solution constituents by a factor of two. For example, in a 50 cm<sup>3</sup> plating solution 0.08 g Ru(NH<sub>3</sub>)<sub>6</sub>Cl<sub>3</sub> was used, this was increased to 0.48 g for a 150 cm<sup>3</sup> plating solution. In 6 h the 150 cm<sup>3</sup> plating solution deposited 40% of the available ruthenium. Therefore, an increase in the concentration resulted in ruthenium deposition of a similar order. The use of new plating containers improved performance so that 68% of the available ruthenium could be deposited. The deposition

of 68% of metal may be the best performance which the solution is capable, because of the instability of ruthenium (II) species.

*Effect of the alkali concentration.* The concentrations of NaOH, NH<sub>4</sub>OH and hydrazine hydrate under which the best plating performance occurred was achieved by the variation of each component in turn from an otherwise constant solution. The results for variation of NaOH and NH<sub>4</sub>OH are given in Figures 17 and 18 respectively. It can be seen that there is a performance maximum for both components. The curve shown for NaOH was obtained from a plating solution which contained the optimum composition of NH<sub>4</sub>OH; and similarly for NH<sub>4</sub>OH.

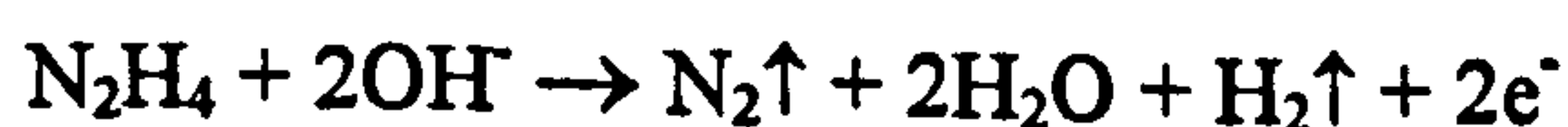
*Effect of reductant concentration.* The effect of hydrazine hydrate concentration on the amount of ruthenium deposited can be seen in Table 6. In the first two experiments 9 cm<sup>3</sup> of 1 M hydrazine was used, which resulted in ruthenium deposition of 14%. A decrease in hydrazine hydrate volume to 6 cm<sup>3</sup> resulted in twice the ruthenium deposition over the same 3 h plating time. These results indicate that there is an optimum concentration of reductant necessary to perform electroless plating. Above this optimum concentration the amount of ruthenium deposited declines. The reason for this decline is unclear, although a similar effect has been observed in other electroless plating processes.

*The effect of substrate surface area.* Although the plating solution performance can be described by an optimum composition, the amount of ruthenium deposited is also dependent on the surface area of the substrate. Figure 19 shows how the amount of ruthenium deposited from 150 cm<sup>3</sup> optimised plating solution varies with substrate

surface area. It can be seen that, for a 150 cm<sup>3</sup> plating solution, there is an optimum surface area of 24 cm<sup>2</sup>, above or below which ruthenium deposition is reduced.

Due to plating solution decomposition, the amount of ruthenium which can be deposited in the lifetime of the plating solution, typically 5 h, is limited to circa 65%. An increase in surface area of the substrate increases the number of active sites at which deposition of ruthenium can occur, and this results in both a greater and faster deposition of metal. Initially, the rate of deposition is determined by the rate of electron transfer. As ruthenium and/or hydrazine in the vicinity of the surface is depleted a concentration gradient develops. Therefore, the rate determining process for deposition becomes controlled by the diffusion of ruthenium ions and/or hydrazine down the concentration gradient. The greater the surface area the earlier deposition becomes diffusion controlled in a bath of a given size. Therefore, as the substrate area is reduced, so the total amount of ruthenium deposited per unit area of substrate in 5 h increases. The amount of ruthenium deposited is further reduced by decomposition of electrolessly active ruthenium species into electrolessly inactive species.

*Variation in pH.* Figure 20 shows the variation in pH with time for an optimised plating solution. The decline over the first 0.5 to 1 h is commonly observed in many electroless processes. In this first 0.5 h the deposition process becomes established and requires a greater usage of the reductant. Consequently, the deposition rate during this period is possibly at its highest. The unified reaction mechanism proposed by van den Meerakker<sup>103</sup> requires OH<sup>-</sup> in the oxidation of hydrazine according to;





Thus, a high deposition rate, or rapid oxidation of hydrazine, will result in a corresponding drop in pH. Once the plating process is established the plating rate tends to become steady requiring a lower consumption of hydroxide ions. The cessation of plating or the decomposition of the plating solution has no effect on the pH of the solution which remains constant.

*Deposition in a closed system.* The performance of the process in a closed system resulted in a quite different pH variation, shown in Figure 21. As in systems which were open to the atmosphere, during the first 0.5 h there is a rapid decline in pH. But after this period there is a recovery in the pH before it becomes steady. The reason for the increase in pH is the release of more alkali into the solution. Repetition of the closed system plating experiment produced the same variation in pH with time. The cause of the release of alkali into the solution is not fully understood and requires further investigation. The retention of  $\text{NH}_3$  gas above the plating solution is unlikely to have such a large influence on the pH of the solution. When  $\text{NH}_3$  gas was trapped in the space above the plating solution, an equilibrium between  $\text{NH}_3$  in solution and that above the solution was established. It was observed that for deposition to occur the presence of both NaOH and  $\text{NH}_3$  (in the form of  $\text{NH}_4\text{OH}$ ) was necessary. The role of the NaOH was to attain, and maintain, the required pH whereas the role of  $\text{NH}_4\text{OH}$  was to regulate the stability of the ruthenium species in the plating solution. It was observed, from experiments which investigated the effect of  $\text{NH}_4\text{OH}$  concentration on deposition, that too high an  $\text{NH}_4\text{OH}$  concentration resulted in lower ruthenium deposition. The other consequence of the use of a closed system was that the rate of ruthenium deposition was decreased. Therefore, retention of a higher concentration of

$\text{NH}_3$  available to the solution by use of a closed system apparently improved the solution stability to a point where it decreased in plating rate.

*Deposition in an inert atmosphere.* The use of a flow of argon to prevent the build up of gases in the space above the solution resulted in plating solution decomposition after 2 h. In effect the plating was performed in an inert atmosphere. Decomposition was observed as a pale green solution with a heavy extraneous deposit of ruthenium on the sides of the plating vessel. The use of a flow of argon gas had the effect of removing any interactions between the plating solution and the gases enclosed above it. In the open system there would be a very small interaction of the  $\text{NH}_3$  above the surface of the solution and the plating solution. As plating progresses this effect will become less significant as  $\text{NH}_3$  is driven off from the solution. An enclosed system represents one limiting condition. The  $\text{NH}_3$  in the space above the solution attains an equilibrium with the solution as described above and is present for longer and in greater concentration, than is the case when the system is open. The use of a flow of argon represents the opposite limiting condition. Above the solution there is no  $\text{NH}_3$  present because it is removed by the flow of argon. As a result the stabilising influence of  $\text{NH}_3$  is lost more rapidly than in an open system. Consequently, the plating solution decomposes earlier.

A further effect of the use of argon to produce an inert system is that the amount of oxygen available to the plating solution is reduced. In electroless plating processes the presence of oxygen is an essential component which generally improves the stability of the metal complexes and increases the plating rate although, in ruthenium plating sufficient exposure to air resulted in the formation of a black precipitate. An increase in the amount of oxygen in the solution, attained by sparging with air, resulted in a brown

solution after 20 minutes (thought to be due to the formation of  $[\text{Ru}(\text{NH}_3)_5\text{NO}]^{2+}$ ) which became green after a further 2 h. Therefore, a decrease in the amount of oxygen in the plating solution resulted in a greater stability, especially of the ruthenium (II) ammines, but a lower plating rate. Thus, for optimum ruthenium plating the use of ordinarily oxygenated solutions is preferred.

*Colloid Investigation.* At one point in the investigation it was suspected that the appearance of the green colour in the plating solution, which precedes the formation of a black precipitate, might be due to the presence of colloidal ruthenium. Colloidal ruthenium, if it was formed, would provide an alternative site for the electroless reduction of ruthenium complexes and might result in the plating solution undergoing rapid decomposition. To determine if colloidal material was present in the solution a Nephelometer was used to measure the light scattered from the solution. The results for the analysis of the plating solution were compared to solutions which were known to contain colloidal material. These results, shown in Table 5, show that no colloidal material was present. The readings of  $<1$  NTU for the plating solution were indistinguishable from the distilled water that was used to prepare the plating solution. The measurements obtained for von Weimarn's gold indicate that the reading is dependent on the size and concentration of the colloid. The larger particle blue colloid gave a reading of 10 NTU whereas the red gold colloid gave readings of 54 NTU. Analysis of the red gold colloid over 2 h resulted in a decrease in the reading obtained. After 2 h reading had fallen to 18 NTU. The decrease in the reading resulted from the formation of particulates caused by the coagulation of the colloid. After 16 h the colloid had precipitated.

*Effects due to mixing.* Investigation into the method by which the plating solutions were prepared indicated that addition of small volumes of alkali of high concentration to solutions of  $[\text{Ru}(\text{NH}_3)_6]\text{Cl}_3$  may have resulted in effects related to slow mixing. By the addition of larger volumes of alkali of lower concentration (to  $[\text{Ru}(\text{NH}_3)_6]\text{Cl}_3$ , after the addition of methylamine, under constant stirring conditions,) a plating solution was obtained which behaved in a more reproducible manner.

*Extension of coating thickness.* The instability of the plating solution did not allow replenishment with  $\text{Ru}(\text{NH}_3)_6\text{Cl}_3$  and/or hydrazine hydrate so as to extend the plating lifetime of the solution. Therefore, to produce coatings of thickness over  $3\ \mu\text{m}$  it was necessary to immerse the substrate into a sequence of fresh plating solutions. A further indication of the ease with which the ruthenium complexes can be reduced to metal was observed when a coating of ruthenium was immersed into a fresh plating solution. Immersion of a ruthenium coating into a plating solution resulted in almost immediate evolution of hydrogen at the surface. Coatings of ruthenium required no activation to catalyse further deposition of ruthenium, even after exposure to air for several days. The lack of a requirement for activation was believed to be due to the chemical inertness of ruthenium metal when exposed to air. With many metals a thin oxide layer is formed on the metal surface after a short exposure to air. This layer is sufficient to prevent further deposition of an electroless coating. Tables 6 and 7 show that resumed deposition onto a ruthenium-coated substrate occurs at the same rate and to the same extent as that at a fresh copper substrate.

*Deposition onto various substrates.* One of the advantages of the electroless deposition process is its ability to deposit coatings onto materials other than metals, such as glass

and plastics. Ruthenium has been deposited successfully onto pure metals (nickel, copper and gold) and alloys (electroless nickel-phosphorus and nickel superalloy). The deposition of ruthenium onto polymethylmethacrylate (perspex) was attempted. The coatings tended to be of poor quality, though well adhered. This may indicate that the preparation of the perspex surface was imperfect.

Deposition onto substrates with a smooth finish (gold, nickel, and the nickel superalloy) resulted in exfoliation of the coating. This was overcome by mechanically roughening the surface, usually by grit blasting, indicating that mechanical binding of the coating to the substrate is as necessary as chemical bonding to produce adherent deposits.

The nickel superalloy (MAR M002) to be coated was provided by Johnson Matthey as a batch of twelve rods. The requirement was to deposit coatings of 2, 5 and 10  $\mu\text{m}$  on three batches of four rods. This was successfully achieved by initially grit blasting the surface to increase the roughness and prevent exfoliation of the coating. The 5 and 10  $\mu\text{m}$  coatings were obtained by successive immersions of the rods in fresh plating solutions.

*Summary.* Throughout this study the instability of the ruthenium (II) species has impaired the performance of the plating solution. Investigation into the behaviour of the plating solution has indicated that, to produce a fully satisfactory plating solution, more stable ruthenium complexes need to be identified. This may be achievable by use of a ruthenium starting material other than hexaammine ruthenium (III) trichloride. Despite the instability of the plating solution good quality bright, adherent coatings were attained.

### 3.4.2 The Characterisation of Electroless Ruthenium Coatings

#### *3.4.2.1 Scanning electron microscopy*

Scanning electron microscopy has shown that when the coating thickness is greater than 2  $\mu\text{m}$ , a “flat” surface is obtained. This indicates that deeper ruthenium deposition has occurred in the valleys of the substrate surface. As the coating thickness increased the grains of the coating merged to produce a smoother texture. It was observed that the surface roughness increased with coating thickness above 2  $\mu\text{m}$ . This increased roughness was caused by nodule formation. As the coating grows some of the grains stand proud of the surface. This is possibly due to favoured deposition at particular points on the surface.

A further factor which may have influenced the topography and surface roughness of the coating was the necessity of immersing the substrate in a sequence of plating solutions to achieve coating of 5 to 10  $\mu\text{m}$ . Though ruthenium coatings do not require an activation procedure, and thus are not reliant on adsorbing a dense monolayer of palladium atoms, the question arises: is deposition initiated uniformly over the entire surface? The concentration of activation sites over a surface can have significant effects on the coating obtained. Too low a concentration of activation sites results in a patchy coating with areas of the substrate remaining uncoated. A high concentration of activation sites results in a coherent coating which is made up of small grains, this generally produces a coating which has a fine texture and no discernible flaws.

#### *3.4.2.2 Action of ammonium persulphate*

Ammonium persulphate was used to determine the porosity of the electroless ruthenium coatings. As the amount of copper dissolved decreased with increasing

coating thickness, so did porosity. However, a 10  $\mu\text{m}$  electroless ruthenium coating did not perform as well as a 5  $\mu\text{m}$  electrodeposited gold coating. Pores in the coating can be the result of a flaw in the substrate surface or the deposition process of the coating. An important part of the preparation of materials for electroless deposition is the activation procedure. This procedure requires the adsorption of catalytic amounts of palladium on to the substrate surface. To produce a good quality pore free coating it is necessary to adsorb a uniform high coverage layer. This is so that the grains of deposited ruthenium can quickly merge to produce a continuous coating. In electrodeposition the uniform dense coverage of activation sites is provided by an external electric current, and as such may be more effective in the production of low porosity coatings.

#### *3.4.2.3 Potentiodynamic corrosion analysis*

The polarisation profiles of the metals presented in Figure 26 (the aerated system) show significant differences from their respective profiles in Figure 27 (the de-aerated system). The differences can be attributed to the removal of oxygen from the system by purging with argon before and during analysis. For an electroless ruthenium coating on copper it might be possible for a battery to be set up between the copper substrate and oxygen in the solution. As a consequence an erroneous characterisation of the corrosion performance of the ruthenium coating could be obtained. A purge of the system with argon was performed to suppress this battery effect by the removal of oxygen. It was observed, however, that the removal of oxygen from the system had no significant effect on the value of  $E_{\text{corr}}$  obtained, although the value of the open circuit potential (OCP) was increased. Generally, the platinum group metals were more

resistant to corrosion in the de-aerated system.

The OCP values for copper in aerated and de-aerated conditions are negative and a similar value of  $E_{\text{corr}}$  was obtained under both conditions. For the platinum group metals the values of the OCP were significantly higher in the de-aerated system. The OCP is the potential obtained when the metals were exposed to  $\text{H}_2\text{SO}_4$ , either aerated or de-aerated, before the overpotential was applied. In Figure 27 values of the OCPs obtained for the various metals in the de-aerated system have been plotted onto their respective corrosion profiles. It can be seen for the platinum group metals that the OCP occurs in the region of the profile associated with chemical unreactivity. For copper the OCP occurs in the region of the copper profile consistent with corrosion. As a result copper will corrode in accordance with the Tafel equation (2.2.2.2i) whereas the platinum group metals remain inert. It should be noted that the corrosion characteristics of platinum group metals have always been difficult to determine.<sup>104</sup>

### 3.4.3 Investigation into other possible ruthenium compounds as starting materials

#### *3.4.3.1 Ammonium pentachloroaquo ruthenium (III)*

In the absence of a complexant, the addition of hydroxide ions to a solution of  $[\text{RuCl}_5(\text{H}_2\text{O})]^{2-}$  resulted in substitution of some of the labile ligands. In the presence of a reducing agent the formation of a ruthenium oxide resulted. Use of complexants such as EDTA and ethylenediamine (en) result in the formation of complexes which are too stable to undergo electroless deposition. The addition of EDTA to  $[\text{RuCl}_5(\text{H}_2\text{O})]^{2-}$  results in the formation of the yellow complex  $[\text{Ru}(\text{HEDTA})\text{Cl}]$ , which undergoes substitution to  $[\text{Ru}(\text{EDTA})\text{OH}]^{2-}$  on the addition of hydroxide ions.<sup>92</sup> The formation of a blue colour in some of these solutions is thought to result from the presence of both



ruthenium (II) and (III) complexes.<sup>93</sup> Addition of ethylenediamine to  $[\text{RuCl}_5(\text{H}_2\text{O})]^{2-}$  resulted in the formation of the green  $[\text{Ru}(\text{en})\text{Cl}_3]_2$ .<sup>92</sup> In alkaline solution substitution of chloride ions by  $\text{OH}^-$  is possible.

The green tris-oxalato ruthenium (III) complex produced by the addition of oxalate to a solution of  $[\text{RuCl}_5(\text{H}_2\text{O})]^{2-}$  is insufficiently stable to prevent the production of ruthenium oxide on addition of hydroxide ions.

The addition of methylamine to  $[\text{RuCl}_5(\text{H}_2\text{O})]^{2-}$  may result in the formation of  $[\text{Ru}(\text{NH}_2\text{CH}_3)_6]^{3+}$  or a mixed complex of the type  $[\text{Ru}(\text{NH}_2\text{CH}_3)_x\text{Cl}_y]^{(3-y)+/-}$ . The subsequent addition of  $\text{NaOH}$  and  $\text{NH}_4\text{OH}$  may result in the formation of a complex of the type  $[\text{Ru}(\text{NH}_2\text{CH}_3)_x(\text{NH}_3)_y]^{3+}$ . In alkaline solution the deep yellow colour produced may be due to the formation of a deprotonated species, similar to  $[\text{Ru}(\text{NH}_2\text{CH}_3)_5(\text{NHCH}_3)]^{2+}$ , (c.f.  $[\text{Ru}(\text{NH}_3)_5(\text{NH}_2)]^{2+}$ ). This methylamine/ammine complex is similar to hexaammine ruthenium (III) and deposited ruthenium onto activated copper without an accompanying extraneous deposit onto the sides of the glass plating vessel. The presence of methylamine ligands in the ruthenium complex may have had a beneficial effect on the stability of the plating solution. However, further work is necessary to indicate whether this complex would perform better than the hexaammine ruthenium (III) used.

### 3.3.3.2 Potassium pentachloronitrosyl ruthenium (III)

In alkaline solution, replacement of the chlorine ligands by hydroxide ions may be preferred to replacement by ammonia. However, plating solutions involving the use of a nitrosyl complex can provide electrolessly deposited ruthenium, but may need to be further stabilised by the addition of a complexant, such as methylamine.

### 3.5 CONCLUSIONS

#### 3.5.1 The electroless ruthenium plating solution

The electroless deposition of ruthenium was achieved from a 150 cm<sup>3</sup> plating solution having the following optimum composition:

[Ru(NH <sub>3</sub> ) <sub>6</sub> ]Cl <sub>3</sub>	0.48 g
0.25 M methylamine	6 cm <sup>3</sup>
1 M NaOH	45 cm <sup>3</sup>
14% NH <sub>4</sub> OH	15 cm <sup>3</sup>
1 M hydrazine hydrate	6 cm <sup>3</sup>
pH	13
Temperature	60°C

The plating solution is prepared as follows: [Ru(NH<sub>3</sub>)<sub>6</sub>]Cl<sub>3</sub> is dissolved in 50 cm<sup>3</sup> distilled water; under constant stirring methylamine is added followed by NaOH then NH<sub>4</sub>OH; the volume is made up to 144 cm<sup>3</sup> with the addition of 28 cm<sup>3</sup> distilled water; the plating solution is then heated to 60°C and hydrazine hydrate is added followed immediately by immersion of the activated substrate.

Both methylamine and NH<sub>4</sub>OH have a stabilising influence on the plating solution and the pH during plating is constant. Plating is observed with hydrogen and nitrogen evolved at the substrate surface within 60 s of immersion of the substrate. The substrate appears to be completely coated after 5 to 10 min.

The plating solution will deposit approximately 65% of the total ruthenium in solution onto a substrate with a surface area of 25 cm<sup>2</sup> in 5 h. This corresponds to a coating

thickness of 3  $\mu\text{m}$ . Using clean polypropylene containers it is possible to deposit ruthenium without an extraneous deposit onto the sides of the container. However, repetitive use of the same container may result in a greater likelihood of an extraneous deposit of ruthenium occurring.

The coatings produced are bright, adherent, and continuous. Scanning electron microscopy shows the coatings to be dense with no observable defects or pores. The plating solution has been successfully used to deposit ruthenium onto activated metals and plastics.

The porosity of electroless ruthenium coatings decreases with increasing coating thickness. However, the performance of a 10  $\mu\text{m}$  coating is inferior to a 5  $\mu\text{m}$  electrodeposited gold coating. It may be possible to improve the porosity of the coatings by improvement in the process of absorbing palladium atoms on to the substrate surface to ensure a constant high surface coverage.

Although the corrosion properties of platinum group metals are difficult to determine, exposure to aerated or de-aerated  $\text{H}_2\text{SO}_4$  resulted in the metals having a value of  $E_{\text{corr}}$  lower than that for copper. However, the natural potential (or OCP) of the metals exposed under these conditions lies in the region of the polarisation profile which can be associated with passivity, unlike that of copper which lies in the anodic Tafel region which corresponds to corrosion.

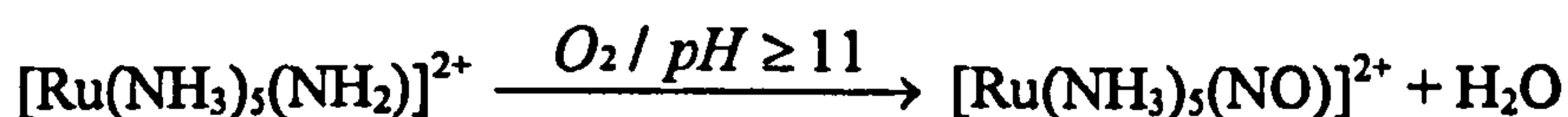
### 3.5.2 Chemistry of the plating solution

In neutral solution dissolution of  $[\text{Ru}(\text{NH}_3)_6]\text{Cl}_3$  gives the complex ion  $[\text{Ru}(\text{NH}_3)_6]^{3+}$ .

Addition of NaOH results in an equilibrium between the hexaammine and a deprotonated species, which gives rise to an intense yellow colour:<sup>25</sup>



At  $\text{pH} \geq 11$  in the presence of oxygen, the oxidation of an ammine ligand may occur which results in the formation of pentaammine nitrosyl ruthenium(III)<sup>98</sup> complex according to:



Ultra violet spectra of the intense yellow and deep yellow/brown solutions both show two absorbances. In each of the two spectra one absorbance (at 275 nm) is the same and corresponds to  $[\text{Ru}(\text{NH}_3)_6]^{3+}$ . The difference in the position of the absorbance maximum of the other peak may indicate that one can be assigned to the deprotonated species (400 nm) and the other is attributable to a product of the oxidation of the deprotonated species. A report by Pell and Armor<sup>99</sup> suggests that the oxidation produces a 30% yield of the nitrosyl complex. The addition of methylamine appears to prevent this oxidation.

It is believed that the electroless deposition proceeds via a two step process. The first is the reduction of ruthenium(III) complexes to their ruthenium(II) analogues and occurs in the bulk of solution. The second step is the reduction of ruthenium(II) species to ruthenium metal at a catalytically active surface. Ruthenium(II) amines however, are unstable in solutions containing  $\text{NH}_3$  and oxygen. Therefore, not only does electroless deposition occur, but the decomposition of ruthenium(II) species into electrolessly

inactive species also takes place. This decomposition is observed as the formation of a green colour during plating, which ultimately leads to a cessation in plating.

Deposition in an inert atmosphere results in premature solution decomposition. A purge with air or oxygen can also result in premature decomposition of the plating solution.

Analysis of the plating solution with a Nephelometer shows that decomposition of the solution does not involve the formation of colloidal ruthenium.

### **3.6 LIST OF TABLES**

**Table 4. Ruthenium deposition from a "RuCl<sub>3</sub>.xH<sub>2</sub>O" solution with variation in NaOH and NH<sub>3</sub> concentration**

**Table 5. Nephelometric analysis of electroless ruthenium plating solutions**

**Table 6. Reproducibility in plating performance of a [Ru(NH<sub>3</sub>)<sub>6</sub>]Cl<sub>3</sub> solution without the presence of methylamine**

**Table 7. Reproducibility in plating performance of a [Ru(NH<sub>3</sub>)<sub>6</sub>]Cl<sub>3</sub> solution with the presence of methylamine**

**Table 8. Average surface roughness, Ra, of various metal substrates**

**Table 9. Values of the average surface roughness of electroless ruthenium coatings of various thickness**

**Table 10. Copper content of ammonium persulphate solutions with variation in ruthenium coating thickness**

**Table 11. Potentiodynamic corrosion analysis of some platinum group metals**

**Table 12. Electrode potentials of some ruthenium compounds**

**Table 4. Ruthenium deposition from a "RuCl<sub>3</sub>.xH<sub>2</sub>O" solution with variation in NaOH and NH<sub>3</sub> concentration**

NaOH <sup>†</sup> /cm <sup>2</sup>	NH <sub>3</sub> <sup>‡</sup> /cm <sup>2</sup>	Weight /mg	Thickness /μm	Surface Area/cm <sup>2</sup>	Ruthenium Deposited/%	mg/cm <sup>2</sup>
4.5	5	2.0	0.3	5.7	8.0	0.35
6	5	3.3	0.5	5.6	13.0	0.59
9	5	3.9	0.6	4.6	15.0	0.85
9	5	4.1	0.6	5.1	16.0	0.80
7.5	4	2.3	0.4	4.6	9.0	0.50
7.5	5	5.2	0.5	7.6	20.0	0.68
7.5	8	2.4	0.3	6.0	9.5	0.40
7.5	8	1.9	0.3	5.1	7.6	0.37
7.5	10	2.8	0.5	4.5	11.2	0.62

<sup>†</sup> as 1 M NaOH.

<sup>‡</sup> as 28% NH<sub>3</sub> solution.

**Table 5. Nephelometric analysis of electroless ruthenium plating solutions**

Colloidal system	Reading/ NTU
Standard (0-100 NTU)*	56.00
Standard (0-10 NTU)*	5.70
MnO <sub>2</sub> Colloid	30.00
von Weirmarns Gold (blue)	10.00
von Weirmarns Gold (red)	54.00
Plating solution (4 h)	<1
Plating solution (5 h)	<1
Plating solution (6 h)	<1
Distilled water	<1

\*These standards were supplied with the instrument by the manufacturers



**Table 6. Reproducibility in plating performance of a  $[\text{Ru}(\text{NH}_3)_6]\text{Cl}_3$  solution without the presence of methylamine**

Solution Number	1 <sup>a</sup>	2 <sup>a</sup>	3 <sup>b</sup>	4 <sup>b</sup>
Surface Area /cm <sup>2</sup>	6.90	←	←	←
Total Coating Weight /mg	10.4	19.5	43.9	65.1
Coating Thickness /μm	1.2	1.0	2.8	2.4
Total Coating Thickness/μm	-	2.2	5.0	7.4
Surface Area /cm <sup>2</sup>	7.80	6.68	7.95	8.10
Coating Weight /mg	11.5	12.4	24.9	21.0
Coating Thickness /μm	1.2	1.1	2.5	2.0
Ruthenium Utilised /%	14	14	32	27

<sup>a</sup>experiments using 9 cm<sup>3</sup> 1 M hydrazine solution

<sup>b</sup>experiments using 6 cm<sup>3</sup> 1 M hydrazine solution

**Table 7. Reproducibility in plating performance of a  $[\text{Ru}(\text{NH}_3)_6]\text{Cl}_3$  solution with the presence of methylamine**

Solution Number	1	2
Surface Area /cm <sup>2</sup>	24.5	←
Coating Weight /mg	32.5	43.0
Coating Thickness /μm	1.1	1.4
Total Coating Thickness/μm	-	2.5
Surface Area /cm <sup>2</sup>	24.5	24.5
Coating Weight /mg	34.1	43.8
Coating Thickness /μm	1.1	1.4
Ruthenium Utilised /%	20	20

**Table 8. Average surface roughness, Ra, of various metal substrates**

Substrate	<sup>a</sup> Ra /Å	<sup>b</sup> Maximum Thickness /μm
Etched Cu sheet	1185	N/R <sup>d</sup>
E/less Ni-P on Cu	858	3.8
<sup>c</sup> AISI 304 SS	241	-
Electro-Ni on 304SS	204	-
Ni sheet	183	2.5

<sup>a</sup> Average surface roughness

<sup>b</sup> Coating Thickness reached before exfoliation observed

<sup>c</sup> Stainless Steel

<sup>d</sup> Exfoliation not observed on 10 μm coating

**Table 9. Values of the average surface roughness of electroless ruthenium coatings of various thickness**

Coating	Coating Thickness / $\mu\text{m}$	Surface Roughness / $\text{\AA}$
Copper substrate	0	1185
Ruthenium	2	607
Ruthenium	4	1426
Ruthenium	10	1815

**Table 10. Copper content of ammonium persulphate solutions with variation in electroless ruthenium coating thickness**

Coating	Coating Thickness / $\mu\text{m}$	Copper Content /ppm
Ruthenium	4	120
Ruthenium	6	100
Ruthenium	10	70
Gold*	5	5

\*electrodeposited (supplied by Johnson Matthey plc.)

**Table 11. Potentiodynamic corrosion analysis of some platinum group metals**

Item Under Test	$E_{\text{corr}}/V$		O. C. P./V <sup>†</sup>	
	Argon	Air	Argon	Air
Copper sheet	-0.156	-0.036	-0.046	-0.003
Platinum sheet	-0.199	-0.244	+0.661	+0.642
Palladium sheet	-0.157	-0.216	+0.362	+0.857
Copper/Ruthenium (10 $\mu\text{m}$ )	-0.237	-0.233	+0.474	+0.236

<sup>†</sup>Open Circuit Potential

**Table 12. Electrode potentials of some ruthenium compounds**

Half Reaction	$E^\circ$ vs SHE /V
$\text{Ru}^{3+} + e \rightleftharpoons \text{Ru}^{2+}$	0.249
$\text{Ru}^{2+} + 2e \rightleftharpoons \text{Ru}$	0.455
$\text{RuO}_2 + 4\text{H}^+ + 2e \rightleftharpoons \text{Ru}^{2+} + 3\text{H}_2\text{O}$	1.120
$\text{RuO}_4 + 6\text{H}^+ + 4e \rightleftharpoons \text{Ru}(\text{OH})_2 + 2\text{H}_2\text{O}$	1.400
$[\text{Ru}(\text{NH}_3)_6]^{3+} + e \rightleftharpoons [\text{Ru}(\text{NH}_3)_6]^{2+}$	0.100
$[\text{Ru}(\text{NH}_3)_5\text{H}_2\text{O}]^{3+} + e \rightleftharpoons [\text{Ru}(\text{NH}_3)_5\text{H}_2\text{O}]^{2+}$	0.066
$[\text{Ru}(\text{H}_2\text{O})_6]^{3+} + e \rightleftharpoons [\text{Ru}(\text{H}_2\text{O})_6]^{2+}$	0.230
$[\text{Ru}(\text{en})_3]^{3+} + e \rightleftharpoons [\text{Ru}(\text{en})_3]^{2+}$	0.210
$[\text{Ru}(\text{bipy})_3]^{3+} + e \rightleftharpoons [\text{Ru}(\text{bipy})_3]^{2+}$	1.240

### **3.7 LIST OF FIGURES**

**Figure 14. Schematic diagram of nephelometric analysis**

**Figure 15. Schematic diagram of holder assembly used for porosity determination**

**Figure 16. Schematic diagram for surface profile determination**

**Figure 17. Effect of variation in NaOH concentration on ruthenium deposition**

**Figure 18. Effect of variation in  $\text{NH}_4\text{OH}$  concentration on ruthenium deposition**

**Figure 19. Effect of surface area on ruthenium deposition**

**Figure 20. Variation in pH during plating of electroless ruthenium plating solutions when exposed to air**

**Figure 21. Comparison of pH variation of enclosed (curve 1) and exposed (curve 2) electroless ruthenium plating solutions**

**Figure 22. Scanning electron micrograph of polished nickel sheet**

**Figure 23. Scanning electron micrograph of acid etched copper sheet**

**Figure 24. Scanning electron micrographs of electroless ruthenium coatings on copper of various thickness. (a) 1  $\mu\text{m}$ , (b) 2  $\mu\text{m}$ , (c) 5  $\mu\text{m}$ , and (d) 10  $\mu\text{m}$**

**Figure 25. Scanning electron micrographs of electroless ruthenium coatings in cross-section. (a) 5  $\mu\text{m}$ , and (b) 10  $\mu\text{m}$**

**Figure 26. Polarisation profiles of platinum group metals in aerated 0.5 M sulphuric acid**

**Figure 27. Polarisation profiles of platinum group metals in argon de-aerated sulphuric acid**

**Figure 28. Summary of the chemistry of ruthenium trichloride**

**Figure 29. Summary of the chemistry of hexaammine ruthenium trichloride**

**Figure 14. Schematic diagram of nephelometric analysis**

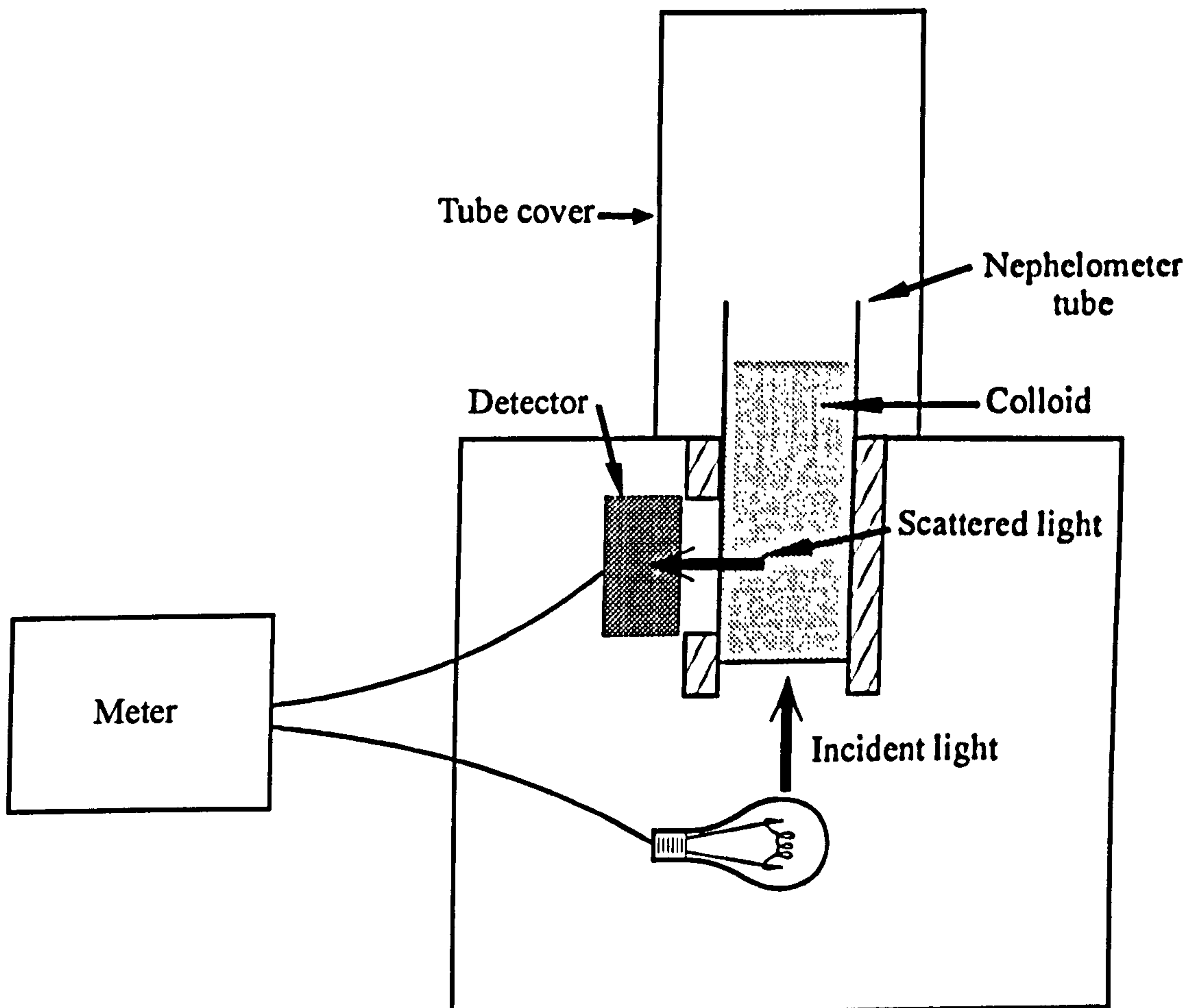


**Figure 15. Schematic diagram of holder assembly used for porosity determination**

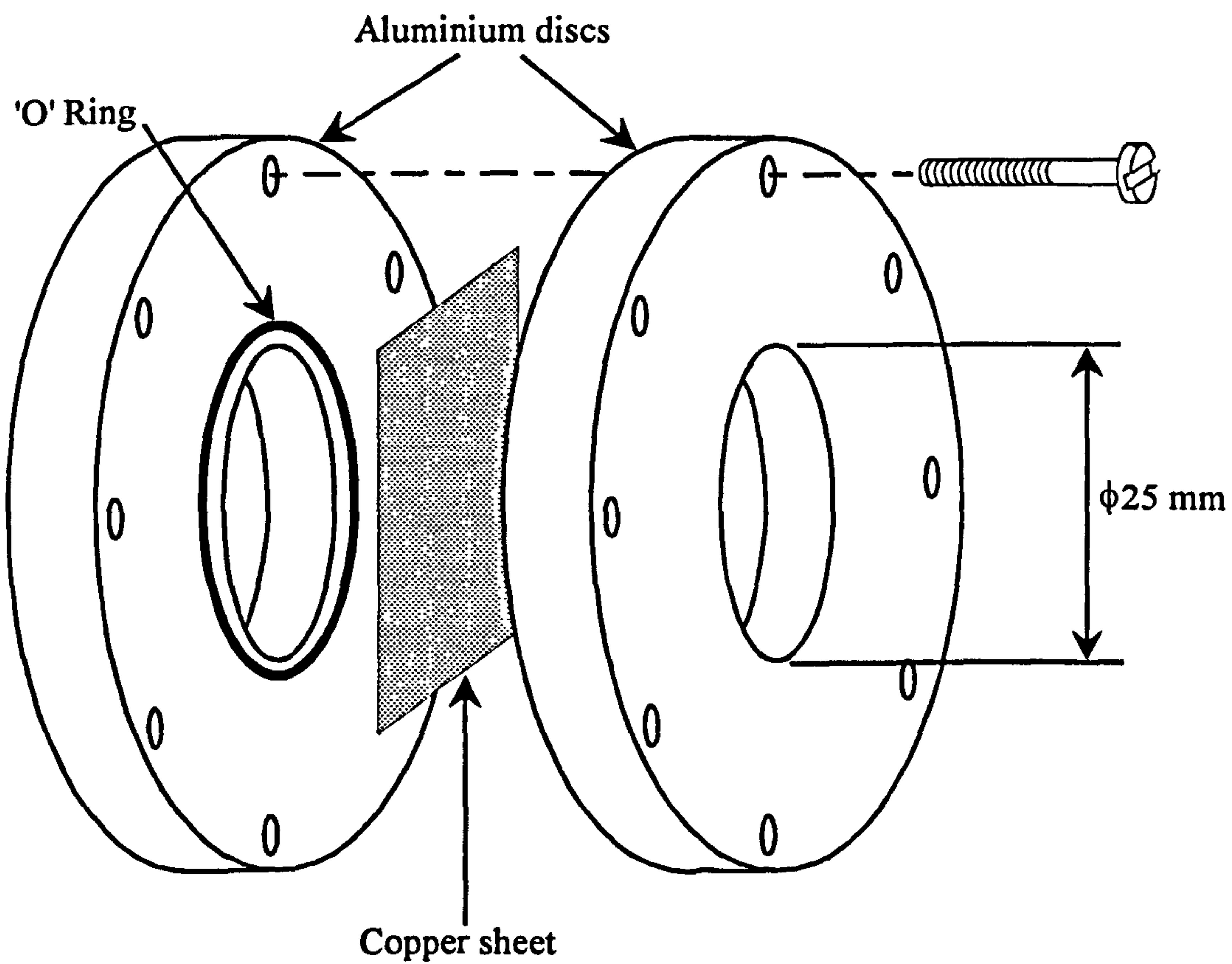
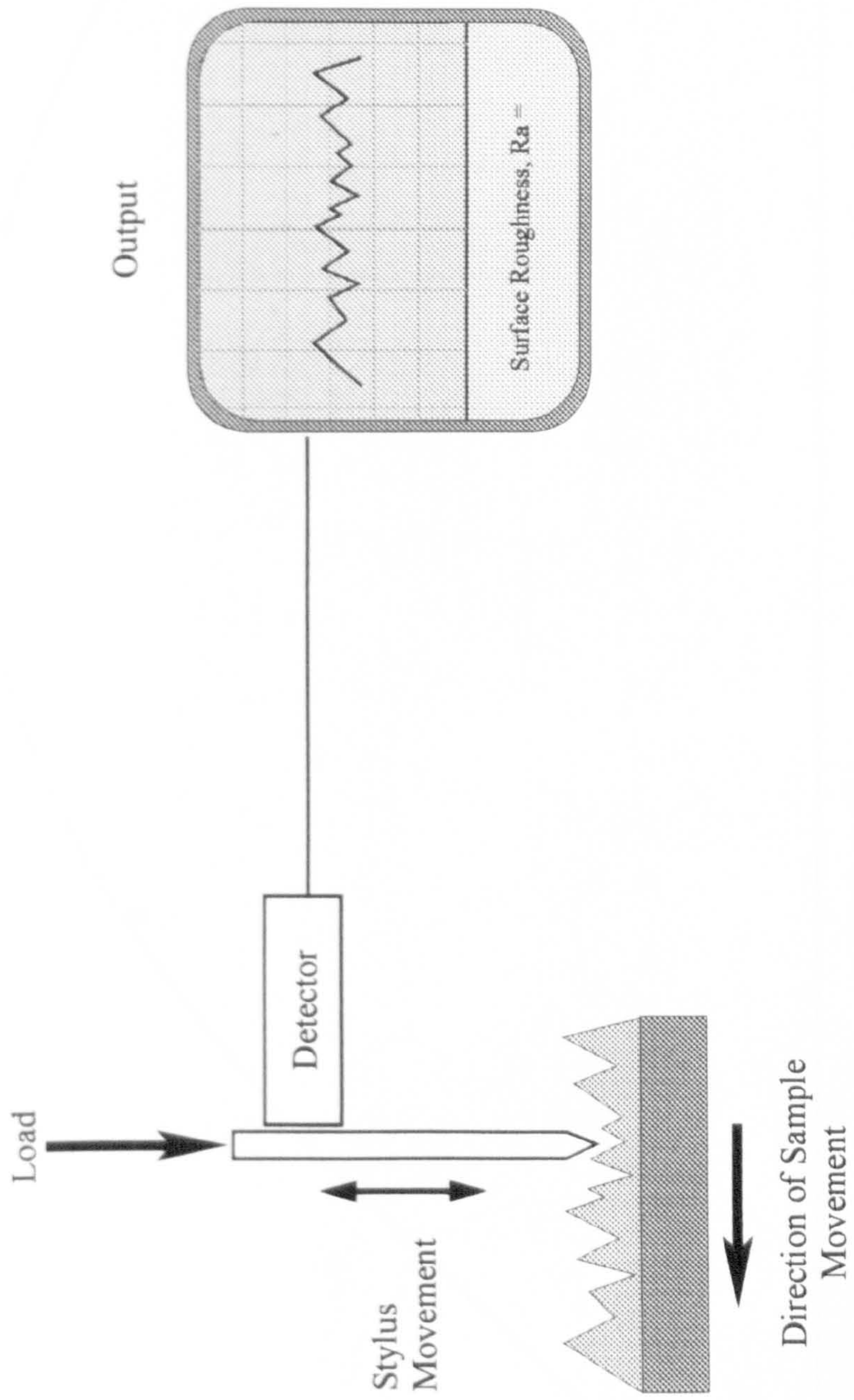


Figure 16. Schematic diagram for surface profile determination





**Figure 17. Effect of variation in NaOH concentration on ruthenium deposition**

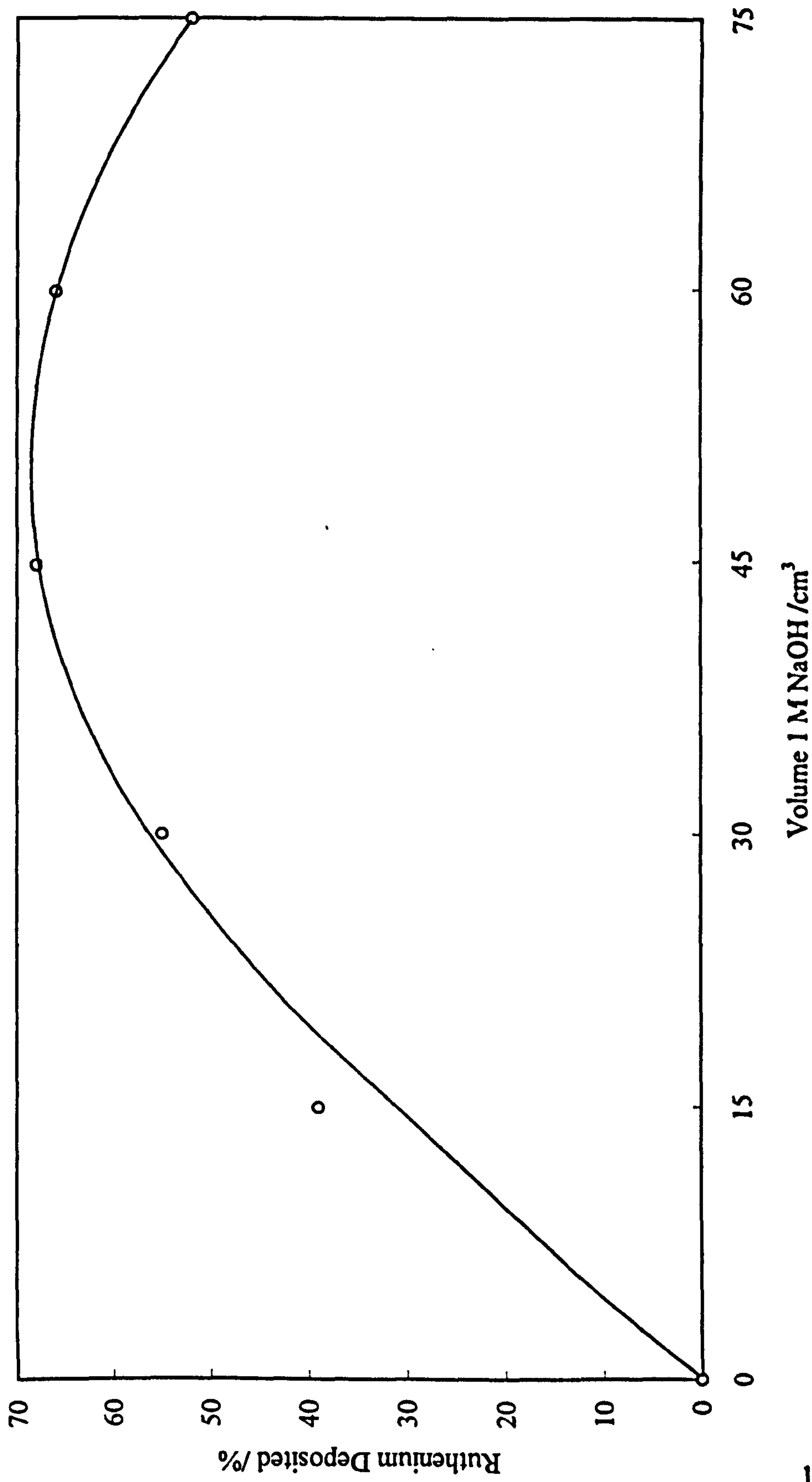
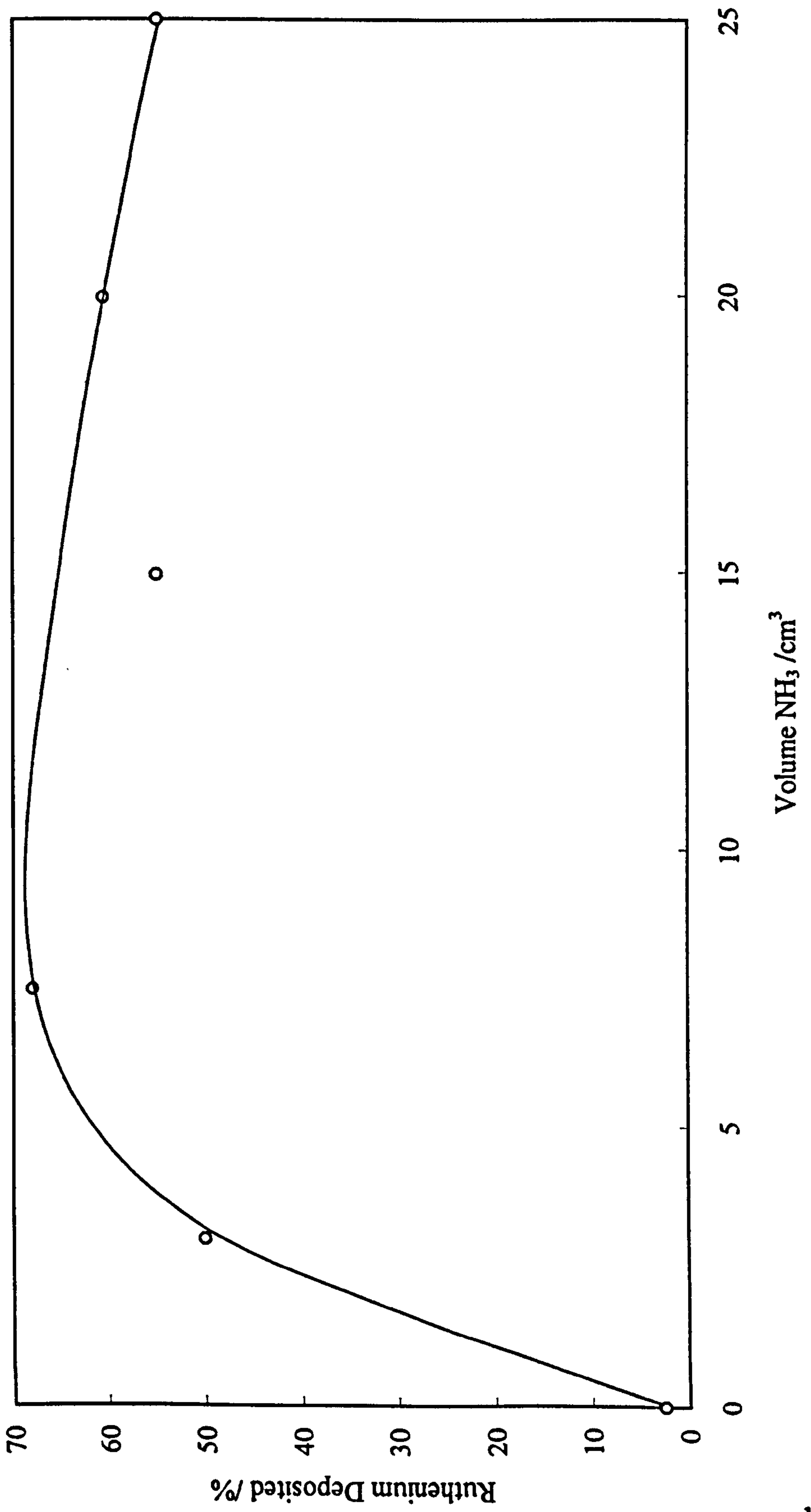


Figure 18. Effect of variation in  $\text{NH}_3$  concentration on ruthenium deposition



**Figure 19. Effect of substrate surface area on ruthenium deposition**

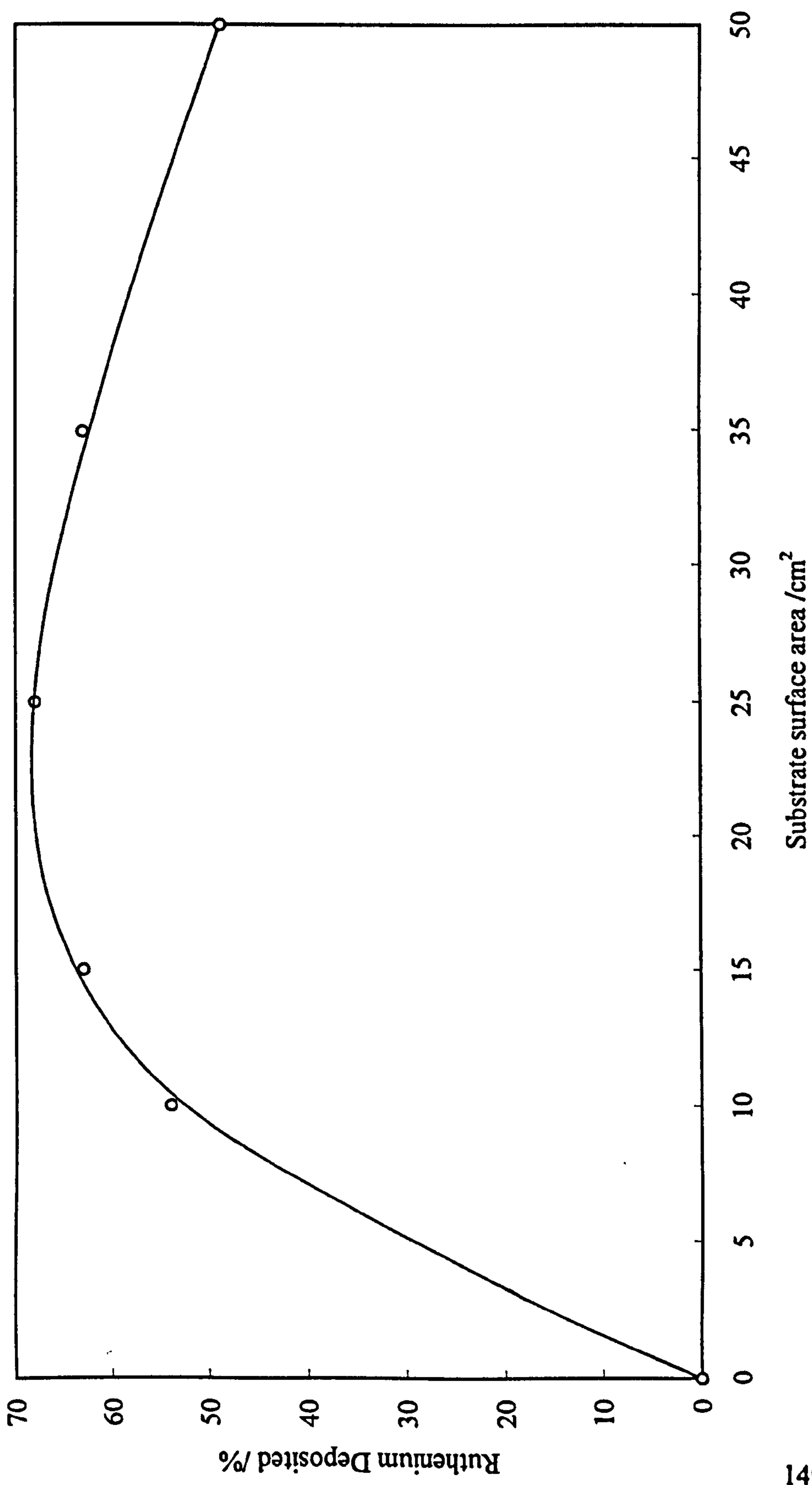


Figure 20. Variation in pH during plating of electroless ruthenium plating solutions when exposed to air

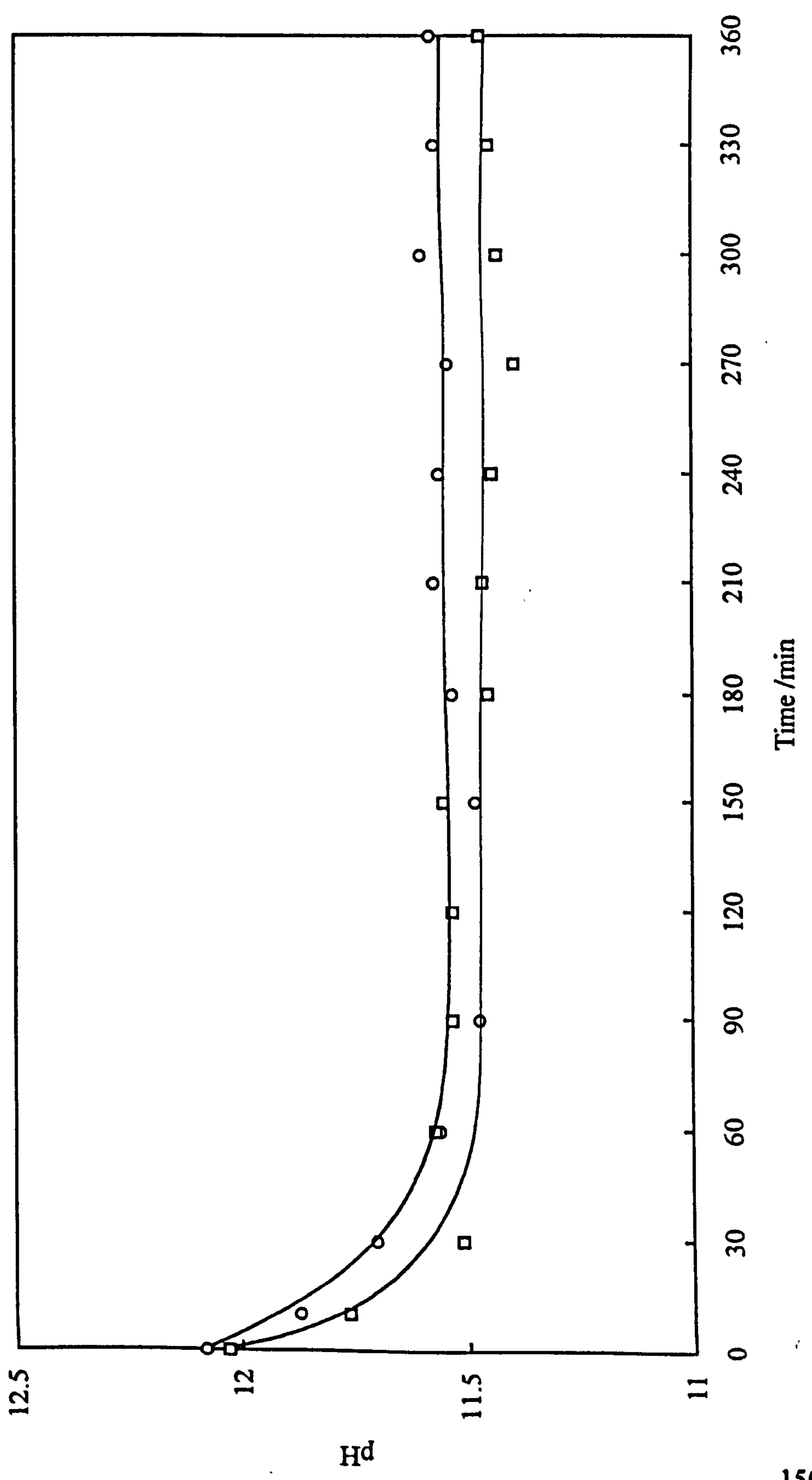
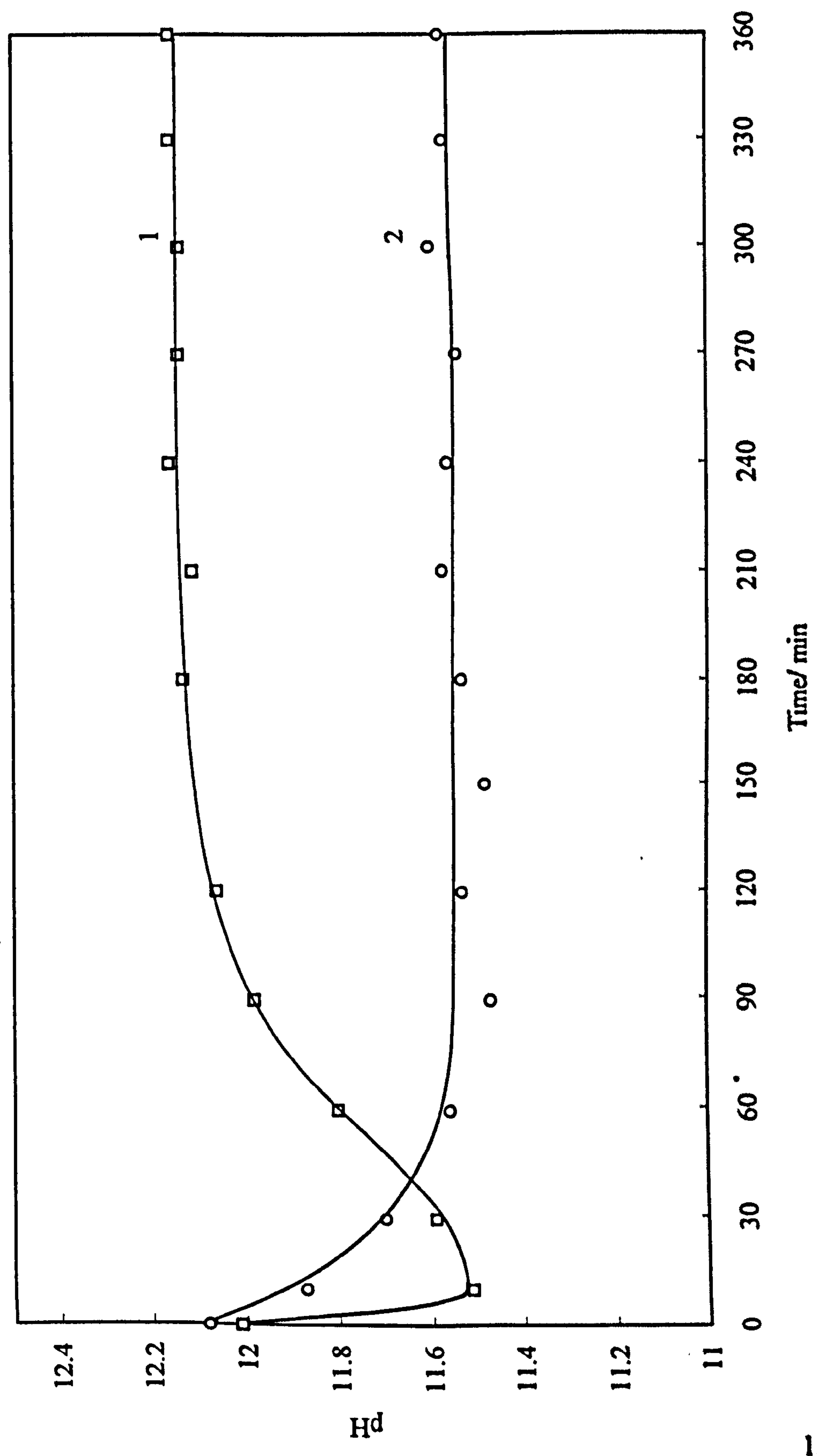
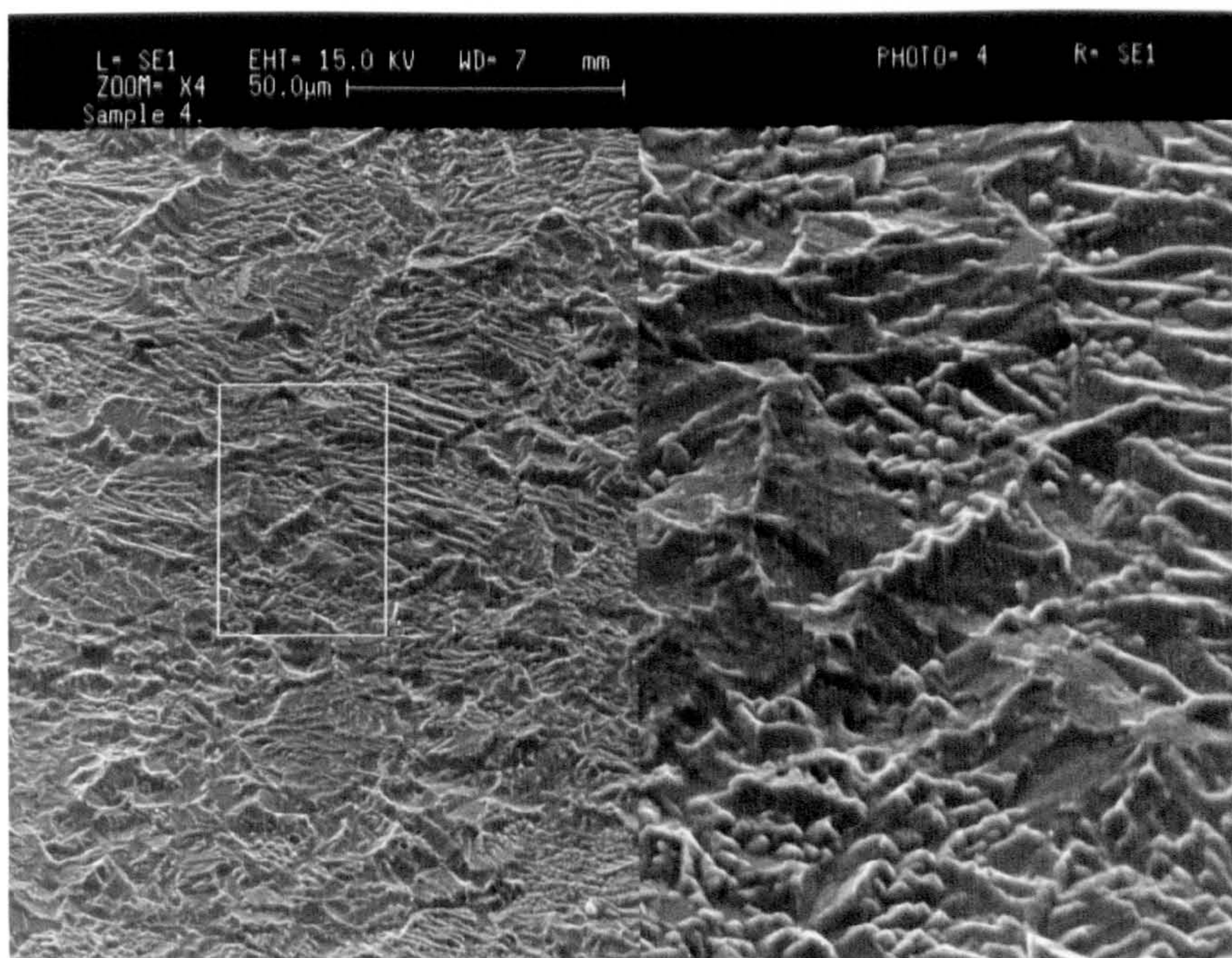


Figure 21. Comparison of pH variation of enclosed (curve 1) and exposed (curve 2) electroless ruthenium plating solutions





**Figure 22. Scanning electron micrograph of nickel sheet**



**Figure 23. Scanning electron micrograph of acid etched copper sheet**

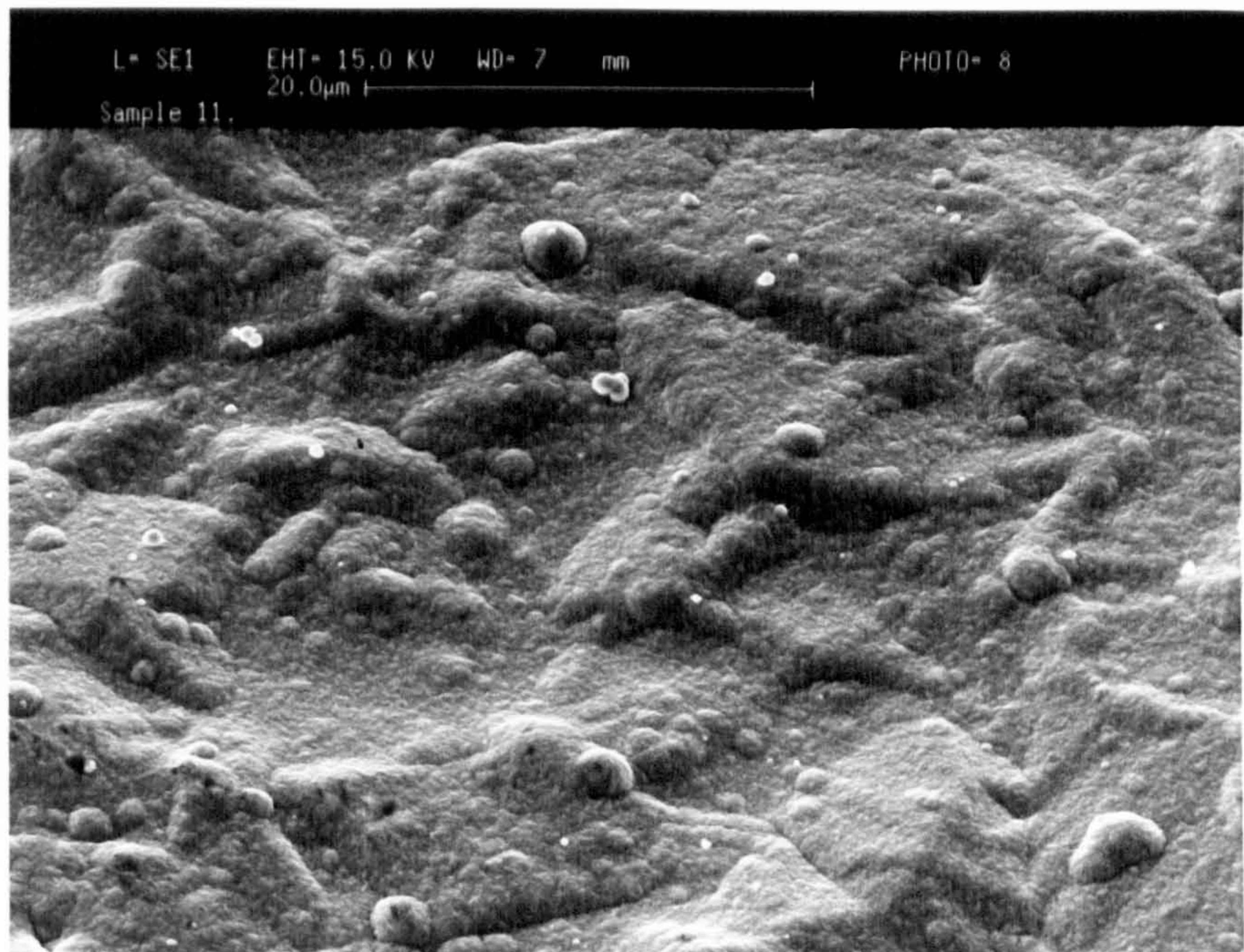


**Figure 24(a). Scanning electron micrograph of 1 μm electroless ruthenium on copper sheet**

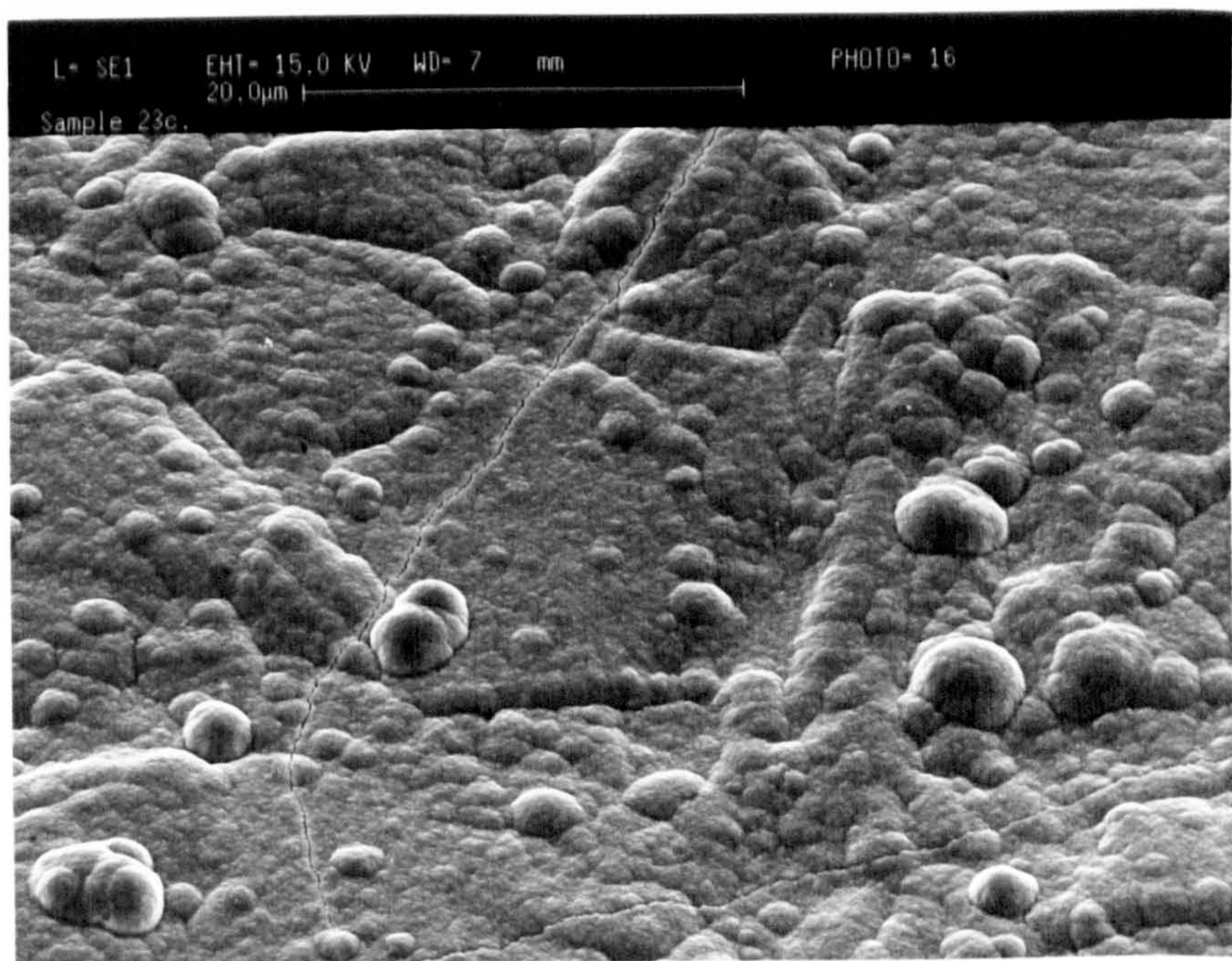


**Figure 24(b). Electron micrograph of 2 μm electroless ruthenium on copper sheet**

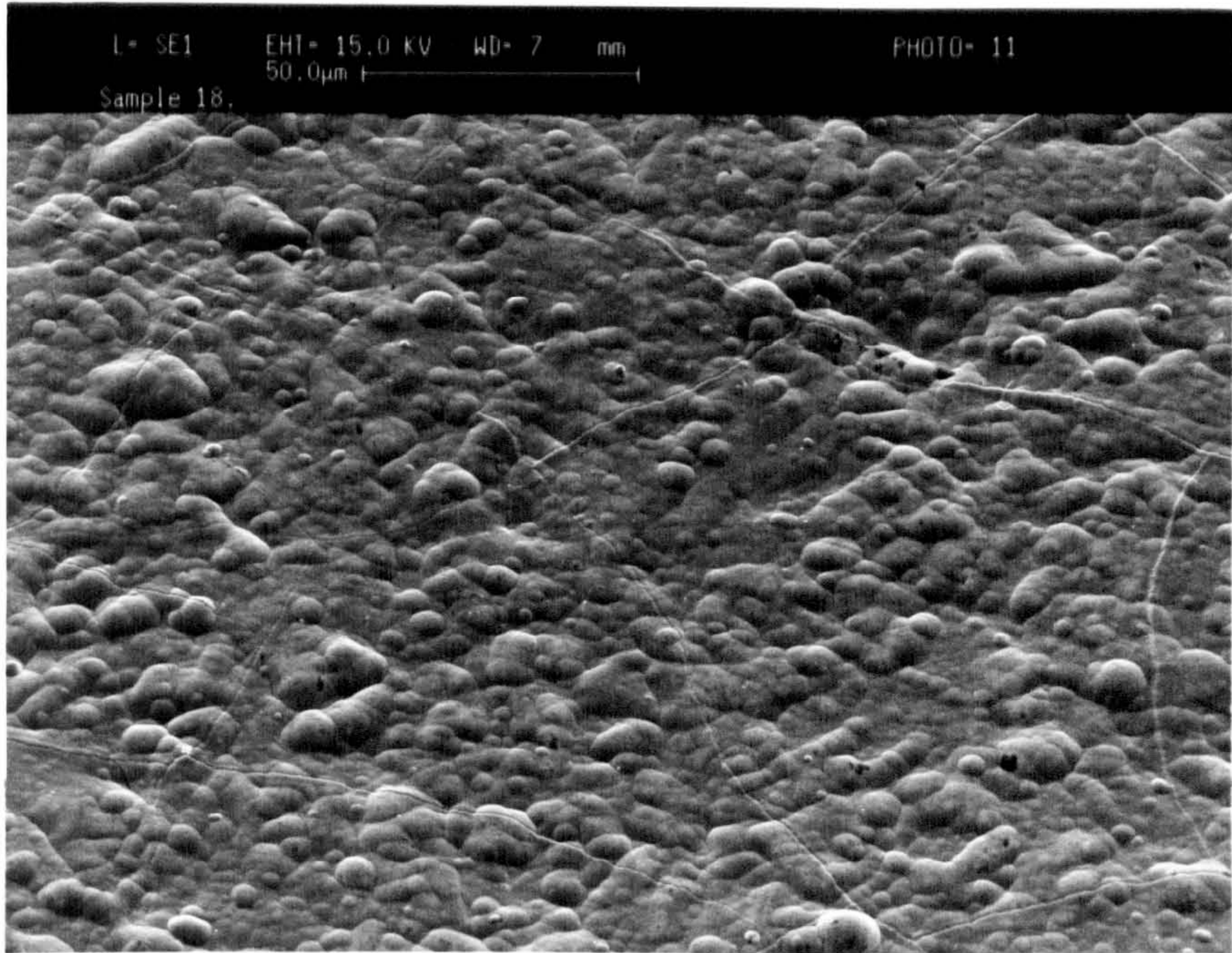


**Figure 24(c). Scanning electron micrograph of 5 μm electroless ruthenium on copper sheet**

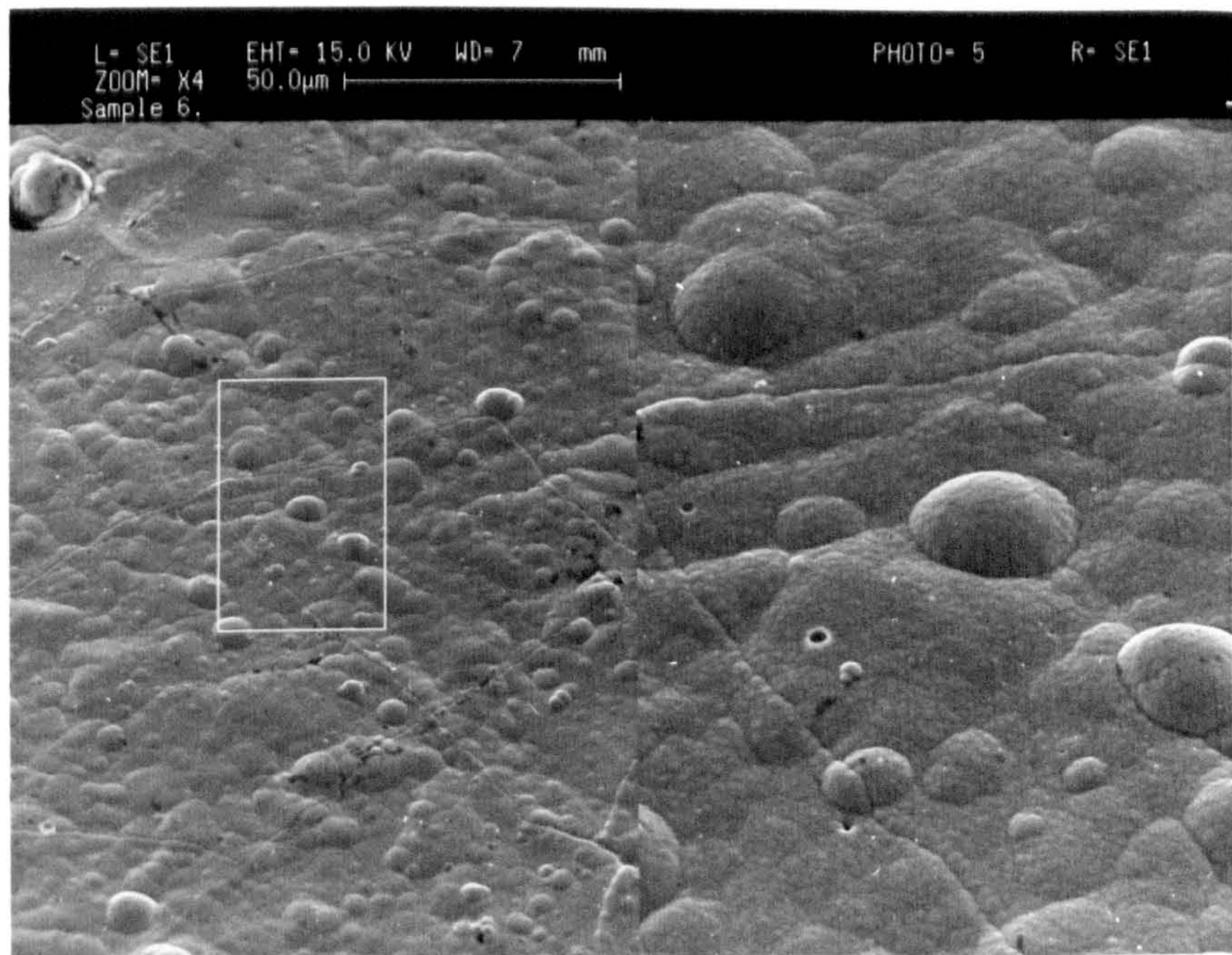


**Figure 24(d). Scanning electron micrograph of 10 μm electroless ruthenium on copper sheet**



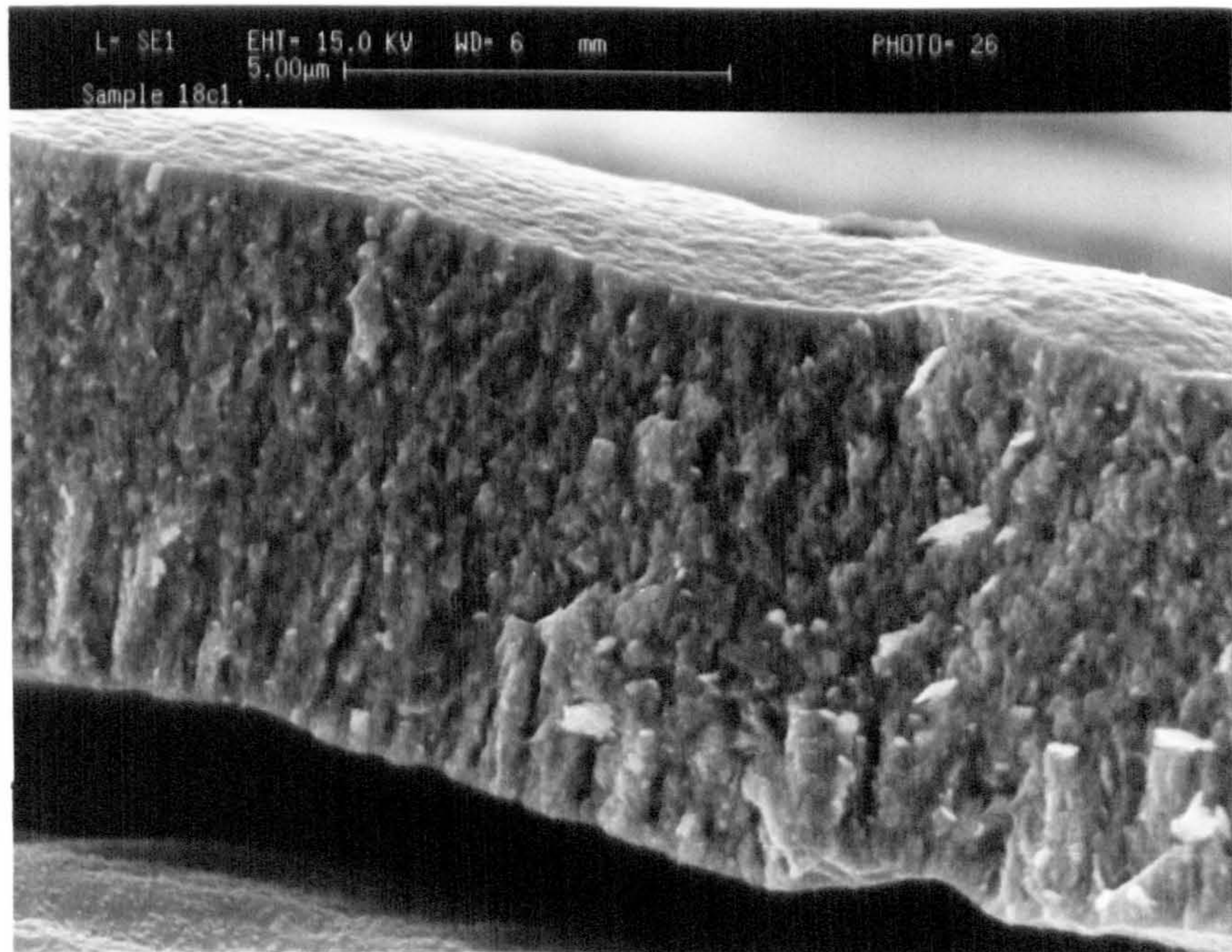


**Figure 25(a). Cross sectional scanning electron micrograph of 5 μm electroless ruthenium**

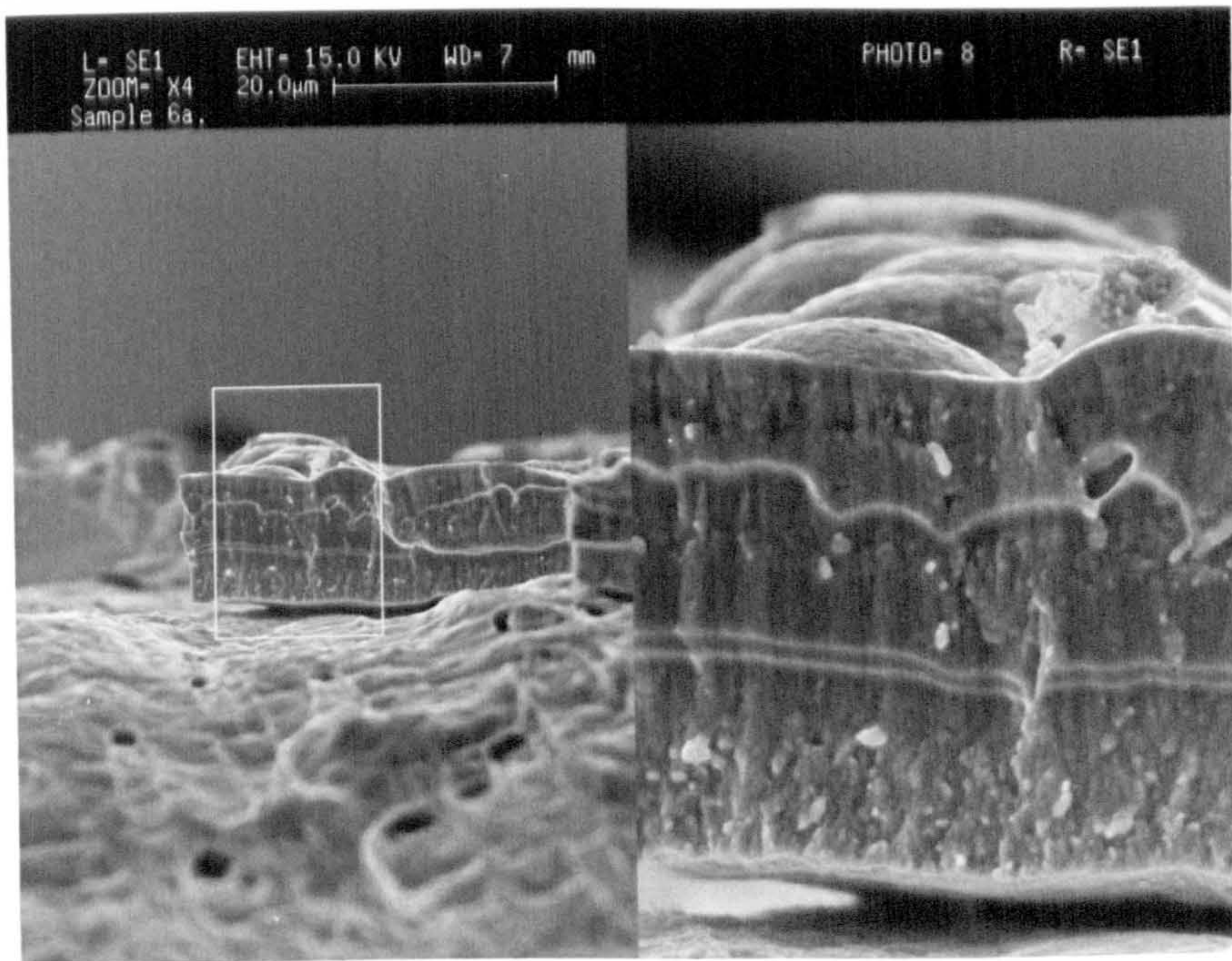


**Figure 25(b). Cross sectional scanning electron micrograph of 10 μm electroless ruthenium**

Figure 26. Polarisation profiles of various platinum group metals in aerated 0.5 M sulphuric acid

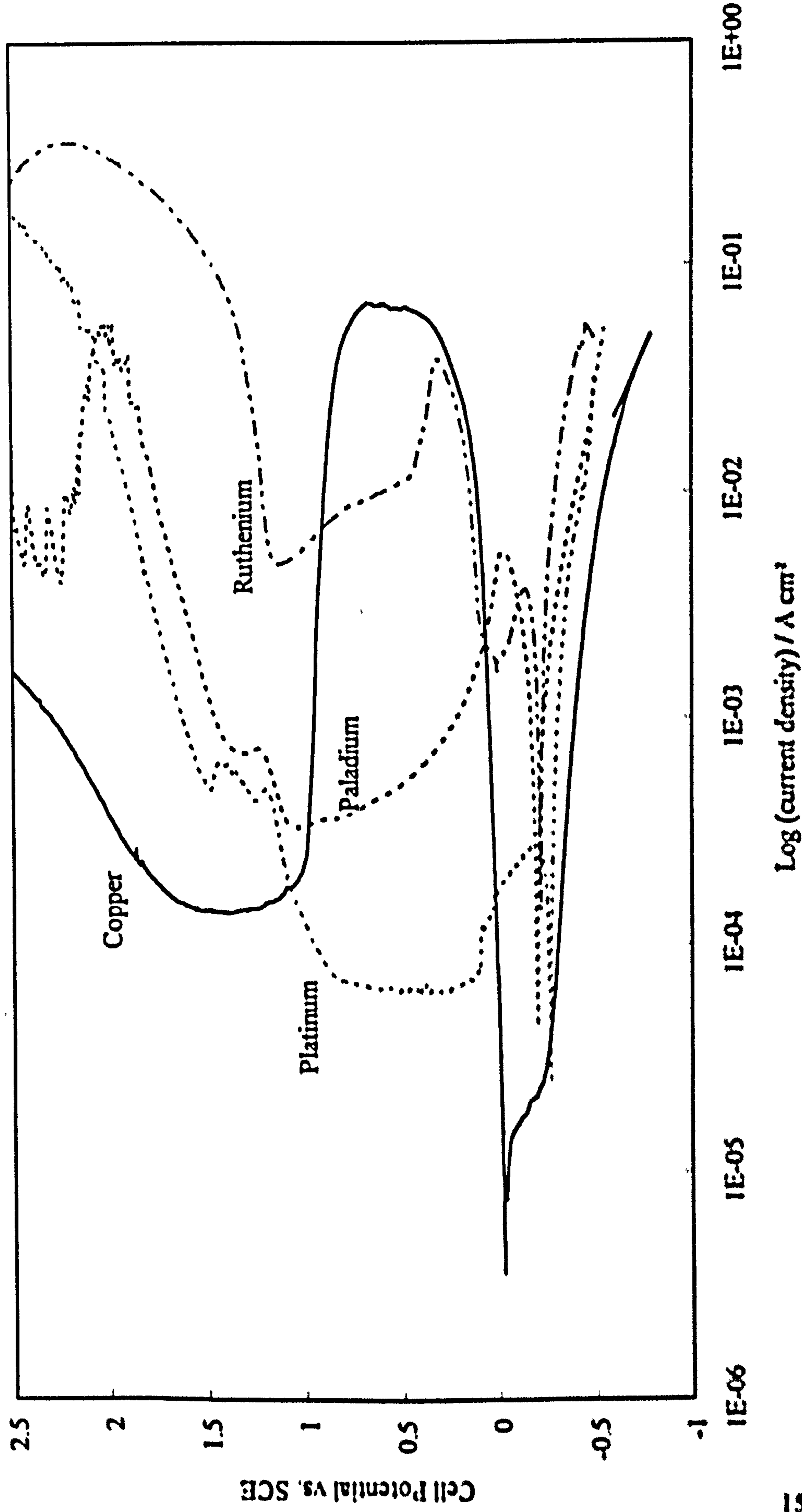


Figure 27. Polarisation profiles of platinum group metals in argon de-aerated 0.5 M sulphuric acid

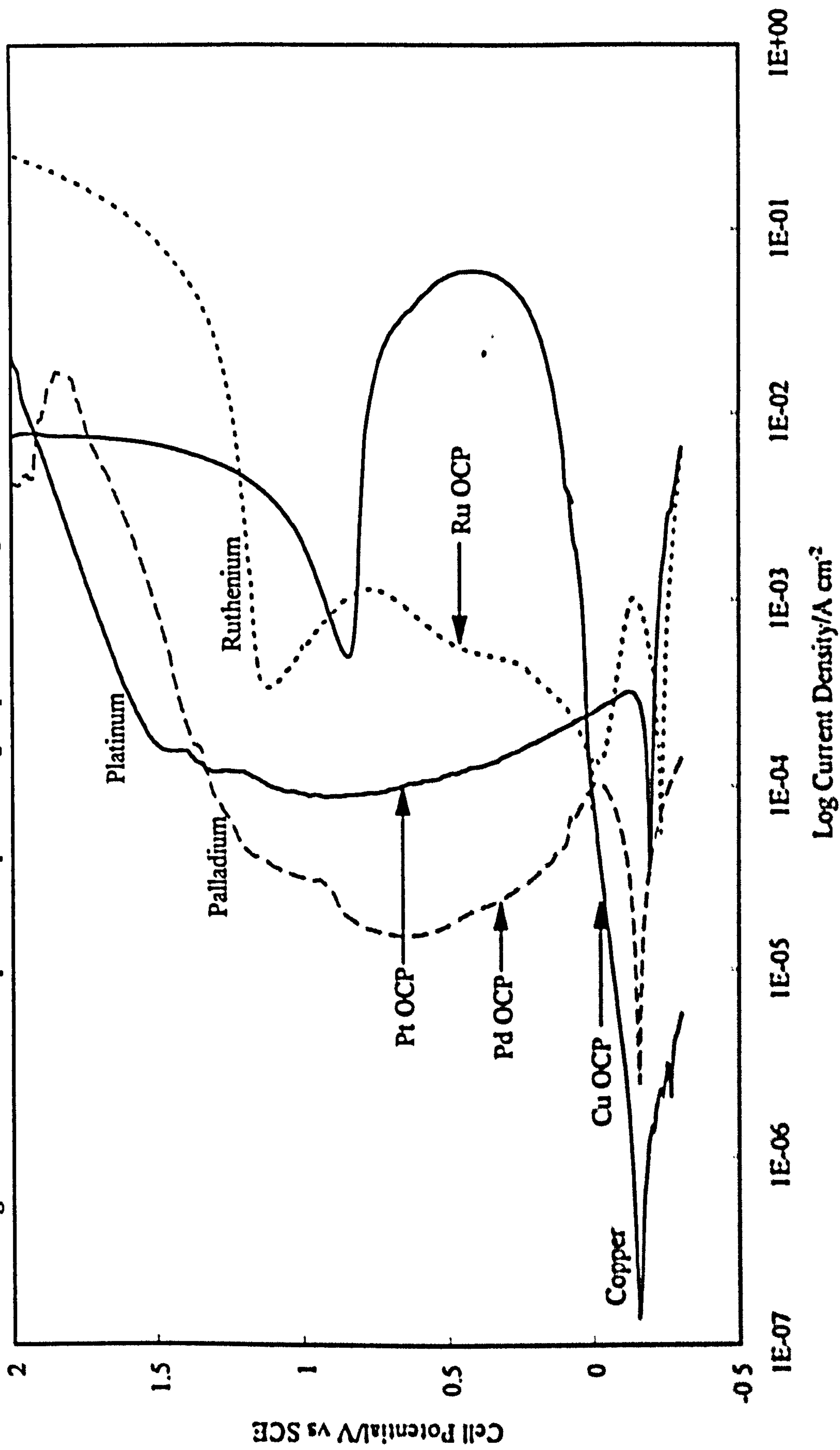
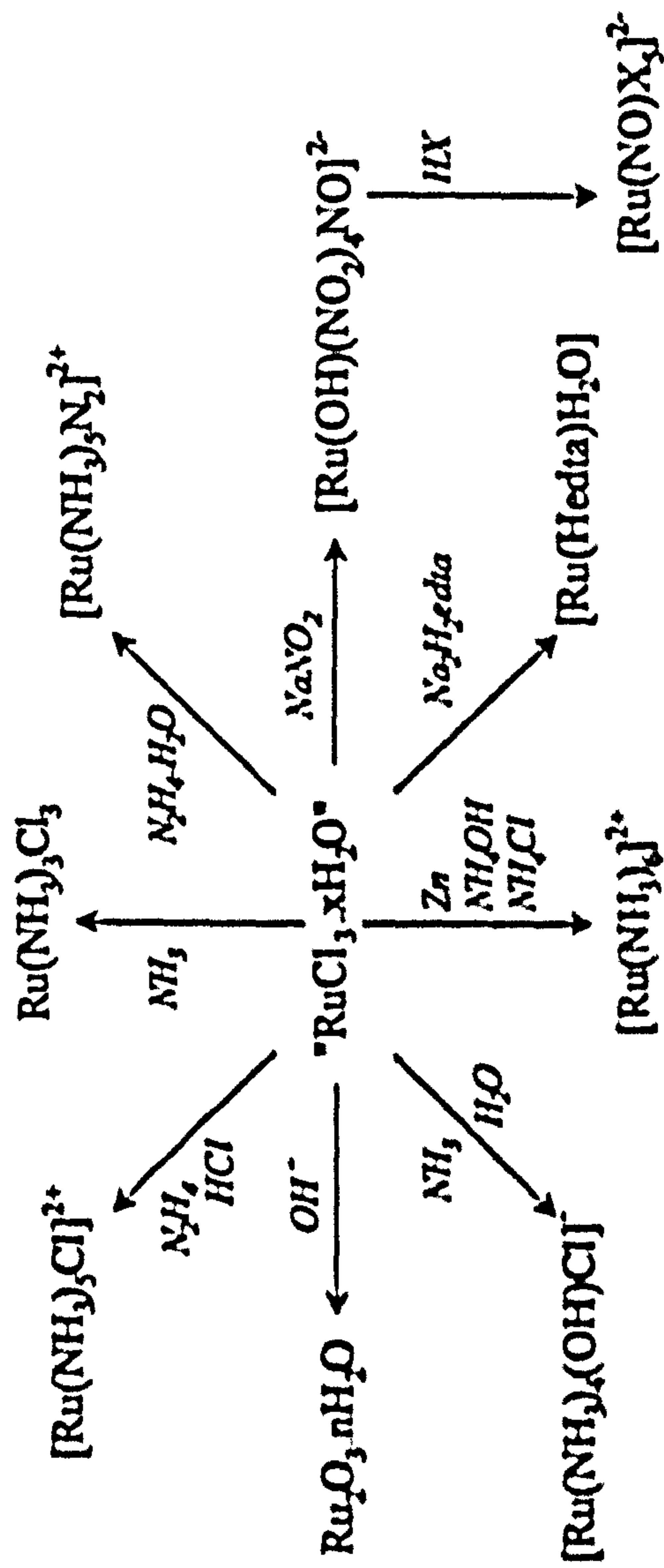


Figure 28. Summary of the chemistry of ruthenium trichloride





## **CHAPTER 4**

### ***B*ibliography**

#### **4 BIBLIOGRAPHY**

1. A. Brenner and G. Riddell, *J. Nat. Bur. Stnds.*, 1946, 37, 31; 1947, 39, 385.
2. A. Wurtz, *Ann. Chim. et Phys.*, 1844, 3, 11.
3. P. Breteau, *Bull. Soc. Chim.*, 1911, 2, 515.
4. F. A. Roux, U. S. Patent 1,207,218 (1916).
5. "Electroless Plating: Fundamentals and Applications" Eds. G. O. Mallorety and J. B. Hajdu, American Electroplaters and Surface Finishers Society, Ohio, 1990.
6. H. Deng and P. Moller, *Pltg. Surf. Finish.*, 1994, 81(3), 73.
7. G. J. Shawhan and R. P. Tracy, *Metal Finishing*, 1988, 6, 85.
8. R. A. Jeanmenne, *Pltg. Surf. Finish.*, 1994, 81(3), 39 and 104.
9. F. Pearlstein, *Metal Finishing*, 1955, 53(8), 59.
10. "Electroless Nickel Plating" W. Riedel, ASM International, Ohio, 1991.
11. D. J. Levy, *Electrochem. Techn.*, 1963, 1(1/2), 38.
12. K. Lang, *Galvanotechnik.*, 1965, 56, 347.
13. R. D. Fisher and N. H. Chilton, *J. Electrochem. Soc.*, 1962, 109(6), 485.
14. F. Pearlstein and R. F. Weightman, *Plating*, 1974, 61, 154.
15. W. Goldie, *Plating*, 1964, 11, 1069.
16. Y. Okinaka, *Pltg. Surf. Finish.*, 1970, 57, 914.
17. F. Pearlstein and R. F. Weightman, *J. Electrochem. Soc.*, 1974, 121(8), 1023.
18. R. N. Rhoda, *Trans. I. M. F.*, 1959, 36, 82.
19. R. N. Rhoda, *J. Electrochem. Soc.*, 1961, 108(7), 707.
20. W. V. Hough, J. L. Little and K. E. Warheit, U.S. Patent 4,255,194 (1981).
21. R. N Rhoda and R. F. Vines, U. S. Patent 3,486,928 (1969).

22. J. Valsiunienne, J. Vinkevicius and A. Yu. Prokopchick, *Leit. TSR Moksulu Akaid. Darb., Ser. B*, 1976, 5, 25.
23. V. Strejcek, German Patent (Ger. Offen.), DE 2607988 (1977).
24. E. Torikai, Y. Kawami and K. Takenaka, Japanese Patent (Kokai Tokkyo Koho), 84-80766 (1984).
25. Y. S. Chang and M. L. Chou, *J. Appl. Phys.*, 1991, 69(11), 7848.
26. J. Valsiunienne and A. Norgailaite, *Leit. TSR Moksulu Akaid. Darb., Ser. B*, 1980, 2, 3.
27. D. W. Baudrand, *Pltg. Surf. Finish.*, 1979, 11, 18.
28. K. Parker, *Pltg. Surf. Finish.*, 1992, 79(3), 29.
29. J. W. Dini and P. R. Coronado, *Plating*, 1967, 54, 385.
30. G. O. Mallory, *Plating*, 1971, 58(4), 319.
31. A. W. Goldenstein, W. Rostoker, F. Schossberger and G. Gutzeit, *J. Electrochem. Soc.*, 1957, 104(2), 104.
32. A. H. Graham, R. W. Lindsay and H. J. Read, *J. Electrochem. Soc.*, 112(4), 401.
33. P. S. Kumar and P. K. Nair, *J. Mater. Sci. Ltrrs.*, 1994, 13, 671.
34. Q. X. Mai, R. D. Daniels and H. B. Harpalani, *Thin Solid Films*, 1988, 166, 235.
35. K.-H. Hur, J.-H. Jeong and D. N. Lee, *J. Mater. Sci.*, 1990, 25, 2573.
36. M. Erming, L. Shofu and L. Pengxing, *Thin Solid Films*, 1988, 166, 273.
37. M. Bayes, I. Sinitskaya, K. Schell and R. House, *Trans. I.M.F.*, 1991, 69(4), 140.
38. K. M. Gorbunova, M. V. Ivanov and V. P. Moiseev, *J. Electrochem. Soc.*, 1973, 120(5), 613.
39. P. B. Bedingsfield, D. B. Lewis, P. K. Datta, J. S. Gray, and P. B. Wells, *Trans. I.M.F.*, 1991, 70(1), 19.



40. W. T. Evans and M. Schlesinger, *J. Electrochem. Soc.*, 1994, 141(1), 78.
41. P. B. Bedingfield, Ph.D. Thesis, University of Northumbria, 1993.
42. A. J. Gould, *Trans. I.M.F.*, 1988, 66, 58.
43. A. P. van Gool, P. J. Boden and S. J. Harris, *Trans. I.M.F.*, 1987, 65, 108.
44. Z. Longfei, L. Shoufu and L. Pengxing, *Surf. Coat. Technol.*, 1988, 36, 455.
45. P.-H. Lo, W.-T. Tsai, J.-T. Lee and M.-P. Hung, *Surf. Coat. Technol.*, 1994, 67,  
27.
46. J. Flis and D. J. Duquette, *Corrosion*, 1985, 41(12), 700.
47. P. K. Datta, K. N. Strafford and S. Allaway in "Surface Engineering Practice" Ellis  
Horwood, 1990, p. 643.
48. J. Bielinski and K. Kaminski, *Surf. Coat. Technol.*, 1987, 31, 223.
49. "Advances in Electrochemical Science and Engineering" Eds. H. Gerischer and C.  
N. Tobia, VCH, Weinheim and New York, 1993, Volume 3, p. 55.
50. A. Hung and K.-M. Chen, *J. Electrochem. Soc.*, 1989, 136(1), 72.
51. H. Honma and T. Kobayashi, *J. Electrochem. Soc.*, 1994, 141(3), 730.
52. T. Berzins, U.S. Patent 3,338,726 (1967).
53. Y. H. Chang, C. C. Lin, M. P. Hung and T. S. Chin, *J. Electrochem. Soc.*, 1986,  
133, 985.
54. E. I. Saranov, N. K. Bukalov and A. B. Lunden, *Prot. Met.*, 1969, 6, 563.
55. A. Molenaar and J. J. C. Coumans, *Surface Tech.*, 1982, 16, 265.
56. Y. Okinaka and C. Wolowodiuk, *Plating*, 1971, 58, 1080.
57. M. Matsuoka, S. Imanishi, M. Sahara and T. Hayashi, *Pltg. Surf. Finish.*, 1988,  
75(5), 102.
58. C. D. Iacovangelo, *J. Electrochem. Soc.*, 1991, 138(4), 976.

59. S. D. Swan and E. L. Gostin, *Met. Finish.*, 1961, 59(4), 52.
60. E. L. Gostin and S. D. Swan, U.S. Patent 3,032,436 (1962).
61. J. Ushio, O. Miyazaura, A. Tonizawa, H. Yokono, N. Kanda, N. Matsaura, S. Ando, H. Okahira and K. Mori, Japanese Patent (Kokai Tokkyo Koho), 89-268876 (1989).
62. M. Kuto, k. Niikura, S. Hoshino and I. Ohno, *J. Surf. Finish. Soc. Jpn.*, 1991, 42, 729.
63. F. Pearlstein and R. F. Weightman, *Plating*, 1969, 56, 1158.
64. H. Ocken, C. C. Lin and D. H. Lister, *Thin Solid Films*, 1989, 171, 323.
65. S. N. Athanvale and M. K. Totalni, *Met. Finish.*, 1989, 87, 23.
66. H. Ocken, B. G. Pound and D. H. Lister, *Thin Solid Films*, 1989, 171, 313.
67. P. Steinmetz, S. Alperine, A. Friant-Costantini and P. Josso, *Surf. Coat. Technol.*, 1990, 43/44, 500.
68. M. L. Chou and H. Chen, *Thin Solid Films*, 1992, 208, 210.
69. M. L. Chou, N. Manning, and H. Chen, *Thin Solid Films*, 1992, 213, 64.
70. W. V. Hough, J. L. Little, and K. E. Warheit, U. S. Patent 4,279,951 (1981).
71. Y. Okinaka, *Plating and Surface Finishing*, 1970, 57, 914.
72. "The Palladium Hydrogen System" F. A. Lewis, Academic Press, New York, 1967.
73. R. Burch and F. A. Lewis, *Trans. Faraday Soc.*, 1970, 66(3), 727.
74. O. Stern, *Z. Elektrochem.*, 1924, 30, 508.
75. H. L. F. von Helmholtz, *Wiss. Abhandl. Physik-tech. Reichsanstalt*, 1879, 1, 925.
76. G. Gouy, *J. Phys.*, 1910, 9, 457.
77. D. L. Chapman, *Phil. Mag.*, 1913, 25, 475.

78. "Basic Corrosion and Oxidation" J. M. West, 2<sup>nd</sup> Edition, Ellis Horwood, New York, 1992.
79. M. Stern and A. L. Geary, J. Electrochem. Soc., 1957, 104, 56.
80. Siemens Aktiengesellschaft D5000 Diffractometer Manual, 1989, 3.
81. M. R. Kalantary, personal communication.
82. L. Brown, Trans. I. M. F., 1985, 62, 139.
83. J. B. Nelson and D.P. Riley, Proc. Phys. Soc. (London), 1945, 57, 160.
84. Y. Okinaka, J. Electrochem. Soc., 1973, 120(6), 739.
85. J. A. Gardiner and J. W. Collat, Inorganic Chemistry, 1965, 4(8), 1208.
86. Y. L. Lo and B. J. Hwang, Ind. Eng. Chem. Res., 1994, 33(1), 56.
87. M. R. Kalantary, K. A. Holbrook and P. B. Wells, Proc. 60<sup>th</sup> International Conference on Surface Finishing, 23<sup>rd</sup>-25<sup>th</sup> September, 1992, Telford, England, p. 570
88. K. Okuno, Plating and Surface Finishing, 1990, 77(2), 48.
89. Y. S. Chang and J. J. Chu, Materials Letters, 1987, 5(3), 67.
90. D. Donoval, L. Stoli, H. Norde, J. de Sousa Pires, P. A. Tove and C. S. Petersson, J. Appl. Phys., 1982, 53, 5352.
91. "A Textbook of Quantitative Inorganic Analysis" 3<sup>rd</sup> Edition, A. I. Vogel, Longman, London, 1972, p. 847.
92. "The Chemistry of Ruthenium" E. A. Seddon and K. R. Seddon, Elsevier, Amsterdam, 1984, p. 155.
93. M. Nagata, T. Esaka and H. Iwahara, Denki Kagaku, 1992, 60(9), 792.
94. "Advanced Inorganic Chemistry," F. A. Cotton and G. Wilkinson, 5<sup>th</sup> Edition, J. Wiley and Sons, New York, 1988, chp. 19.

95. "The Chemistry of the Rarer Platinum Group Metals," W.P. Griffith, J. Wiley and Sons, New York, 1967, chp. 4.
96. K. Okuno, *Plating and Surface Finishing*, 1990, 77(2), 48.
97. D. Wayshart and G. Navon, *J. Chem. Soc. Chem. Commun.*, 1971, 1410
98. J. N. Armor, H. A. Scheidegger and H. Taube., *J. Am. Chem. Soc.*, 1968, 90, 5928.
99. S. D. Pell and J. N. Armor, *J. Am. Chem. Soc.*, 1975, 97, 502.
100. P. C. Ford, *Coord. Chem. Rev.*, 1970, 5, 75.
101. F. M. Lever and A. R. Powell, *Chem. Soc. Spec. Publ. No. 13*, 1959, 135.
102. J. F. Endicott and H. Taube, *Inorg. Chem.*, 1965, 4(4), 437.
103. J. E. A. M. van den Meerakker, *J. Appl. Electrochem.*, 1981, 11, 395.
104. D. Cameron, personal communication.
105. S. D. Pell and J. N. Armor, *J. Am. Chem. Soc.*, 1972, 94, 686.
106. N. M. Sinitsyn, *Zh. Neorg. Khim.*, 1982, 27, 2042.
107. F. Bottomley, *J. Chem. Soc. Chem. Commun.*, 1971, 200.
108. J. A. Broomhead and H. Taube, *J. Am. Chem. Soc.*, 1969, 91, 1261.
109. C. T. Morgan, *J. Chem. Soc.*, 1936, p. 43.
110. A. Jolly, *Compt. Rend.*, 1892, 115, 1299.